https://doi.org/10.26219/heal.aueb.5641

ATHENS UNIVERSITY
OF ECONOMICS AND BUSINESS

DEPARTMENT OF STATISTICS

POSTGRADUATE PROGRAM

ON THE SCALING PROPERTIES OF SPATIALLY AVERAGED RAIN FIELDS

By

Georgios D. Makatis

A THESIS
Submitted to the Department of Statistics
of the Athens University of Economics and Business
in partial fulfillment of the requirements for
the degree of Master of Science in Statistics

Athens, Greece
1997

ISBN : 960-7929-06-3

https://doi.org/10.26219/heal.aueb.5641

ATHENS UNIVERSITY OF ECONOMICS AND BUSINESS

DEPARTMENT OF STATISTICS

ON THE SCALING PROPERTIES OF SPATIALLY AVERAGED RAIN FIELDS

By

Georgios D. Makatis

A THESIS
Submitted to the Department of Statistics
of the Athens University of Economics and Business
in partial fulfillment of the requirements for
the degree of Master of Science in Statistics

Athens, Greece
1997

https://doi.org/10.26219/heal.aueb.5641

ΟΙΚΟΝΟΜΙΚΟ ΠΑΝΕΠΙΣΤΗΜΙΟ ΑΘΗΝΩΝ

ΤΜΗΜΑ ΣΤΑΤΙΣΤΙΚΗΣ

ΠΕΡΙ ΤΩΝ ΙΔΙΟΤΗΤΩΝ ΚΛΙΜΑΚΩΣΗΣ ΧΩΡΙΚΩΝ ΜΕΣΩΝ ΠΕΔΙΩΝ ΒΡΟΧΗΣ

Γεώργιος Δ. Μακάτης

ΔΙΑΤΡΙΒΗ
Που υποβλήθηκε στο Τμήμα Στατιστικής
του Οικονομικού Πανεπιστημίου Αθηνών
ως μέρος των απαιτήσεων για την απόκτηση
Μεταπτυχιακού Διπλώματος Ειδίκευσης στη Στατιστική

Αθήνα
1997

https://doi.org/10.26219/heal.aueb.5641

ATHENS UNIVERSITY OF ECONOMICS AND BUSINESS

DEPARTMENT OF STATISTICS

A Thesis submitted in partial fulfillment of
the requirements for the degree of
Master of Science

ON THE SCALING PROPERTIES OF SPATIALLY AVERAGED RAIN FIELDS

Georgios Makatis

Supervisor :
Dr. Ch. Pavlopoulos

External examiner :
Prof. Dr. Wolfgang Urfer
Fachbereich Statistic,
Universitat Dortmund,
Germany

Approved by the Graduate Committee

Professor E. Xekalaki
Director of the Graduate Program
September 1997

https://doi.org/10.26219/heal.aueb.5641

DEDICATION

To all who love me.

https://doi.org/10.26219/heal.aueb.5641

ACKNOWLEDGEMENTS

I would like to thank my supervisor Dr. Haralabos Pavlopoulos not only for the trust that he showed, assigning me this specific project, but also for the continuous instruction, his valuable advice and his support during the development of this project.

We express our thanks to Dr. David Short of NASA/Goddard Space Flight Center , for providing us with the TOGA-COARE data set.

I would also like to thank my parents for their financial help all these years and for their love and support.

https://doi.org/10.26219/heal.aueb.5641

VITA

I was born in Athens in 1973. I graduated the 5-th High School of Ilion in 1990. I was admitted for undergraduate studies in Mathematics (16-th position) of the Athens University. In 1995 I graduated with B.Sc. degree in Mathematics and emphasis in Applied Mathematics with grade 7.2 out of 10. In 1995, I was admitted in the M.Sc. Program of the department of Statistics of the Athens University of Economics and Business. Part of my graduate studies was done in the Katholic University of Leuven in Belgium , where I enrolled as ERASMUS student.

https://doi.org/10.26219/heal.aueb.5641

ABSTRACT

Georgios D. Makatis

ON THE SCALING PROPERTIES OF SPATIALLY AVERAGED RAIN FIELDS

1997

Notions of simple- and multi- scaling, both in the strict and the wide sense, are reviewed and discussed, in connection with some recent empiricism regarding the scaling properties of probability moments of spatially averaged random fields of rain rate, conditional on rain. A theoretical explanation is provided for the wide sense multi-scaling of these moments, based on a general multiplicative representation of strictly multi-scaling positive random processes, with respect to scale magnification. This explanation has recently led to the consideration of random cascade models for the study and analysis of the spatial structure of rain rate. However, random cascade models do not account for the evolution of a spatial structure through time. In this dissertation the validity of scaling properties has been explored in the spectral and the correlation structures of time series of spatially averaged rain rate. Both of these structures have been estimated on the basis of real data from a regularly observed (by radar) tropical rain field during the well known TOGA-COARE experiment. The results of this empirical non-model-based analysis point to the multi-scaling behavior of the normalized spectral distribution, across the entire spectrum of frequencies, and also to the multi-scaling behavior of the corresponding spectral moments. However, the same study shows that both the raw and the smoothed periodogram, as well as the

https://doi.org/10.26219/heal.aueb.5641

correlation structure do not comply with any scaling. An opinion is then expressed, that these findings may constitute a useful hint towards the development of more sophisticated space-time theoretical models, perhaps a special class of space-time random cascades, complying with the hereby evidence for the enlarged set of scaling properties of rain rate fields.

Key Words and Phrases : Strict and Wide Sense Simple-Scaling, Strict and Wide Sense Multi-Scaling, Random Cascade, Spatially Averaged Rain Rate, Spatial Scale Parameter, Spectral Distribution, Spectral Moments, Spectral Multi-Scaling.

https://doi.org/10.26219/heal.aueb.5641

ΠΕΡΙΛΗΨΗ

Γεώργιος Δ. Μακάτης

ΠΕΡΙ ΤΩΝ ΙΔΙΟΤΗΤΩΝ ΚΛΙΜΑΚΩΣΗΣ ΧΩΡΙΚΩΝ ΜΕΣΩΝ ΠΕΔΙΩΝ ΒΡΟΧΗΣ

1997

Γίνεται μία ανασκόπηση των εννοιών αυστηρής και ασθενούς , απλής και πολλαπλής κλιμάκωσης στοχαστικών διαδικασιών, καθώς και κάποιων πρόσφατων εμπειρικών αποτελεσμάτων σχετικά με τις ιδιότητες κλιμάκωσης των ροπών πιθανότητας χωρικών μέσων πεδίων βροχής, δοθέντος ότι βρέχει. Επίσης δίνεται μία θεωρητική εξήγηση της ασθενούς πολλαπλής κλιμάκωσης αυτών των ροπών, βασισμένη σε μια γενική πολλαπλασιαστική αναπαράσταση η οποία ισχύει για θετικές στοχαστικές διαδικασίες με την ιδιότητα της αυστηρής πολλαπλής κλιμάκωσης. Αυτή η εξήγηση έχει πρόσφατα οδηγήσει στη θεώρηση των λεγομένων τυχαίων υποδειγμάτων “καταρράκτωσης” (cascading) για τη μελέτη και ανάλυση της χωρικής δομής της έντασης της βροχής. Ωστόσο, τα τυχαία υποδείγματα καταρράκτωσης δεν εξηγούν την εξέλιξη της χωρικής δομής μέσα στο χρόνο. Σε αυτή τη διατριβή, η ισχύς των ιδιοτήτων κλιμάκωσης διερευνάται για τη φασματική δομή και τη δομή αυτοσυσχέτισης χρονολογικών σειρών χωρικών μέσων πεδίων βροχής. Αυτές οι δύο δομές έχουν εκτιμηθεί με βάση πραγματικά δεδομένα ενός τακτικά παρατηρούμενου (από ραντάρ) τροπικού πεδίου βροχής κατά τη διάρκεια του πειράματος TOGA-COARE. Τα αποτελέσματα αυτής της εμπειρικής και όχι βασισμένης σε πρότυπο ανάλυσης, δείχνουν την

πολλαπλής κλιμάκωσης συμπεριφορά της κανονικοποιημένης φασματικής συνάρτησης κατανομής σε όλο το φάσμα των συχνοτήτων, καθώς επίσης και την πολλαπλής κλιμάκωσης συμπεριφορά των αντίστοιχων φασματικών ροπών. Ωστόσο, η ίδια έρευνα δείχνει ότι το περιοδόγραμμα , το εξομαλυθέν περιοδόγραμμα και οι συναρτήσεις αυτο-συνδιασποράς και αυτο-συσχέτισης δεν επιδέχονται καμμία κλιμάκωση. Τέλος, εκφράζεται η άποψη ότι αυτά τα ευρήματα μπορούν να αποτελέσουν χρήσιμες υποδείξεις για την ανάπτυξη πιο περίπλοκων θεωρητικών υποδειγμάτων χώρου-χρόνου, ίσως μιας ειδικής κατηγορίας υποδειγμάτων τυχαίας καταρράκτωσης σε χώρο και χρόνο, τα οποία υπακούουν στις ιδιότητες κλιμάκωσης των πεδίων βροχής, συμπεριλαμβανομένων και αυτών που αναδεικνύονται στην παρούσα διατριβή.

<u>Λέξεις Κλειδιά και Φράσεις :</u> Αυστηρή και Ασθενής Έννοια της Απλής Κλιμάκωσης , Αυστηρή και Ασθενής Έννοια της Πολλαπλής Κλιμάκωσης, Τυχαία Καταρράκτωση, Χωρικοί Μέσοι Πεδίων Βροχής, Παράμετρος Χωρικής Κλιμάκας, Φασματική Κατανομή, Φασματικές Ροπές, Φασματική Πολλαπλή Κλιμάκωση.

https://doi.org/10.26219/heal.aueb.5641

TABLE OF CONTENTS

https://doi.org/10.26219/heal.aueb.5641

LIST OF TABLES

https://doi.org/10.26219/heal.aueb.5641

LIST OF FIGURES

https://doi.org/10.26219/heal.aueb.5641

https://doi.org/10.26219/heal.aueb.5641

CHAPTER 1

INTRODUCTION

This dissertation is concerned with the investigation of multi-scaling properties in the spectral structure and in the correlation structure of time series of spatially averaged rain rate processes. Rain rate is a physical variable with units of millimeters per hour (mm/hr), associated with the instantaneous intensity of rainfall at any given point of a region over which a rain field is distributed. Given an instantaneous map or snapshot of a rain field (over a fixed region), its average intensity is the spatial average rain rate of the field at that very instant. Sample functions of such averages during a time interval are treated as realizations of a stochastic process which is referred to as **spatially averaged rain rate process** or simply as spatially averaged rain field. The scaling properties of the spectral distribution, of its spectral moments, and of the auto-correlation structure of such processes, are the subject of interest in this work.

The notion of ''wide sense multi-scaling'' has been introduced in the work of *Gupta and Waymire (1990)*, where it was first shown that empirical moments of spatially averaged hydrological variables, such as rainfall intensity and river flow, deviate from ''simple scaling'' behavior. Similar multi-scaling behavior has also been detected in turbulent velocity fields by *Anselmet et al. (1984)* and *Frisch and Parisi (1985)*. The new element of scientific interest in the present work is that multi-scaling behavior is investigated with respect to the spectral distribution of spatially averaged rain fields, instead of with respect to their probability distribution.

In Section 2 the notions of strict and wide sense simple scaling and multi-scaling of stochastic processes are defined. A general multiplicative ''random cascade'' representation is derived for the class of positive stochastic processes with strict sense multi-scaling behavior. This derivation relies on the invariance of the finite dimensional probability distributions under re-scaling by a *random* function of the scale parameter λ. The notion of strict sense multi-scaling is actually a generalization of the invariance of finite dimensional probability distributions of simple scaling processes. That is, in the case

https://doi.org/10.26219/heal.aueb.5641

of simple scaling processes, the invariance holds under re-scaling by a *non-random* function λ^θ, of the scale parameter $\lambda>0$, and $\theta\in\mathbf{R}$ is a so called *scaling exponent.*

Section 3 is concerned with the probabilistic structure of rain fields, addressing the probability measure induced by the random element which represents the instantaneous spatial average rain rate (or intensity of rain) over a given region at some fixed instant of time. Following *Gupta and Waymire (1990)*, the multi-scaling properties of the spatial structure of rain fields are briefly reviewed, in terms of the above probability measure.

In Section 4 new notions of multi-scaling are proposed for investigation, notions analogous to that of wide sense multi-scaling, but referring to the spectral distribution and its moments, instead of the probability distribution and its moments.

Section 5 describes a very reliable data set of rainfall measurements collected during the Intensive Observing Period (IOP) of the Tropical Ocean Global Atmosphere (TOGA) Coupled Ocean-Atmosphere Response Experiment (COARE). This data set was made available by the Laboratory for Atmospheres, Goddard Space Flight Center of the National Aeronautics and Space Administration (NASA), and it is used in this dissertation for the detection of *''spectral multi-scaling''* in spatially averaged rain fields. This data set is analyzed so that time series of spatially averaged rain fields are extracted for several sub-regions of various spatial scales with respect to the initial TOGA-COARE region. Estimates of the spectral cumulative distribution function, of its spectral moments, and of the auto-correlation function are obtained for these time series, and they are used in order to investigate the validity of multi-scaling properties in them, at least for the case of TOGA-COARE-like rain fields. Indeed, these estimates do provide supporting evidence for the validity of multi-scaling behavior of the cumulative spectral distribution function, and of its spectral moments, but they do not support the hypothesis of multi-scaling behavior by the auto-correlation function.

Section 6 concludes with some remarks on, and discussion of the obtained results, including also some thoughts about how these results may contribute to the efforts for development of space-time models, capturing both the spatial structure and its evolution through time, for spatially averaged rain rate fields.

https://doi.org/10.26219/heal.aueb.5641

CHAPTER 2

BACKGROUND ON THE THEORY OF SCALING PROCESS

2.1 Simple Scaling

Definition 2.1.1 Let $X:=\{X_s \,;\, s\in S\}$ be a real valued stochastic process defined on an arbitrary, probability space (Ω, F, P), and parametrized by a general index set S, such that $\lambda\cdot S=\{\lambda\cdot s\,;s\in S\}\subseteq S$, for every scalar $\lambda>0$. The process **X** is called ***simple scaling process in the strict sense*** if and only if for every $\lambda>0$, there is a positive scale function C_λ, such that the stochastic processes $X_\lambda:=\{X_{\lambda s}\,;\, s\in S\}$ and $C_\lambda X:=\{C_\lambda X_s\,;\, s\in S\}$ have the same probability distribution in the sense of finite dimensional distributions. That is, for every $\lambda>0$, for every $n\geq1$, for every choice of indices $s_1, s_2, \ldots,$ s_n from S, and for every vector $\mathbf{x}=(x_1, x_2, \ldots, x_n)\in\mathbf{R}^n$ the following equality holds:

$$P\left(X_{\lambda s_1}\le x_1, X_{\lambda s_2}\le x_2,\ldots,X_{\lambda s_n}\le x_n\right)=P\left(C_\lambda\cdot X_{s_1}\le x_1, C_\lambda\cdot X_{s_2}\le x_2,\ldots,C_\lambda X_{s_n}\le x_n\right)\ (1).$$

For brevity this property of strict simple scaling is denoted by writing $\{X_{\lambda s}\}\overset{d}{=}\{C_\lambda X_s\}$.

The form of the scale function C_λ is given by $C_\lambda=\lambda^\theta$ where the parameter θ is referred to as the scaling exponent [*Lamperti , 1962 , Thm. 1*]. In the following lines, using the definition of simple scaling , we prove this fact.

Given two positive scalars λ_1, λ_2, equation (1), implies that for every $y\in\mathbf{R}$, and for every index $s\in S$, such that $\lambda_1\cdot\lambda_2\cdot s\in S$ and also $\lambda_2\cdot s\in S$

$$P(X_{\lambda_1\lambda_2 s}\le y)=P(X_{(\lambda_1\lambda_2)\cdot s}\le y)=P\{(C_{\lambda_1\lambda_2})X_s\le y\}=P(X_s\le\frac{y}{C_{\lambda_1\lambda_2}})$$

and also that

$$P(X_{\lambda_1\lambda_2 s}\le y)=P(X_{(\lambda_1)\cdot\lambda_2 s}\le y)=P(C_{\lambda_1}X_{\lambda_2 s}\le y)=P(X_{\lambda_2 s}\le\frac{y}{C_{\lambda_1}})=$$

$$=P(C_{\lambda_2}X_s\le\frac{y}{C_{\lambda_1}})=P(X_s\le\frac{y}{C_{\lambda_1}\cdot C_{\lambda_2}})$$

Thus, the positive scale function $C_\lambda=C(\lambda)$ must satisfy the functional equation $C(\lambda_1\cdot\lambda_2)=C(\lambda_1)\cdot C(\lambda_2)$, provided that X_s has a non-degenerate probability distribution

https://doi.org/10.26219/heal.aueb.5641

function. In order to solve this functional equation , we consider the function $f(x)=\ln C(e^x)$, which is well defined for every $x\in\mathbf{R}$.

Then,

$$f(x_1+x_2)=\ln C(e^{x_1+x_2})=\ln C(e^{x_1}\cdot e^{x_2})=\ln\left\{C\left(e^{x_1}\right)\cdot C\left(e^{x_2}\right)\right\}=\ln C\left(e^{x_1}\right)+\ln C\left(e^{x_2}\right)=$$

$=f(x_1)+f(x_2)$.

It is well known that the only measurable , non-constant function f which satisfies the functional equation $f(x_1+x_2)= f(x_1)+ f(x_2)$, is the linear function $f(x)=\theta\cdot x$, with fixed $\theta\in\mathbf{R}$ (see *Port (1994)*). Thus, $C(e^x)=e^{\theta\cdot x}$, for every $x\in\mathbf{R}$, with fixed $\theta\in\mathbf{R}$.

Finally, setting $x = \ln\lambda$, for $\lambda>0$, it follows that $C(\lambda)=\lambda^\theta$.

A well known example of stochastic processes which are simple scaling in the sense of (1) is the class of the so called ***Levy stable processes*** , provided they start from 0 , and that they are suitably centered . For such a process, say $\{X_s\ ;\ s\geq 0\}$, the increments $\{X_s-X_t,\ 0\leq t<s\}$ are stationary and independent, with $X_s - X_t$ distributed according to a stable law with exponent α . Stable laws are easily defined in terms of their characteristic function (Fourier transform), which in turn depends on four parameters : the "characteristic exponent " $0<\alpha\leq 2$, a "location parameter '' $-\infty<\mu<+\infty$, a "scale parameter " $\sigma>0$, and a "skewness parameter " $-1\leq\beta\leq 1$. Accordingly, $\{X_s-X_t\}$ has a characteristic function given by [*Gnedenko and Kolmogorov 1954* ; *Ito ,1984*],

$$\phi(\zeta)=E\left[\exp\{i\zeta(X_t-X_s)\}\right]=\begin{cases}\exp\left\{-\sigma^\alpha(s-t)^\alpha|\zeta|^\alpha\left[1-i\beta\cdot\mathrm{sign}(\zeta)\cdot\tan\left(\dfrac{\pi\cdot\alpha}{2}\right)\right]+i\mu\zeta\right\}, & \text{if } \alpha\neq 1\\ \exp\left\{-\sigma\ (s-t)\ |\zeta|\ \left[1+i\beta\cdot\left(\dfrac{2}{\pi}\right)\cdot\mathrm{sign}(\zeta)\cdot\log|\zeta|\right]+i\mu\zeta\right\}, & \text{if } \alpha=1\end{cases}$$

where $\mathrm{sign}(\zeta)$ is 1 if $\zeta>0$, -1 if $\zeta<0$, and 0 if $\zeta=0$. This and the independence of increments determines the joint probability distribution of the process $\{X_s\ ;\ s\geq 0\}$. Thus, if $X_0=0$ and $\mu=0$, then indeed $\{X_s\ ,\ s\geq 0\}$ satisfies (1) with scaling exponent $\theta=1$.

Another example , celebrated in a physical theory of simple scaling, is the ***Holtzmark distribution*** of the inverse square force field due to a spatial distribution of either massive stars in space, or of charged particles suspended in an atmosphere ; see *Chandresekhar* [*1943*] , *Feller* [*1971*] . According to this application, let $Y(\rho)$ denote ,

https://doi.org/10.26219/heal.aueb.5641

respectively , the gravitational or Coulomb inverse square law force due to randomly distributed masses or charges in space with mean density ρ . Since the length unit is proportional to $\rho^{-1/3}$, this and the inverse square law provide the scaling relationship, $\{Y(\rho)\} \stackrel{d}{=} \{\rho^{2/3} Y(1)\}$, meaning that $\{Y(\rho)\}$ is a simple scaling process in the strict sense, with scaling exponent $\theta = 2/3$.

Similar attempt was made by *Lovejoy and Mandelbrot (1985)* to construct simple scaling models for rainfall processes (rain rate). However, as we shall explain later in more detail , the physical base of these models is not well founded, since the empirical evidence presented by several other authors is not in accord with simple scaling of rain rate processes (*Waymire (1985), Kedem and Chiu (1987) , Gupta and Waymire (1990)*).

If X_s has finite moments $E[X_s^h]$ of order $h \geq 1$, then strict sense simple scaling implies that $X_{\lambda s}^h$ and $(\lambda^\theta \cdot X_s)^h$ have the same probability distribution, whence equality of moments must also hold , so that $E[X_{\lambda s}^h] = \lambda^{\theta h} \cdot E[X_s^h]$, or equivalently $\log E[X_{\lambda s}^h] = \theta \cdot h \cdot \log\lambda + \log E[X_s^h]$.

Definition 2.1.2 The process **X** of Definition 2.1.1 is called ***simple scaling in the wide sense*** if and only if there is a constant $\theta \in \mathbf{R}$ such that for every $\lambda > 0$, for every $s \in S$ and for every $h \geq 1$, holds the equation:

$$\log m_\lambda(h) = \theta \cdot h \cdot \log\lambda + \log m_1(h) \qquad (2),$$

where, $m_\lambda(h) = E\left[X_{\lambda s}^h\right]$.

Wide sense simple scaling expressed by equation (2) may be summarized as follows:

(i) log -log linearity of $m_\lambda(h)$ with respect to the scale λ

(ii) The slope of the log-log linear relationship is a linear function $h \to h\theta$ of the moment's order h , whose slope equals the scaling exponent θ .

Clearly, wide sense simple scaling follows directly from strict sense simple scaling. However, the reverse is not necessarily true. In the work of *Gupta and Waymire (1990)* it has been shown , via analysis of real rainfall data , that rain rate processes deviate from this

https://doi.org/10.26219/heal.aueb.5641

wide sense of simple scaling , and therefore they also cannot be simple scaling in the strict sense. Nevertheless, that same work pointed to a different , and rather interesting new notion of scaling referred to as **multi-scaling**. Multi-scaling is also a notion defined in a strict and wide sense in the following sub-section.

2.2 Multi-Scaling

Definition 2.2.1 The stochastic process $\mathbf{X}:=\{X_s\ ;\ s\in S\}$ of Definitions 2.1.1 and 2.1.2 is called ***multi-scaling process in the strict sense*** if and only if there is a positive stochastic process $\mathbf{C} := \{C_\lambda\ ;\ \lambda > 0\}$, defined also on (Ω,F,P) , such that for every $\lambda>0$ the stochastic processes $\mathbf{X}_\lambda := \{X_{\lambda s}\ ;\ s \in S\}$ and $C_\lambda \cdot \mathbf{X} := \{C_\lambda \cdot X_s\ ;\ s \in S\}$ have the same probability distribution in the sense of finite dimensional distributions. That is, for every $\lambda>0$, for every $n\geq 1$, for every choice of indices $s_1,s_2,\ldots,s_n$ from S , and for every vector $\mathbf{x}=(x_1, x_2,\ldots, x_n) \in \mathbf{R}^n$ the following equality holds :

$$P\left(X_{\lambda s_1} \leq x_1, X_{\lambda s_2} \leq x_2,\ldots, X_{\lambda s_n} \leq x_n\right) = P\left(C_\lambda \cdot X_{s_1} \leq x_1, C_\lambda \cdot X_{s_2} \leq x_2,\ldots, C_\lambda X_{s_n} \leq x_n\right) \quad (3).$$

In short, the notation $\{X_{\lambda s}\} \stackrel{d}{=} \{C_\lambda \cdot X_s\}$ is used, as for simple scaling, but now C_λ is a random scale function. Note that both equations (1) and (3) express invariance of the probability distribution of the process $\mathbf{X}$, under scaling operations $\lambda^{-\theta}$ and C_λ^{-1} on the random variable $X_{\lambda s}$, with scaled parameter by a scale factor λ. However, the dramatic qualitative difference between the two invariances is that $\lambda^{-\theta}$ is a non-random factor and C_λ^{-1} is a random factor.

In the sequel , we shall restrict our interest to the case of $0<\lambda\leq 1$, that is, to scales λ which act as ''magnifying lenses'' for the study of the process of interest $\mathbf{X}$ in its finer detail, with respect to the index $s\in S$. For such scales, a positive and strictly multi-scaling process $\mathbf{X}$ admits a rather interesting representation which is presented in the following lemma.

https://doi.org/10.26219/heal.aueb.5641

Lemma 2.2.1

Let $\mathbf{X} := \{X_s \,;\, s\in S\}$ be a positive and strictly multi-scaling process, in accord with Definition 2.2.1, and $0<\lambda\le 1$. Then, there exists a real-valued stochastic process $\mathbf{Z} := \{Z_u \,;\, u \ge 0\}$ satisfying the following three properties:

(I) Starts at zero almost surely : $P(Z_0 = 0) = 1$.

(II) Has stationary increments (but not necessarily independent increments).

(III) For every magnifying scale $0<\lambda\le 1$, holds the multiplicative representation

$$\{X_{\lambda s}\} \stackrel{d}{=} \left\{X_s \cdot \exp\left[\theta \cdot \log\lambda + Z_{\log\left(\frac{1}{\lambda}\right)}\right]\right\},$$ in the sense of finite dimensional distributions,

where θ is an arbitrary fixed real number .

Proof : Since $\{X_s\}$ is strictly multi-scaling , by definition there is a positive process $\{C_\lambda \,;\, 0<\lambda\le 1\}$ such that for every $\lambda\in(0,1]$ we have $\{X_{\lambda s}\} \stackrel{d}{=} \{C_\lambda \cdot X_s\}$. Now, setting $\lambda = e^{-u}$ for $u\ge 0$, and choosing arbitrarily a fixed constant $\theta\in\mathbf{R}$, we define a process $\mathbf{Z} := \{Z_u \,;\, u\ge 0\}$ via its finite dimensional distributions, so that $\{Z_u\} \stackrel{d}{=} \{\theta\cdot u + \log C_{\exp(-u)}\}$.

Thus, $$\left\{Z_{\log\left(\frac{1}{\lambda}\right)}\right\} \stackrel{d}{=} \left\{\theta\cdot\log\left(\frac{1}{\lambda}\right) + \log C_\lambda\right\} \stackrel{d}{=} \left\{\log\left(\frac{C_\lambda}{\lambda^\theta}\right)\right\},$$

whence

$$\{C_\lambda\} \stackrel{d}{=} \left\{\lambda^\theta \cdot \exp\left[Z_{\log\left(\frac{1}{\lambda}\right)}\right]\right\}$$

or equivalently

$$\{C_\lambda\} \stackrel{d}{=} \left\{\exp\left[\theta\cdot\log\lambda + Z_{\log\left(\frac{1}{\lambda}\right)}\right]\right\} \qquad (4) \;,$$

which completes the proof of (III).

https://doi.org/10.26219/heal.aueb.5641

For the proof of (I), it is clear by the definition of the $\mathbf{Z}$ process that $Z_0 \overset{d}{=} \log C_1$, and therefore (I) holds if and only if $P(C_1 = 1) = 1$, which obviously holds, since $P(X_s > 0) = 1$ and $X_s \overset{d}{=} C_1 \cdot X_s$. In order to show (II), it suffices to show that for any $u_1 \geq 0$ and $u_2 \geq 0$, it is $Z_{u_1+u_2} \overset{d}{=} Z_{u_1} + Z_{u_2}$. Indeed, for $u_1 \geq 0$ and $u_2 \geq 0$ set $\lambda_1 = e^{-u_1}$ and $\lambda_2 = e^{-u_2}$. Then, strict multi-scaling of the process $\mathbf{X}$ implies that $C_{\lambda_1\lambda_2} \cdot X_s \overset{d}{=} X_{(\lambda_1\lambda_2)\cdot s} \overset{d}{=} X_{\lambda_1\cdot(\lambda_2 s)} \overset{d}{=} C_{\lambda_1} \cdot X_{\lambda_2 \cdot s} \overset{d}{=} C_{\lambda_1} \cdot C_{\lambda_2} \cdot X_s$, whence $C_{\lambda_1 \cdot \lambda_2} \overset{d}{=} C_{\lambda_1} \cdot C_{\lambda_2}$, since $P(X_s > 0) = 1$. Therefore $\log C_{\lambda_1 \cdot \lambda_2} \overset{d}{=} \log C_{\lambda_1} + \log C_{\lambda_2}$, and in light of (4) we have that

$$\theta \cdot \log(\lambda_1 \cdot \lambda_2) + Z_{\log\left(\frac{1}{\lambda_1 \cdot \lambda_2}\right)} \overset{d}{=} \theta \cdot \log\lambda_1 + Z_{\log\left(\frac{1}{\lambda_1}\right)} + \theta \cdot \log\lambda_2 + Z_{\log\left(\frac{1}{\lambda_2}\right)}$$

or equivalently

$$Z_{\log\left(\frac{1}{\lambda_1}\right)+\log\left(\frac{1}{\lambda_2}\right)} \overset{d}{=} Z_{\log\left(\frac{1}{\lambda_1}\right)} + Z_{\log\left(\frac{1}{\lambda_2}\right)}.$$

This completes the proof of the lemma.

The above lemma shows that scaling of the index $s \in S$ by a factor $0<\lambda\leq 1$, implies scaling of the distribution of the $\mathbf{X}$ process by a random factor which is an exponentiated additive process $\mathbf{Z}$ with stationary increments. In this sense, intuitively speaking, the probabilistic structure of the process $\mathbf{X}$ may be thought of as resembling to a ''cascading'' of some initial quantity (corresponding to $\lambda=1$), to finer bits or pieces in a sequence of fragmentations (corresponding to a series of scale magnifications $0<\lambda<1$).

For this reason, the multiplicative representation in (III) of lemma 2.2.1 is often referred to as ''multiplicative random cascade'' representation of the multi-scaling process $\mathbf{X}$. We shall return to this interpretation in Section 3, regarding rain fields in particular.

Let us now assume that the process $\mathbf{C}:=\{ C_\lambda ; \lambda \in (0,1] \}$ associated with a positive and strictly multi-scaling process $\mathbf{X}:=\{X_s ; s \in S \}$, is independent of the process $\mathbf{X}$. Equation $X_{\lambda s} \overset{d}{=} C_\lambda \cdot X_s$ certainly implies that $E(X_{\lambda s}^h) = E(C_\lambda^h \cdot X_s^h)$, provided that the moments

https://doi.org/10.26219/heal.aueb.5641

$E(X^h_{\lambda s})$ of order $h \geq 1$ exist for every $s \in S$. Then , independence of the processes **C** and **X** implies that $m_\lambda(h) = E(C^h_\lambda) \cdot m_1(h)$, with $m_\lambda(h) = E(X^h_{\lambda s})$ as in subsection 2.1.

Consequently, employing the representation (4) we obtain $m_\lambda(h) = E\left\{\lambda^{\theta h} \cdot e^{h \cdot Z_{\log\left(\frac{1}{\lambda}\right)}}\right\}$

or equivalently $m_\lambda(h) = \lambda^{\theta \cdot h} \cdot M_\lambda(h) \cdot m_1(h)$, where $M_\lambda(h) = E\left\{e^{h \cdot Z_{\log\left(\frac{1}{\lambda}\right)}}\right\}$ is the moment generating function of $Z_{\log\left(\frac{1}{\lambda}\right)}$.

Thus , $\log m_\lambda(h) = \theta \cdot h \cdot \log\lambda + \log M_\lambda(h) + \log m_1(h)$ or equivalently

$$\log m_\lambda(h) = \left\{\theta \cdot h + \frac{\log M_\lambda(h)}{\log\lambda}\right\} \cdot \log\lambda + \log m_1(h) \qquad (5).$$

We note that the latter equation expresses again a log-log linear relationship between $m_\lambda(h)$ and λ, if and only if the function $\theta \cdot h + \frac{\log M_\lambda(h)}{\log\lambda}$ is a function of h only , and independent of λ. In that case, obviously $\log M_\lambda(h) = (\log\lambda) \cdot A_0(h)$, where $A_0(h)$ is a function of h only and independent of λ. Moreover , since $\log M_\lambda(h)$ is a cumulant generating function , it is necessarily a convex function of h (see *Billingsley (1979) , pg. 121*), and therefore $\frac{\partial^2[\log M_\lambda(h)]}{\partial h^2} = (\log\lambda) \cdot \frac{d^2 A_0(h)}{dh^2} \geq 0$,which implies that $A_0(h)$ must be a concave function. Thus , if $A(h) = \theta \cdot h + \frac{\log M_\lambda(h)}{\log\lambda}$ is the slope function (of h only and independent of λ) in (5) , it also must be a concave function of h since $\frac{d^2 A(h)}{dh^2} = \frac{d^2 A_0(h)}{dh^2} \leq 0$.The above theoretical considerations lead to a weaker notion of multi-scaling , referred to as wide sense multi-scaling.

Definition 2.2.2 A positive stochastic process $X := \{X_s \,;\, s \in S\}$ possessing finite moments of order $h \geq 1$, is called ***multi-scaling process in the wide sense*** if and only if for every magnifying scale $\lambda \in (0,1]$ the following conditions are satisfied :

https://doi.org/10.26219/heal.aueb.5641

(I) The moments of order $h \geq 1$ of the scaled process $\mathbf{X}_\lambda := \{X_{\lambda \cdot s} ; s \in S\}$ are log-log linearly related with the scale λ :

$$\log m_\lambda(h) = A(h) \cdot \log \lambda + B(h) \qquad (6),$$

where $m_\lambda(h) = E(X^h_{\lambda \cdot s})$ and $B(h) = \log m_1(h)$,

(II) The slope coefficient $A(h)$ is a non-linear concave function of the moment's order $h \geq 1$, and independent of λ.

From the above discussion it is also clear that a positive process $\mathbf{X}$ which is strictly multi-scaling , with finite moments of order $h \geq 1$, and with scaling factor process $\mathbf{C}$ independent of $\mathbf{X}$, can be wide sense multi-scaling if and only if $\log M_\lambda(h) = (\log\lambda) \cdot A_0(h)$, with $A_0(h)$ being a concave function of h only and independent of λ.

Thus, processes which are multi-scaling in this weaker sense may be also processes which are strictly multi-scaling, and therefore processes which obtain the multiplicative representation of Lemma 2.2.1 .

Such an example is the process $\mathbf{Y} := \{Y_\lambda ; \lambda \in (0,1]\}$, defined via a positive random variable Y_1 , and a standard Brownian Motion $\mathbf{B} = \{B_u ; u \geq 0\}$, independent of Y_1 , as follows: $Y_\lambda = Y_1 \cdot \exp\left\{\sigma \cdot B_{\log\left(\frac{1}{\lambda}\right)} + \mu \cdot \log \lambda\right\}$,

where $\sigma > 0$ is a diffusion parameter and $\mu \in \mathbf{R}$. Then , it is immediately noted that each $\frac{Y_\lambda}{Y_1}$ is a lognormally distributed random variable, for every $0 < \lambda \leq 1$, and of course $P(Y_\lambda > 0) = 1$ for every $0 < \lambda \leq 1$. Moreover , since B_u is normally distributed with mean 0 and variance u , we easily obtain by direct calculation that $\log m_\lambda(h) = A(h) \cdot \log\lambda + \log m_1(h)$, where $A(h) = h \cdot \mu - \frac{h^2 \cdot \sigma^2}{2}$ is indeed a concave function of h only and independent of λ.

Despite the abundance of more such examples, the interest is hereon shifted onto examples of natural processes which do possess wide sense multi-scaling structure. Striking examples of wide sense multi-scaling physical processes are :

a) Spatial averages of rain rate fields (conditional on rain) , with respect to magnification of the spatial scale ($0<\lambda\leq 1$).

b) Spatial averages of runoff water supply at river basins , also with respect to magnification of the spatial scale.

c) Velocity differences in a field of fully developed turbulent flow, with respect to magnification of scale in spatial distance.

In all three cases , log-log linearity of the empirical moments with respect to scale magnification $0<\lambda\leq 1$ was verified , as well as concavity of the slope function , in the work of *Gupta and Waymire (1990)* . The detailed description of the data available in each case is given in that same paper , and also in references mentioned therein.

CHAPTER 3

PROBABILISTIC STRUCTURE AND MULTI-SCALING OF RAIN FIELDS

In this section our attention is focused exclusively on rain fields , and the multi-scaling properties of their spatial structure are reviewed in more detail. Let $G\subset \mathbf{R}^2$ be a fixed geographic region on the globe , say a square or disk domain. Given a probability space (Ω,F,P) associated with the randomness of rainfall over the region G, let a non-negative random variable $R_{t,\alpha}:\Omega\to[0, \infty)$ denote the instantaneous intensity of rainfall (measured in units of mm/hr) at the point $\alpha\in G$, at the instant $t\geq 0$. Then, at any fixed instant $t\geq 0$, the collection of random variables $\{ R_{t,\alpha} \ ; \alpha\in G\}$ represents a random field of rain rate over the region G at the instant t.

Let B(G) be the Borel σ-algebra of subsets of the region G, and μ a fixed (non-random) finite measure defined on B(G). Given a sub-region $A\in B(G)$, the random variable $R_{t,A} = R_t(A) = \dfrac{1}{\mu(G)}\cdot\int_A R_{t,\alpha}\mu(d\alpha)$ represents the instantaneous spatial average rain rate (or intensity of rain) over A at the instant t. For example, μ could be 2-D Lebesgue measure (i.e $\mu= l_2$) , or some other more complicated measure accounting for the geographic morphology of the region G.

Thus, for each fixed $t\geq 0$, the collection $\{ R_t(A) \ ; A\in B(G) \}$ is a stochastic process indexed by $A\in B(G)$, and also it may be viewed as a random measure on B(G).

https://doi.org/10.26219/heal.aueb.5641

On the other hand, for each fixed $A \in B(G)$, the collection $\{ R_t(A) ; t \geq 0 \}$ is a stochastic process of spatially averaged rain rate over $A \in B(G)$, indexed by $t \geq 0$.

Moreover, for each fixed $t \geq 0$, and for each fixed $A \in B(G)$, the random variable $R_t(A)$ is non-negative, and induces on $[0, \infty)$ a probability measure $P_{t,A}$ of mixed type. That is, $P_{t,A} = \left(\pi_{t,A} , P^+_{t,A}\right)$, where $\pi_{t,A} = P_{t,A}(\{0\}) = P\{R_t(A) = 0\}$ is an atom probability of no rain over $A \in B(G)$ at the instant t, and $P^+_{t,A}$ is the conditional on rain probability distribution of the positive random variable $R^+_t(A) = [R_t(A) \mid R_t(A)>0]$. Therefore, if $F_{t,A}$ is the distribution function of $P_{t,A}$, and $F^+_{t,A}$ is the distribution function of $P^+_{t,A}$, then for every $u \in \mathbf{R}$ we have that

$$F_{t,A}(u) = \pi_{t,A} \cdot I_{[0,\infty)}(u) + (1 - \pi_{t,A}) \cdot F^+_{t,A}(u) \qquad (7).$$

Moreover, $F^+_{t,A} = 0$ for $u \leq 0$, and $F^+_{t,A}$ is assumed to be absolutely continuous with probability density function $f_{t,A}(u) = \dfrac{dF^+_{t,A}(u)}{du}$, or equivalently $P^+_{t,A}$ is absolutely continuous with respect to the 1-D Lebesgue measure l_1 on $(0, \infty)$, and $f_{t,A} = \dfrac{dP^+_{t,A}}{dl_1}$ is the corresponding Radon-Nikodym derivative .

Under this assumption, for any Borel subset $B \subset (0, \infty)$ we have

$$P^+_{t,A}(B) = P\left\{R^+_t(A) \in B\right\} = P\left\{R_t(A) \in B \middle| \ R_t(A) > 0\right\} = \int_B f_{t,A}(u)du .$$

From equation (7) it is clear that moments of the unconditional distribution function $F_{t,A}$ exist, if and only if the corresponding moments of the conditional on rain distribution function $F^+_{t,A}$ exist.

In particular, $\int_0^\infty u^h \cdot dF_{t,A}(u) = (1 - \pi_{t,A}) \cdot \int_0^\infty u^h \cdot f_{t,A}(u)\, du$

or $E\left[R^h_t(A)\right] = P\left[R_t(A) > 0\right] \cdot E\left[\left(R^+_t(A)\right)^h\right]$

https://doi.org/10.26219/heal.aueb.5641

whence $E\left[\left(R_t^+(A)\right)^h\right] = \dfrac{E\left[R_t^h(A)\right]}{P\left[R_t(A) > 0\right]}$.

Also, for every magnifying scale $0<\lambda<1$, the conditional on rain statistical moments of spatially averaged rain rate are $m_\lambda(h) = E\left[(R_t^+(\lambda \cdot A))^h\right] = \dfrac{E\left[R_t^h(\lambda \cdot A)\right]}{P\left[R_t(\lambda \cdot A) > 0\right]}$.

For fixed $t \geq 0$ corresponding to a single snapshot (map) of rain rates from a rain field over the region G, let us set $Y_A = R_t^+(A)$. Then, the process $\{ Y_A ; A \in B(G) \}$ is a positive stochastic process , indexed by $A \in B(G)$, and is called the process of spatial rain rate averages conditional on rain. It is this process which in the work of *Gupta and Waymire (1990)* was found to satisfy wide sense multi-scaling (see Definition 2.2.2). Indeed, the conditional on rain statistical moments $m_\lambda(h) = E(Y_{\lambda \cdot A}^h) = E\left\{\left(R_t^+(\lambda \cdot A)\right)^h\right\}$ were estimated for h=1,2,3,4,5,6 and scales $\lambda = 1, \frac{1}{2}, \frac{1}{4}, \frac{1}{8}, \frac{1}{16}$, and the log-log linear relationship $\log m_\lambda(h) = A(h) \cdot \log \lambda + B(h)$ was verified with correlation coefficient persistently close to -1, varying from -0.997 to -0.999 . Moreover, the estimate of the slope function A(h) did conform with concave behavior, deviating from simple scaling according to part (II) of Definition 2.2.2. The data used for the estimation of statistical moments conditional on rain, were from phase-I of the Global Atmosphere Research Program, Atlantic Tropical Experiment (GATE).

That evidence did provide a hint towards the possibility of strict sense multi-scaling, since strict and wide sense multi-scaling are not mutually exclusive behaviors as we explained in Section 2. If $\{Y_A ; A \in B(G)\}$ were indeed a strictly multi-scaling process , then according to Lemma 2.2.1, it should admit a suitable multiplicative representation via exponentiation of an additive process with stationary increments. This in turn would allow for an intuitive perception of rain-fields as being randomly cascading structures. In fact, this very intuition has actually triggered some efforts of modeling the spatial structure of rain fields by considering the so called <u>multiplicative random cascade models</u>. The exact definition of random cascade models, with descriptions of their rich probabilistic and fractal geometric structure and properties, and also their use in simulating spatial snapshots

https://doi.org/10.26219/heal.aueb.5641

of rain rate fields, are appearing in explicit detail in more recent works by *Gupta and Waymire (1993)* , *Over and Gupta (1994)*, *Holley and Waymire (1992)*. However, at the present state of the progress made by the use of such models towards the study of rain fields (and of hydrological processes in general), these models do not capture the temporal evolution of rain rate fields, but only some of their spatial features.

This very point has triggered our interest to investigate the possibility of scaling behavior, again with respect to magnification of the spatial scale, in quantitative characteristics of spatially averaged rain rate which do involve the element of time, even in a subtle if not in a direct way.

As a first step towards this direction, in the next Section 4 we propose the investigation of wide sense multi-scaling behavior in the spectral and in the auto-correlation structure of time series obtained from spatially averaged rain rate, on sub-regions of different scales from a given rain field. It is hoped that the new findings may possibly be incorporated into the efforts of modifying random cascade models in such a way as to enable them to capture more physically based features of rain fields, not only with respect to spatial variability, but with respect to temporal variability as well.

CHAPTER 4

SPECTRAL STRUCTURE AND MULTI-SCALING OF RAIN RATE

Motivated by the work presented in Sections 2 and 3, an effort is made here to extend appropriately the notion of wide sense multi-scaling, in such a manner that it may be used for the study of the effects of spatial scale magnification on the spectral structure of spatially averaged rain rate processes. In order to distinguish this notion of multi-scaling from the ones presented earlier, we shall refer to it as ***spectral multi-scaling***.

Given a random field of rain rate over some fixed geographic region G, the variable of interest remains to be the instantaneous spatial average rain rate $R_t(A)$, over a given sub-region $A \in B(G)$, at a given instant $t \geq 0$. So far, the notions of multi-scaling defined in Sections 2 and 3 were concerned with the effects of change of the spatial scale λ, on the

https://doi.org/10.26219/heal.aueb.5641

probability distribution (strict sense), and on the probability moments (wide sense), of the conditional on rain scaled process $\{R_t^+(\lambda \cdot A)\ ;\ A \in B(G)\}$ for scales $0<\lambda\leq 1$. That is, the scaled process has been treated merely as a spatial process, since the only parameter which has been varying is the sub-region $A\in B(G)$ via different scalings corresponding to scale factors $0<\lambda\leq 1$, and the time parameter $t\geq 0$ has been treated as fixed.

Hereforth, we shall let the time $t\geq 0$ also flow discretely as well, and our interest will be focused on the effects that changes of the scale parameter impose on the spectrum of the scaled process $\{R_t(\lambda \cdot A)\ ;t\geq 0\}$, for scales $0<\lambda\leq 1$, and fixed $A\in B(G)$. Note that, $\{R_t(\lambda \cdot A)\ ;t\geq 0\}$ is the <u>unconditional</u> process of spatially averaged rain rate, which is observed only at discrete equidistant time instants (i.e. discrete-time series). Some general assumptions which shall be adopted, are the following :

(A1) For each $A\in B(G)$, and for each $0<\lambda\leq 1$, the (unconditional) process $\{R_t(\lambda \cdot A)\ ;\ t\geq 0\}$ is a stationary process in wide sense. That is, given $A\in B(G)$, and $0<\lambda\leq 1$, the unconditional mean

$$\mu_\lambda(1) := E\{R_t(\lambda \cdot A)\} = P[R_t(\lambda \cdot A) > 0]\cdot E\{R_t^+(\lambda \cdot A)\} = (1-\pi_{t,\lambda A})\cdot m_\lambda(1)$$

does not depend on time $t\geq 0$, and the auto-covariance function

$$\gamma_\lambda(k) := \mathrm{Cov}\{R_{t+k}(\lambda A)\ ,\ R_t(\lambda A)\} = E\{R_{t+k}(\lambda A)\cdot R_t(\lambda A)\} - \mu_\lambda^2(1)$$

is also independent of $t\geq 0$, for every integer lag k.

(A2) For each $A\in B(G)$, and $0<\lambda\leq 1$, the auto-covariance of the unconditional process $\{R_t(\lambda \cdot A)\ ;\ t\geq 0\}$ admits a spectral representation with respect to an absolutely continuous spectral distribution $G_\lambda(\omega)$, with a spectral density function $g_\lambda(\omega) = \dfrac{dG_\lambda(\omega)}{d\omega}$, for $\omega\in(0,\pi]$. That is, $G_\lambda(\omega)$ is a monotonically increasing absolutely continuous function, defined for $\omega\in(0,\pi]$, such that

$$\gamma_\lambda(k) = \int_0^\pi \cos(\omega k)\cdot dG_\lambda(\omega) = \int_0^\pi \cos(\omega k)\cdot g_\lambda(\omega)d\omega \qquad (8)$$

https://doi.org/10.26219/heal.aueb.5641

for every integer k. Equation (8) is known as the spectral representation of auto-covariance $\gamma_\lambda(k)$, and it implies that the variance of the (stationary) process $\{R_t(\lambda A)\}$ satisfies the equation

$$\sigma_\lambda^2 = \gamma_\lambda(0) = \int_0^\pi dG_\lambda(\omega) = G_\lambda(\pi) - G_\lambda(0) = \int_0^\pi g_\lambda(\omega)d\omega \ ,$$

whence it follows that $\sigma_\lambda^2 = \gamma_\lambda(0) = G_\lambda(\pi)$, provided that $G_\lambda(0) = 0$. Thus, the value $G_\lambda(\omega) = \int_0^\omega g_\lambda(u)du$, of the spectral distribution function, for given $\omega \in (0,\pi]$, is interpreted as being the portion of the variance which is attributed to frequencies in the spectral interval $(0, \omega]$; (see *Koopmans (1974)* or *Chatfield (1989)*).

On the other hand, the normalized version $G_\lambda^*(\omega) = \dfrac{G_\lambda(\omega)}{G_\lambda(\pi)}$ is an ordinary probability distribution function on $(0,\pi]$, with density function $g_\lambda^*(\omega) = \dfrac{g_\lambda(\omega)}{\int_0^\pi g_\lambda(\omega)d\omega}$, and may be interpreted as being the proportion of the variance which is attributed to frequencies in the spectral interval $(0, \omega]$. The normalized version is also referred to as being a spectral distribution function, since the auto-correlation function $\rho_\lambda(k) = \dfrac{\gamma_\lambda(k)}{\gamma_\lambda(0)}$ admits the spectral representation

$$\rho_\lambda(k) = \int_0^\pi \cos(\omega k)dG_\lambda^*(\omega) = \int_0^\pi \cos(\omega k)g_\lambda^*(\omega)d\omega \qquad (9).$$

(A3) The spectral moments of the (unconditional) process $\{R_t(\lambda \cdot A) \ ; \ t \geq 0\}$, defined by the integral $s_\lambda(h) := \int_0^\pi \omega^h dG_\lambda(\omega) = \int_0^\pi \omega^h g_\lambda(\omega)d\omega$, exist for every $h \geq 1$ (i.e. $s_\lambda(h) < \infty$).

Thus, in a way analogous to that of Definition 2.2.2, the following Definitions 4.1 and 4.2 are proposed here as extensions of the notion of multi-scaling, concerning the spectral domain of the process $\{R_t(\lambda \cdot A) \ ; \ t \geq 0\}$.

https://doi.org/10.26219/heal.aueb.5641

Definition 4.1 Provided that for $A \in B(G)$, and for $0<\lambda\le 1$, the unconditional process $\{R_t(\lambda \cdot A)\ ;\ t \ge 0\}$ of spatially averaged rain rate satisfies (A1), (A2), and (A3), it will be called a ***spectrally multi-scaling process in the wide sense*** , if and only if

(i) For every $h\ge 1$, the spectral moments $s_\lambda(h)$ are log-log linearly related with the scale parameter λ. That is, for every $h\ge 1$, and $0<\lambda\le 1$,

$$\log s_\lambda(h) = a(h)\cdot \log\lambda + \log s_1(h) \qquad (10)$$

or equivalently

$$\log\left\{\frac{s_\lambda(h)}{s_1(h)}\right\} = a(h)\cdot \log\lambda \qquad (11)$$

(ii) The slope coefficient $a(h)$ is a non-linear function of the spectral moment's order $h\ge 1$, and independent of the scale parameter $0<\lambda\le 1$.

Definition 4.2 Provided that for $A \in B(G)$, and for $0<\lambda\le 1$, the unconditional process $\{R_t(\lambda \cdot A)\ ;\ t \ge 0\}$ of spatially averaged rain rate satisfies (A1) and (A2), it will be called a ***spectrally multi-scaling process in the strict sense*** , if and only if

(i) For every frequency $0<\omega\le\pi$, the spectral distribution function $G_\lambda(\omega)$ is log-log linearly related with the scale parameter λ.

That is, for every $0<\omega\le\pi$, and for every $0<\lambda\le 1$,

$$\log G_\lambda(\omega) = C(\omega)\cdot \log\lambda + \log G_1(\omega) \qquad (12)$$

or equivalently

$$\log\left\{\frac{G_\lambda(\omega)}{G_1(\omega)}\right\} = C(\omega)\cdot \log\lambda \qquad (13).$$

(ii) The slope coefficient $C(\omega)$ in (13), is a non-linear function of the spectral frequency $0<\omega\le\pi$, and independent of the scale parameter $0<\lambda\le 1$.

Under the assumptions (A1),(A2),and (A3), it is not obvious that strict spectral multi-scaling, in the sense of (13), should necessarily imply wide spectral multi-scaling in the sense of (11). That is, the nomenclature introduced with the Definitions 4.1 and 4.2 does not necessarily imply a relationship between the two notions of spectral multi-scaling just defined. In fact, this is a point open to further investigation, yet unsettled in this

https://doi.org/10.26219/heal.aueb.5641

dissertation.

However, if strict spectral multi-scaling holds, then via differentiation with respect to the frequency ω, equation (12) implies that

$$g_{\lambda}(\omega)=\lambda^{C(\omega)}\cdot\left[g_1(\omega)+C'(\omega)\cdot G_1(\omega)\cdot\log\lambda\right] \quad (14).$$

Equation (14) clearly shows that the multi- scaling property of the spectral distribution function $G_{\lambda}(\omega)=\lambda^{C(\omega)}\cdot G_1(\omega)$, is not inherited to the corresponding spectral density function $g_{\lambda}(\omega)$. That is, $g_{\lambda}(\omega)\neq\lambda^{C(\omega)}\cdot g_1(\omega)$, unless $C'(\omega)=0$ in equation (14). Nevertheless, the possibility of $C'(\omega)=0$ is already ruled out, since in that case $C(\omega)$ would have to be a constant function, while part (ii) of Definition 4.2 requires that $C(\omega)$ is a non-linear function. Thus, this contradiction implies that $C'(\omega)$ is not the identically zero function.

Evidence supporting the validity of spectral multi-scaling, both in the strict and the wide sense defined above, is demonstrated in the next Section. It is also shown that the spectral densities, indeed do not comply with any relationship of the log-log linear type

$$\log\left\{\frac{g_{\lambda}(\omega)}{g_1(\omega)}\right\}=D(\omega)\cdot\log\lambda \qquad (15)$$

with $D(\omega)$ being an independent of λ function of ω.

Moreover, it is shown that neither the auto-covariances nor the auto-correlations of $\{R_t(\lambda\cdot A)\ ;\ t\geq 0\}$ possess any multi-scaling properties, again in the sense of log-log linear type of relations

$$\log\left|\frac{\gamma_{\lambda}(k)}{\gamma_1(k)}\right|=H(k)\cdot\log\lambda \qquad (16)$$

$$\log\left|\frac{\rho_{\lambda}(k)}{\rho_1(k)}\right|=E(k)\cdot\log\lambda \qquad (17)$$

respectively, with $H(k)$ and $E(k)$ being independent of the integer lag k.

In fact, if (17) does not hold true, then this implies that (16) cannot hold true either.

https://doi.org/10.26219/heal.aueb.5641

Indeed, if (16) were true, then $\log\left|\frac{\rho_\lambda(k)}{\rho_1(k)}\right| = \log\left|\frac{\gamma_\lambda(k)}{\gamma_1(k)}\right| - \log\left|\frac{\gamma_\lambda(0)}{\gamma_1(0)}\right|$,whence, due to (16) one has that $\log\left|\frac{\rho_\lambda(k)}{\rho_1(k)}\right| = E(k)\cdot\log\lambda$, with E(k)= H(k)- H(0).

CHAPTER 5

DESCRIPTION AND ANALYSIS OF THE DATA

5.1 Description of the TOGA - COARE Rain Field

The data which are analyzed in this dissertation, verifying spectral multi-scaling of spatially averaged rain-fields, constitute a small portion of a much larger data set of rain rate measurements. The data were collected during a 21-day period (00:01 UTC of December 20, 1992 through 23:51 UTC of January 9, 1993), known as Cruise 2 of the Intensive Observing Period (IOP) of the Tropical Ocean Global Atmosphere (TOGA) Coupled Ocean Atmosphere Response Experiment (COARE). The measurements were obtained from two Doppler precipitation radars, which were scanning **every ten minutes** a large tropical region in the China Sea , of approximate size 300km (North to South direction) $\times$ 400km (East to West direction). The two radars , named TOGA and MIT, were on board the ships R | V Xiangyanghong #5 (People's Republic of China) and R | V JV Vickers (U.S.A), respectively. Rain rates were obtained from the reflectivities of each radar snapshot , which then were binned over small square pixels of size 2×2 km^2 each. The data set which is actually used here consists of 25 concurrent time series , each consisting of 2996 instantaneous averages of rain rate over a different one of the 25 contiguous pixels depicted in Figure 1. The region of size 10×10 km^2 obtained from the union of the 25 non-overlapping contiguous pixels of Figure 1 lied entirely within the intersection of the ranges of the two radars, approximately located at 2^0 South and 156^0 East. Thus, it is understood that each radar snapshot gives a rain field of 25 rain-rate averages corresponding to the 25 pixels of Figure 1, and there are 2996 snapshots in total.

More detailed information about TOGA- COARE is given by *Short et.al. (1995)*, *Kucera et.al. (1995) and Ferrier et al. (1995)*.

1	2	3	4	5
6	7	8	9	10
11	12	13	14	15
16	17	18	19	20
21	22	23	24	25

Figure 1 : 10×10 km^2 region consisting of 25 contiguous pixels of size 2×2 km^2 each.

Let A_0 denote the entire 10×10 km^2 region of Figure 1, which can be considered as a sub-region of the much larger 300×400 km^2 region G of the whole experiment. Since A_0 is the largest field available, let us associate it with unitary scale $\lambda_0=1$, and for each $t = 1,2,\ldots,2996$, let $R_t(A_0)$ denote the spatial average of the 25 rain rates corresponding to the t-th snapshot. The set $\{R_t(A_0)\ ;\ t = 1,2,\ldots,2996\}$ forms a time series plotted in Figure 2(a).

Scaling A_0 by a factor $\lambda_1 = \frac{4}{5}$ leads to 4 possible square sub-regions, each of size 8×8 km^2 and consisting of 16 contiguous pixels. From these 4 possibilities, we consider the one obtained by deleting the top row and the left column of pixels from Figure 1. Let A_1 be the remaining (scaled) sub-region. Averaging the 16 rain rates of each snapshot over A_1 we obtain a new time series $\{ R_t(A_1)\ ;\ t = 1,2,\ldots,2996 \}$, depicted in Figure 2(b).

Scaling A_0 by a factor $\lambda_2 = \frac{3}{5}$ leads to 9 possible square sub-regions, each of size 6×6 km^2 and consisting of 9 contiguous pixels. From these 9 possibilities, we consider the one obtained by deleting the top two rows and the left two columns of pixels from Figure 1. Let A_2 be the remaining (scaled) sub-region. Averaging the 9 rain rates of each snapshot over A_2 we obtain a new time series $\{R_t(A_2)\ ;\ t = 1,2,\ldots,2996\}$, depicted in Figure 2(c).

https://doi.org/10.26219/heal.aueb.5641

Scaling A_0 by a factor $\lambda_3 = \frac{2}{5}$ leads to 16 possible square sub-regions, each of size 4×4 km^2 and consisting of 4 contiguous pixels. From these 16 possibilities, let us consider the one obtained by deleting the three top rows and the three left columns from Figure 1. Let A_3 be the remaining (scaled) sub-region. Averaging the 4 rain rates of each snapshot over A_3 we obtain a new time series $\{ R_t(A_3) \ ; \ t = 1,2,...,2996 \}$, depicted in Figure 2(d).

Finally, scaling A_0 by a factor $\lambda_4 = \frac{1}{5}$ leads to 25 possibilities, each one being one individual pixel of size 2×2 km^2 . The time series of the bottom-right pixel of Figure1, $\{ R_t(A_4) \ ; \ t = 1,2,...,2996 \}$, is depicted in Figure 2(e) .

https://doi.org/10.26219/heal.aueb.5641

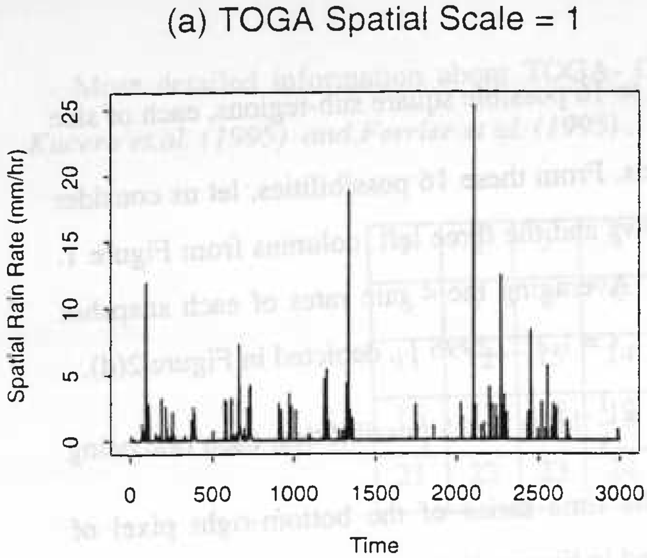

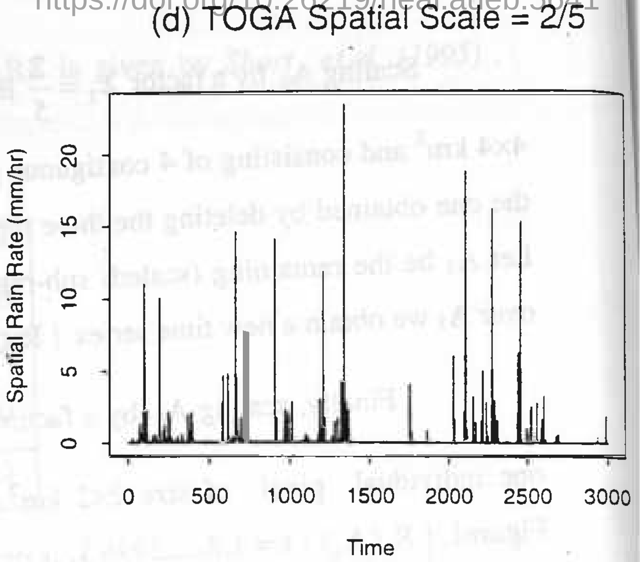

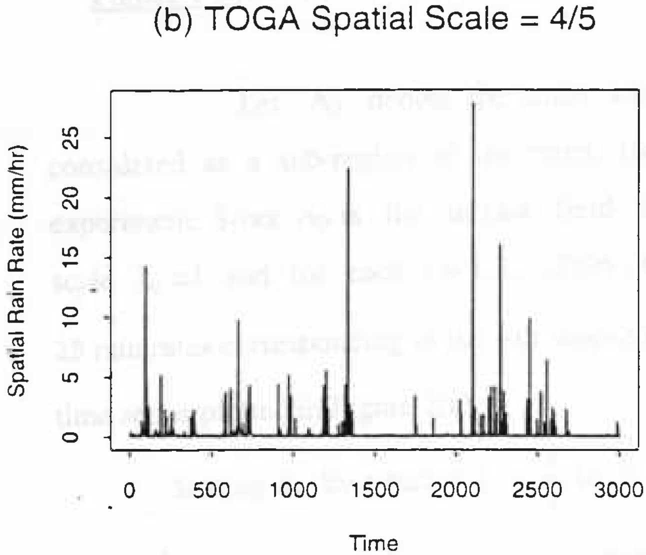

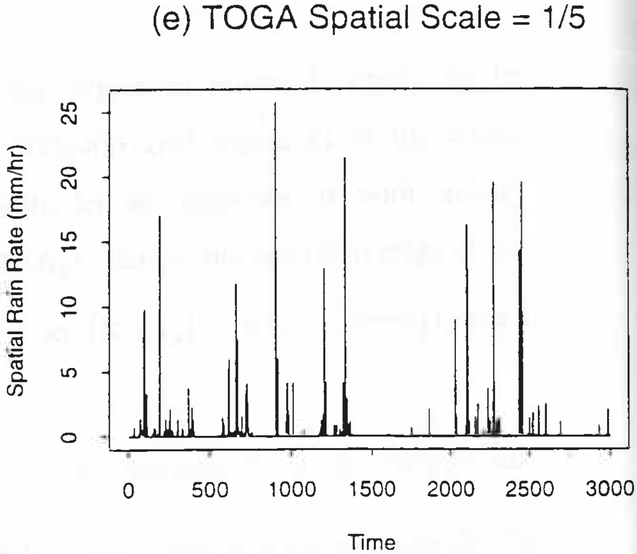

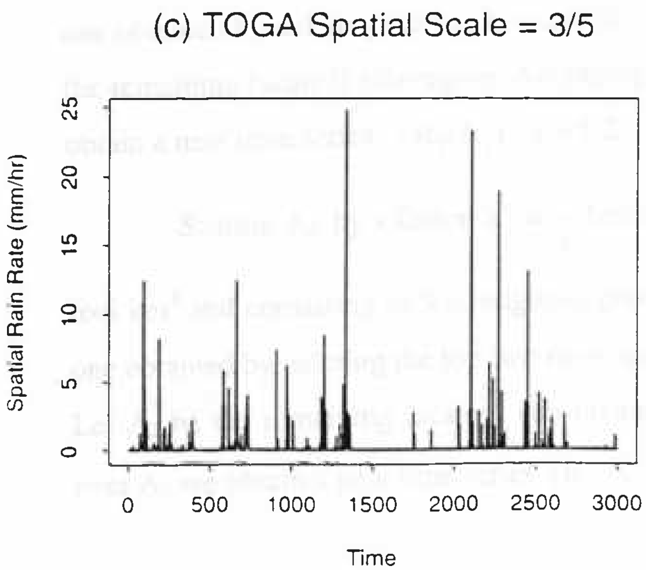

Figure 2:
Plots of the time series
$\{R_t(A_i)\}_{t=1}^{2996}$, i=0,1,2,3,4 .

https://doi.org/10.26219/heal.aueb.5641

Table 1 summarizes some numeric characteristics of the averaged time series: total of observations, sample mean , standard error of the sample mean, sample standard deviation , minimum and maximum observation.

λ	OBSERV	MEAN	ST.ER.M	ST.DEV	MIN	MAX
1	2996	0.211209	0.018	0.985186	0	25.34
4/5	2996	0.212849	0.0195	1.071691	0	27.89
3/5	2996	0.212445	0.02059	1.127126	0	24.75
2/5	2996	0.199889	0.020483	1.121181	0	23.38
1/5	2996	0.193763	0.022098	1.209599	0	25.70

Table 1 : Statistics of the time series $\{R_t(A_i)\}_{t=1}^{2996}$, for i =0,1,2,3,4 .

https://doi.org/10.26219/heal.aueb.5641

5.2 Multi-scaling of Spectral Moments

For each one of the time series $\{R_t(A_i)\}_{t=1}^{N}$, where N=2996 and i=0,1,2,3,4 , defined in the previous sub-section, the raw and the smoothed periodogram are utilized in order to estimate the corresponding spectral density functions $g_{\lambda_i}(\omega)$ and their spectral moments $s_{\lambda_i}(h)$. The so called raw periodogram estimate of the spectral density $g_{\lambda_i}(\omega)$, is given by the finite Fourier transform of the time series $\{R_t(A_i)\}_{t=1}^{N}$:

$$\hat{g}_{\lambda_i}(\omega_v) = \frac{1}{2\pi N}\cdot\left\{\left[\sum_{t=1}^{N} R_t(A_i)\cos(t\omega_v)\right]^2 + \left[\sum_{t=1}^{N} R_t(A_i)\sin(t\omega_v)\right]^2\right\} \qquad (18),$$

evaluated at the Fourier frequencies $\omega_v = \frac{2\pi v}{N}$, for each $v = 1,2,\ldots,\left[\frac{N}{2}\right]$.

A well known fact from the statistical theory of spectral analysis of stationary time series, is that for large time series ($N\to\infty$), the raw periodogram provides an asymptotically unbiased estimator of the spectral density. However, in general, the raw periodogram is not a consistent estimator of the spectral density function *(Koopmans 1974).* An also well known technique by which the raw periodogram may be modified , so as to become a consistent and asymptotically unbiased estimator of the spectral density, is its smoothing via weighted averaging of its values, over a neighborhood of Fourier frequencies, containing the Fourier frequency at which the smoothed periodogram value is estimated. Among the many different ways in which the weights and the length of the smoothing window may be chosen, the simplest and most basic one is the symmetric moving average smoothing suggested by Daniell. According to this kind of smoothing, the smoothed periodogram estimate at a Fourier frequency ω_v is calculated as follows:

$$\tilde{g}_{\lambda_i}(\omega_v) = \frac{1}{n}\cdot\sum_{k=v-\left[\frac{n-1}{2}\right]}^{v+\left[\frac{n}{2}\right]} \hat{g}_{\lambda_i}(\omega_k) \qquad (19).$$

Clearly, the uniform weights $\frac{1}{n}$, and the length of the moving average, are determined by the integer n in (19). According to a well established theory, see *Koopmans (1974)*, in order for the smoothed periodogram estimator to be consistent, n must tend to infinity along with

https://doi.org/10.26219/heal.aueb.5641

N, in such a manner that the bandwidth $\frac{2\pi n}{N}$ of the smoothing window tends to zero. (i.e. $n = o(N)$).

Figure 3 depicts the raw periodogram estimate corresponding to the spectral density function of each one of the time series $\{R_t(A_i)\ ;\ t = 1,2,...2996\}$, for i=0,1,2,3,4. Figure 4 depicts the Daniell smoothed periodogram estimate corresponding to the spectral density function of each one of the above time series. The bandwidth used in the smoothing is $n = [\sqrt{N}] + 1 = 55$ for every time series.

Provided, under assumption (A3), that a spectral moment $s_{\lambda_i}(h) := \int_0^{\pi} \omega^h \cdot g_{\lambda_i}(\omega)\, d\omega$, of order h≥1 exists, one may employ either the raw or the smoothed periodogram estimate of the spectral density $g_{\lambda_i}(\omega)$, and to estimate the above spectral moment via the following Riemann sum approximations, where $\Delta(\omega_v) = \omega_{v+1} - \omega_v = \frac{2\pi(v+1)}{N} - \frac{2\pi v}{N} = \frac{2\pi}{N}$,

$$\hat{s}_{\lambda_i}(h) := \sum_{v=1}^{\left[\frac{N}{2}\right]} \omega_v^h \cdot \hat{g}_{\lambda_i}(\omega_v) \cdot \Delta(\omega_v) = \frac{2\pi}{N} \cdot \sum_{v=1}^{\left[\frac{N}{2}\right]} \omega_v^h \cdot \hat{g}_{\lambda_i}(\omega_v) \qquad (20)$$

$$\tilde{s}_{\lambda_i}(h) := \sum_{v=1}^{\left[\frac{N}{2}\right]} \omega_v^h \cdot \tilde{g}_{\lambda_i}(\omega_v) \cdot \Delta(\omega_v) = \frac{2\pi}{N} \cdot \sum_{v=1}^{\left[\frac{N}{2}\right]} \omega_v^h \cdot \tilde{g}_{\lambda_i}(\omega_v) \qquad (21)$$

Figure 5 shows the growth of the estimated spectral moments $\hat{s}_{\lambda_i}(h)$, for h=1,2,3,4,5,6,7,8, for each of the five time series corresponding to i=0,1,2,3,4 , and the values of $\log \hat{s}_{\lambda_i}(h)$ are given in Table 2.

For each value of the moment's order h=1,2,3,4,5,6,7,8, linear regressions of $\log s_{\lambda_i}(h)$ on $\log \lambda_i$ yield excellent fits whose information is summarized in Table 3. This information includes estimates of the slope and intercept of the best fitting straight line, together with the corresponding correlation coefficient and the sum of squared residuals. Figure 6 depicts the best fitting lines obtained from these linear regressions, and Figure 7 shows the plot of their slopes a(h) versus the spectral moment's order h=1,2,3,4,5,6,7,8.

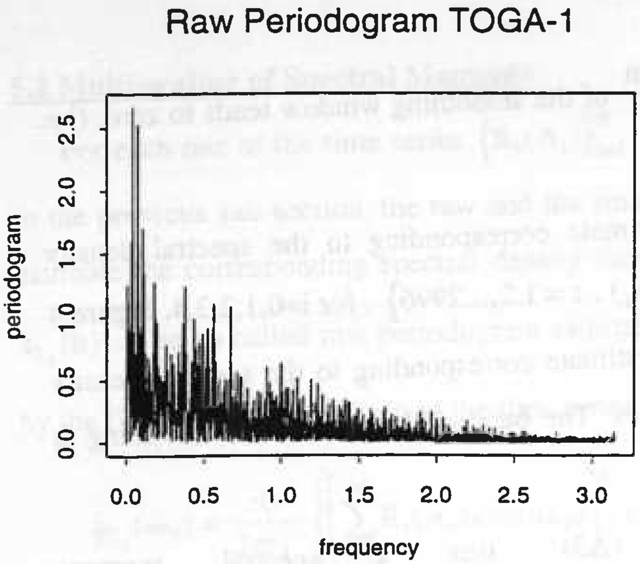

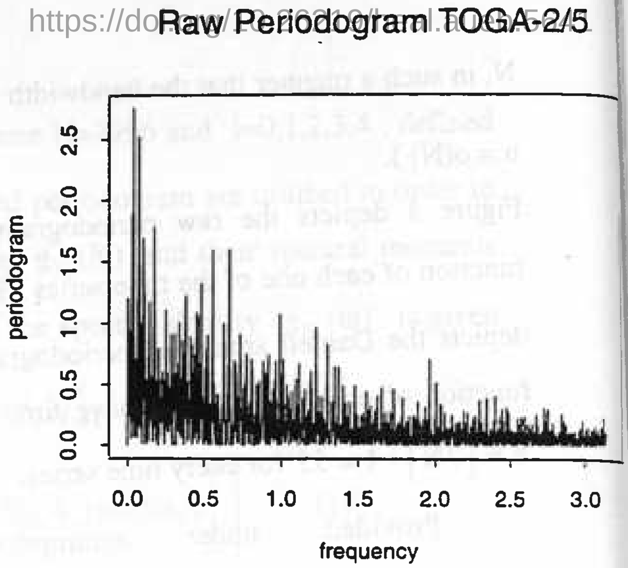

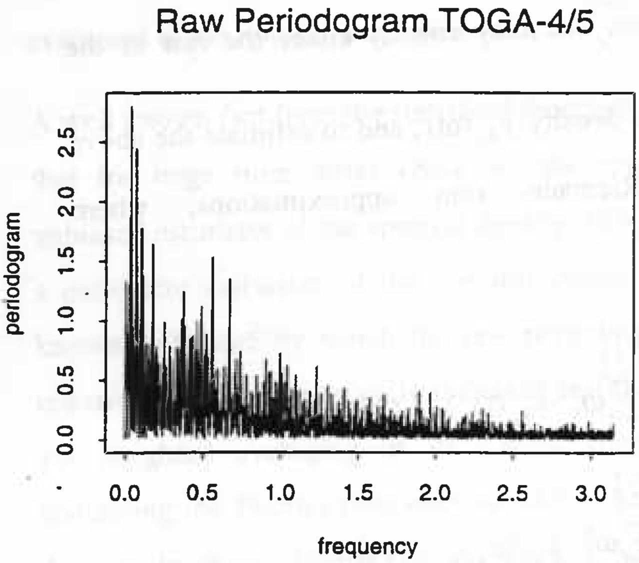

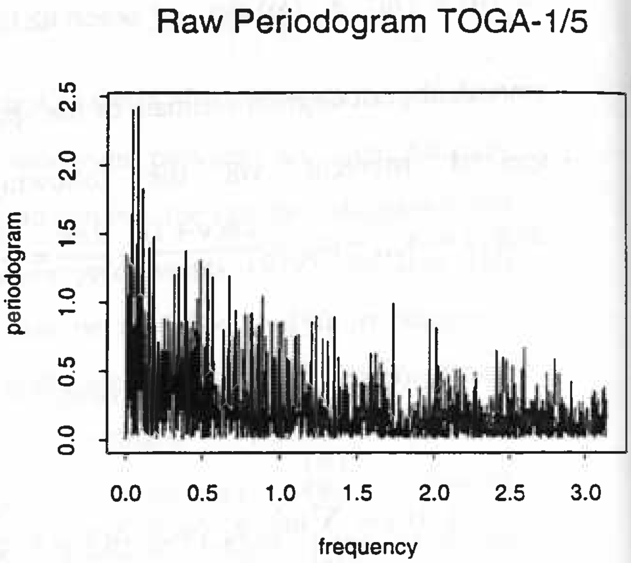

Figure 3:
Plots of the raw periodograms $\hat{g}_{\lambda}(\omega)$, for λ=1,4/5, 3/5, 2/5,1/5.

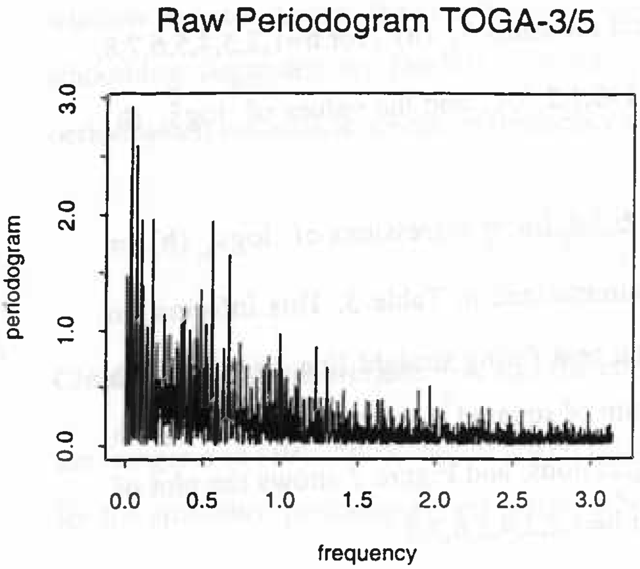

https://doi.org/10.26219/heal.aueb.5641

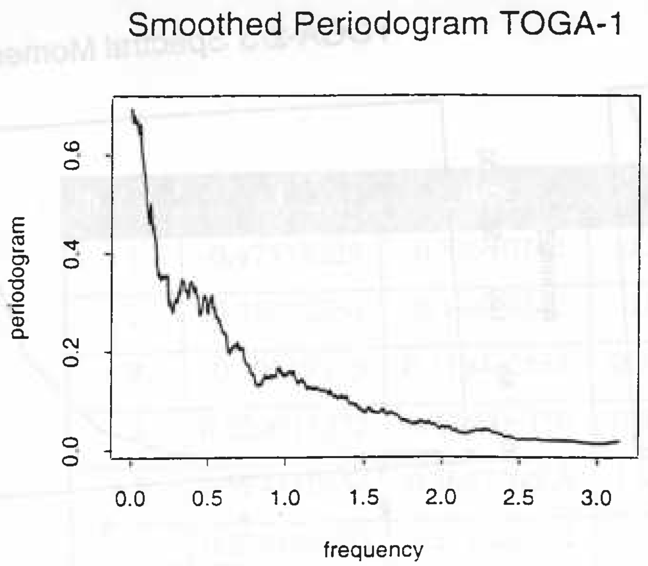

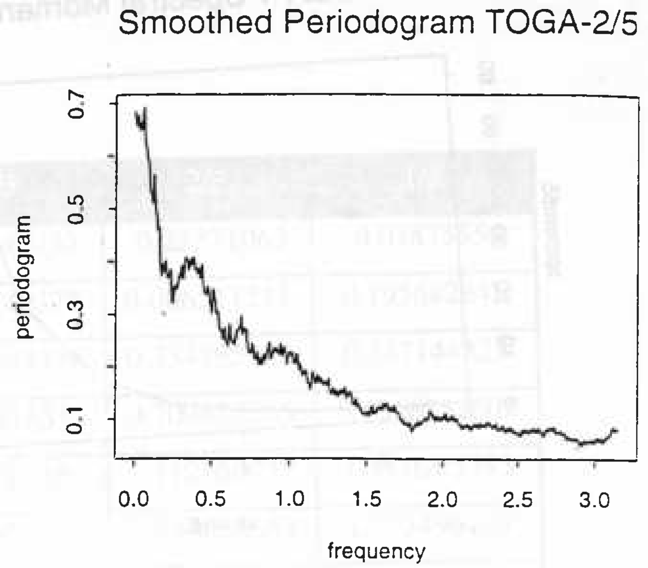

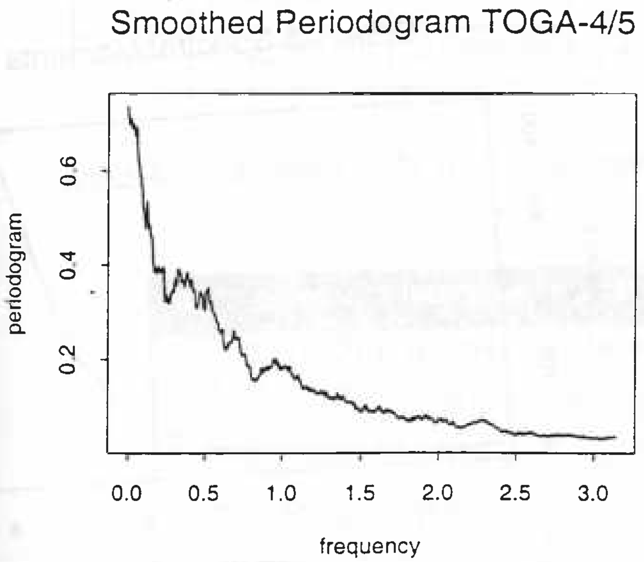

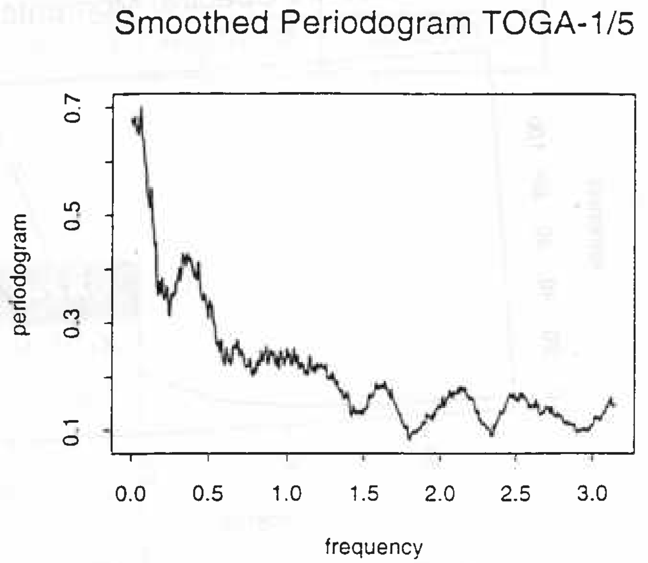

Figure 4:
Plots of the smoothed periodograms $\tilde{g}_{\lambda}(\omega)$, for λ=1,4/5, 3/5, 2/5,1/5 , and bandwidth n=55

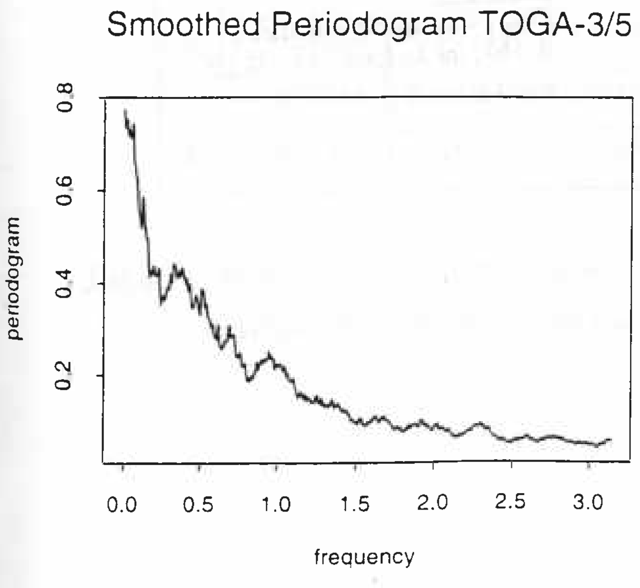

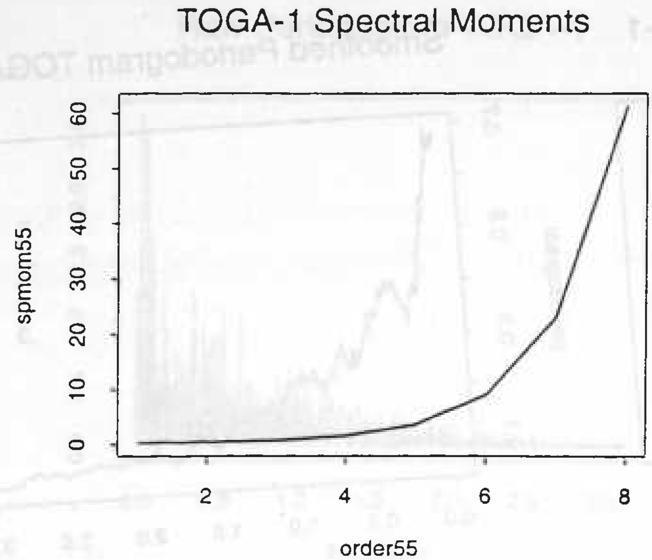

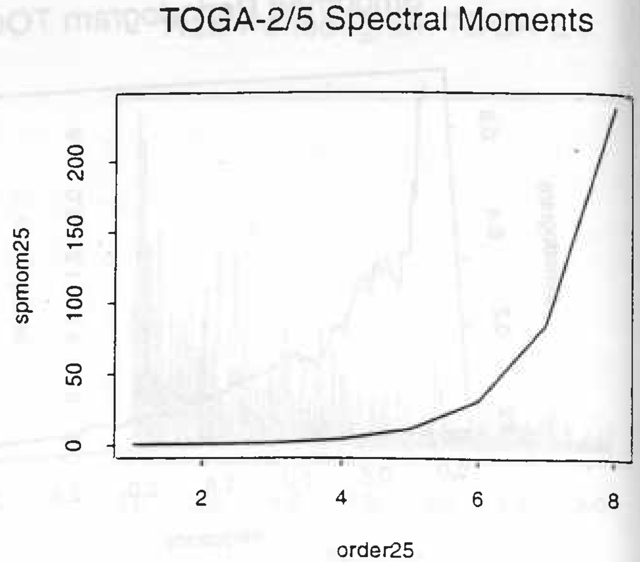

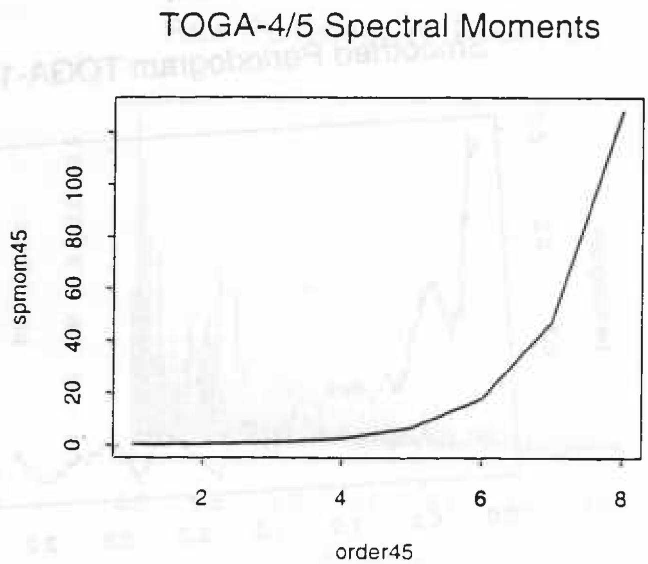

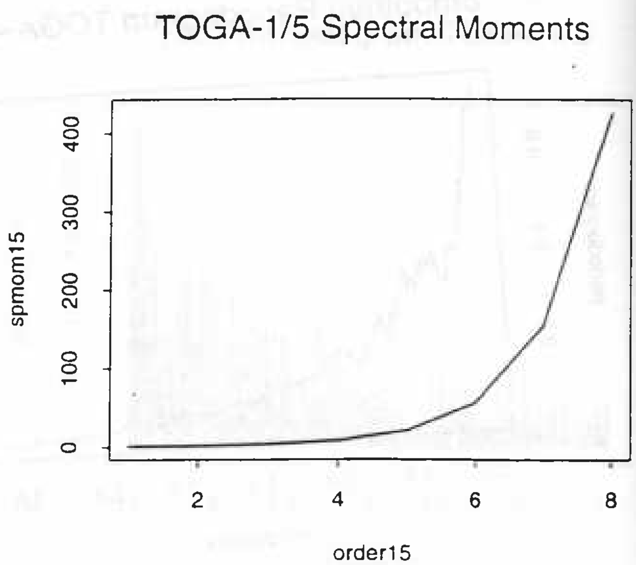

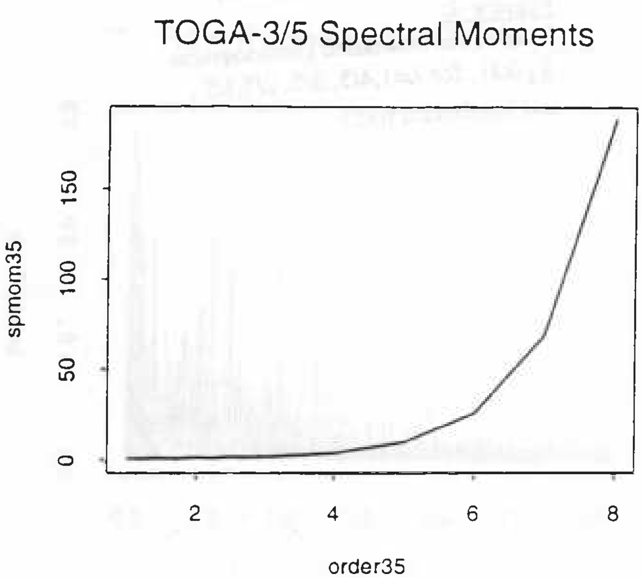

Figure 5:
Plots of the spectral moments $\hat{s}_{\lambda}(h)$, for λ=1,4/5, 3/5, 2/5,1/5, and $1 \leq h \leq 8$.

https://doi.org/10.26219/heal.aueb.5641

h / λ	1	4/5	3/5	2/5	1/5
1	-0.47572229	-0.34910742	-0.26940232	-0.22371063	-0.07875554
2	-0.35272564	-0.17479542	-0.06740878	0.006511211	0.195682843
3	-0.10149315	0.119442688	0.246944146	0.334295122	0.547144323
4	0.220015272	0.474006150	0.615916513	0.709833585	0.9366332601
5	0.584150154	0.862726608	1.015061561	1.112566227	1.34764 5383
6	0.976146253	1.272882172	1.432871185	1.532622689	1.773496129
7	1.387408299	1.697619271	1.863307747	1.964663182	2.209671911
8	1.812587470	2.132889851	2.302874023	2.405507788	2.653599713

Table 2 : Logarithms of the spectral moments $\hat{s}_{\lambda_i}(h)$.

h	slope	intercept	R	S.S.Res
1	-0.517829	-0.425955	0.96986	0.00516
2	-0.717657	-0.281740	0.96939	0.01007
3	-0.844308	-0.009785	0.96375	0.01665
4	-0.927282	0.328676	0.95827	0.02332
5	-0.984143	0.705786	0.95391	0.02920
6	-1.024628	1.107497	0.95067	0.03406
7	-1.054366	1.526008	0.94832	0.03793
8	-1.076794	1.956615	0.94663	0.04096

Table 3 : Slope , Intercept , Correlation Coefficient and Sums of Squared Residuals for the regression lines fitted in Figures 6.

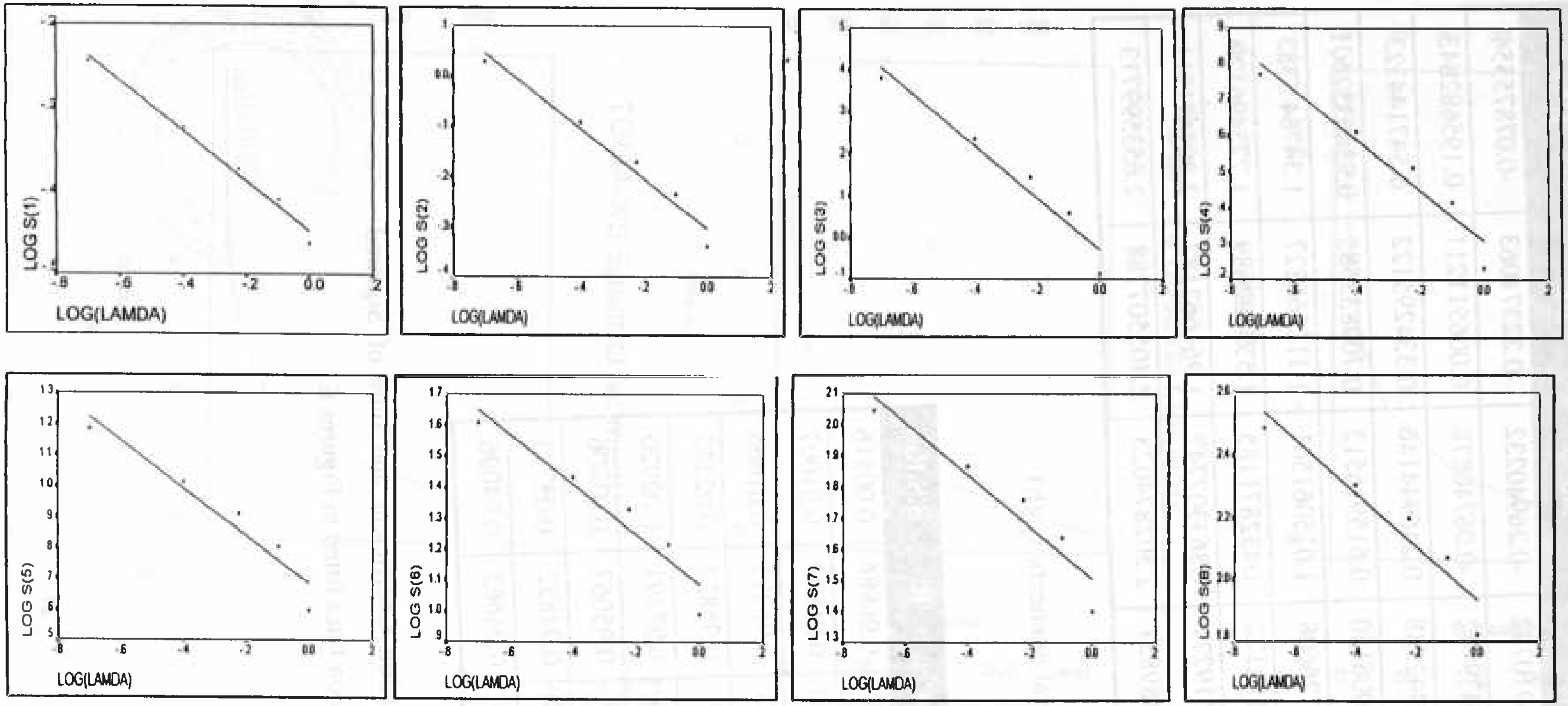

Figure 6:

Plots of log $\hat{s}_{\lambda}(h)$ versus logλ, including best fitting straight lines, for $1 \leq h \leq 8$.

https://doi.org/10.26219/heal.aueb.5641

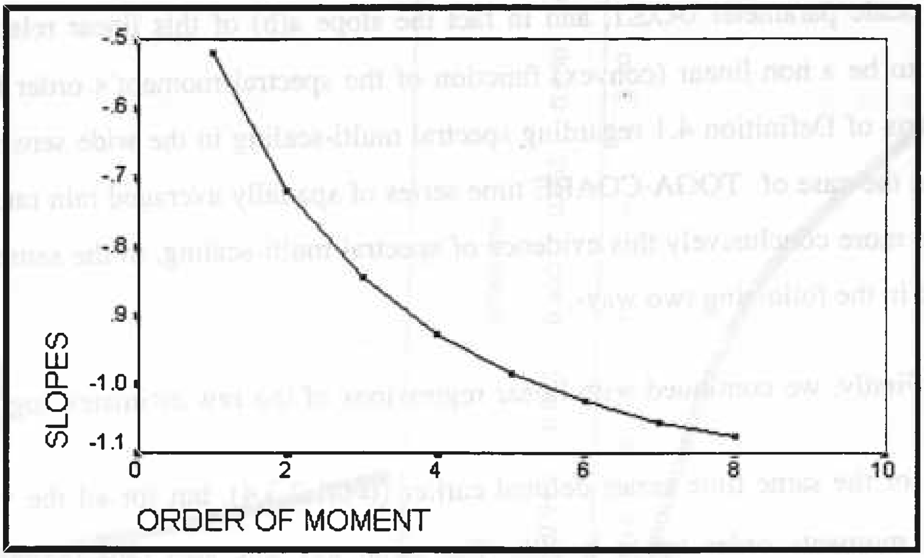

Figure 7: Plot of the slopes a(h) in Table 3 versus the order h of the spectral moment.

This preliminary analysis of TOGA-COARE data does indicate quite clearly that the spectral moments $s_\lambda(h)$ do conform to a log-log linear relationship with respect to the spatial scale parameter $0<\lambda\leq 1$, and in fact the slope a(h) of this linear relationship does appear to be a non-linear (convex) function of the spectral moment's order $h\geq 1$. That is, both parts of Definition 4.1 regarding spectral multi-scaling in the wide sense, do seem to apply in the case of TOGA-COARE time series of spatially averaged rain rate. In order to confirm more conclusively this evidence of spectral multi-scaling, in the sense of (11), we proceed in the following two ways.

Firstly, we continued with linear regressions of the raw estimates $\log\left\{\frac{\hat{s}_{\lambda_i}(h)}{\hat{s}_{\lambda_0}(h)}\right\}$ on $\log\lambda_i$, for the same time series defined earlier (i=0,1,2,3,4), but for all the values of the spectral moments order up to h=200. The same job was also repeated for the linear regressions of the smoothed estimates $\log\left\{\frac{\tilde{s}_{\lambda_i}(h)}{\tilde{s}_{\lambda_0}(h)}\right\}$ on $\log\lambda_i$, again for $1\leq h\leq 200$.

For each case, raw and smoothed , Figures 8 and 9 respectively show the plots of the estimated slope a(h) of the best fitting straight line, the plots of the corresponding squared correlation coefficients, and the plots of the corresponding sums of squared residuals, all versus the values of the spectral moments order h.

The behavior of all three plots is almost identical, comparing between the raw and the smoothed case. In particular, the slope function a(h) is indeed a negative-valued non-linear convex function, there is a quite high lower bound very close to 0.94 for the squared correlation, and a satisfactorily low-valued sum of squared residuals.

https://doi.org/10.26219/heal.aueb.5641

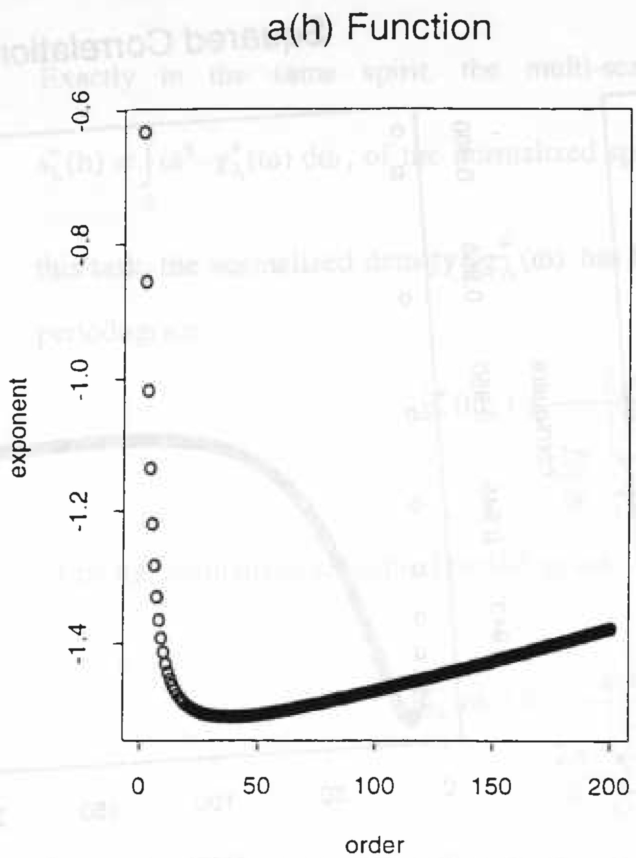

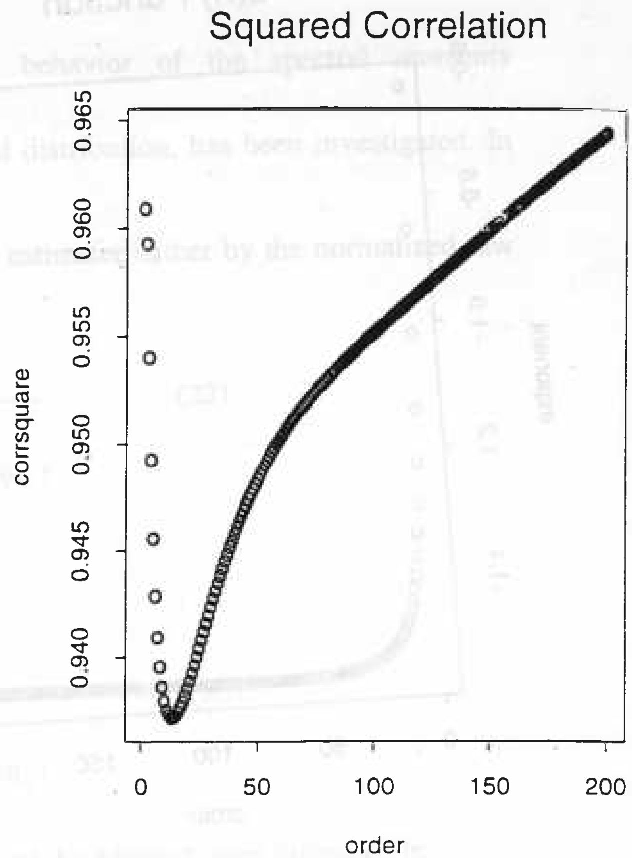

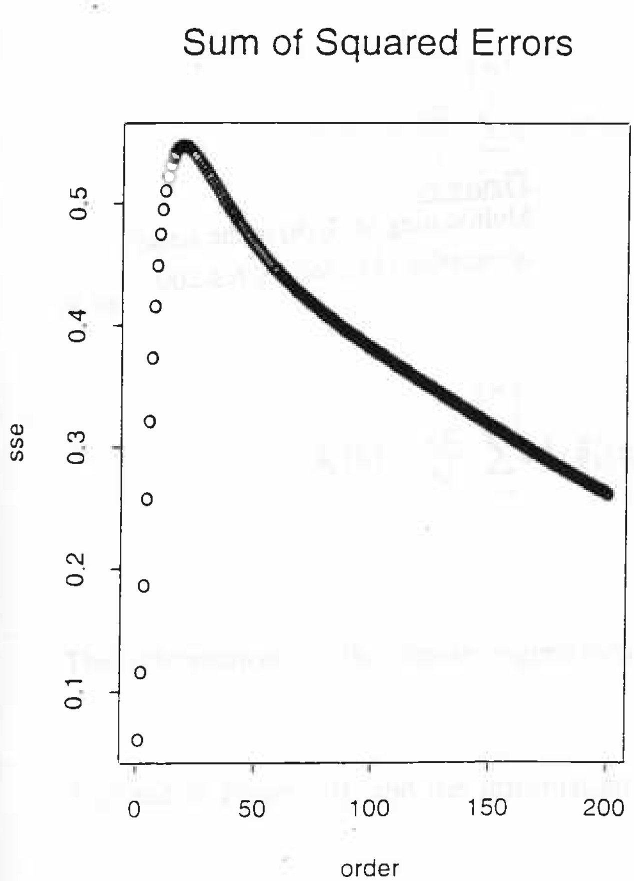

Figure 8:
Multi-scaling of $\hat{s}_{\lambda}(h)$, in the sense of equation (11), for $1 \leq h \leq 200$.

https://doi.org/10.26219/heal.aueb.5641

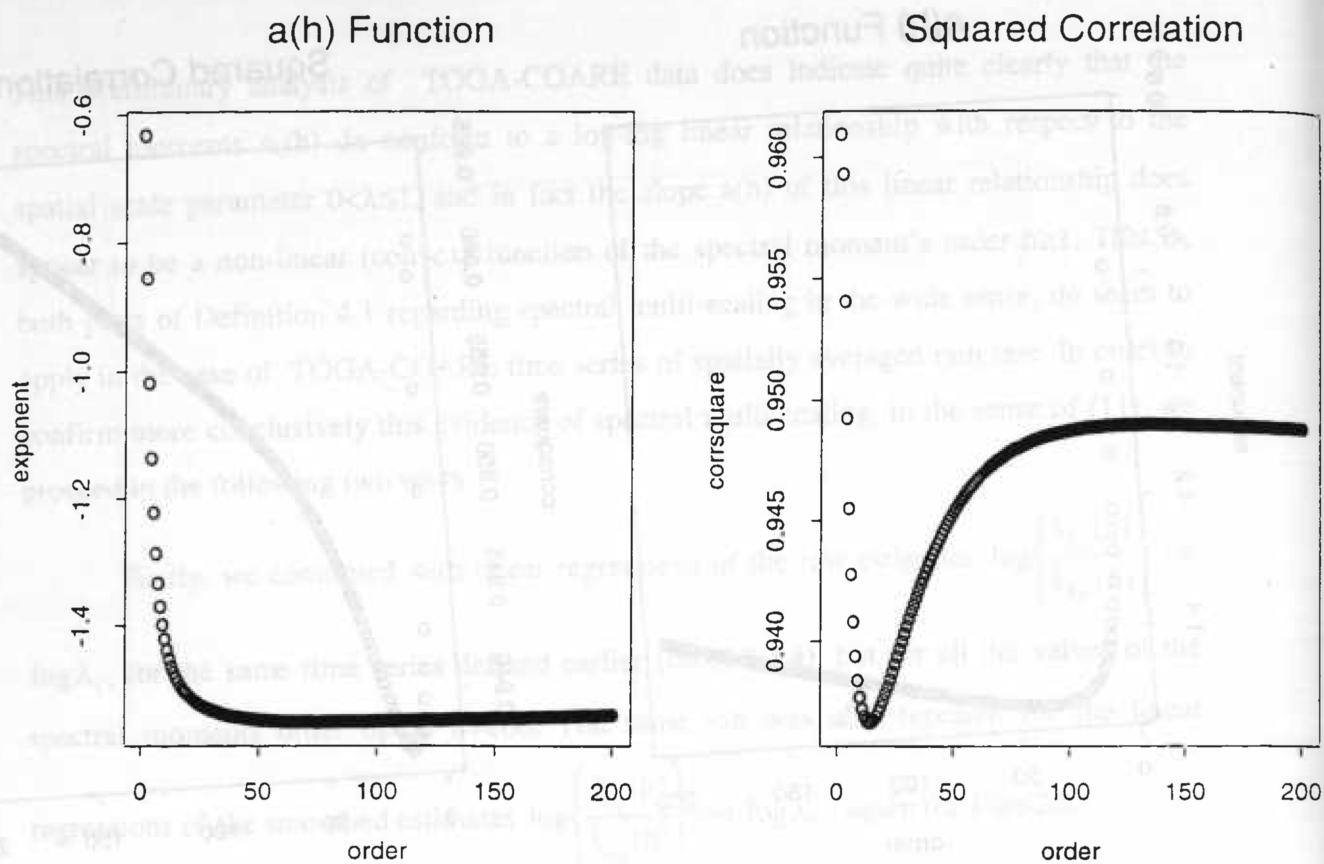

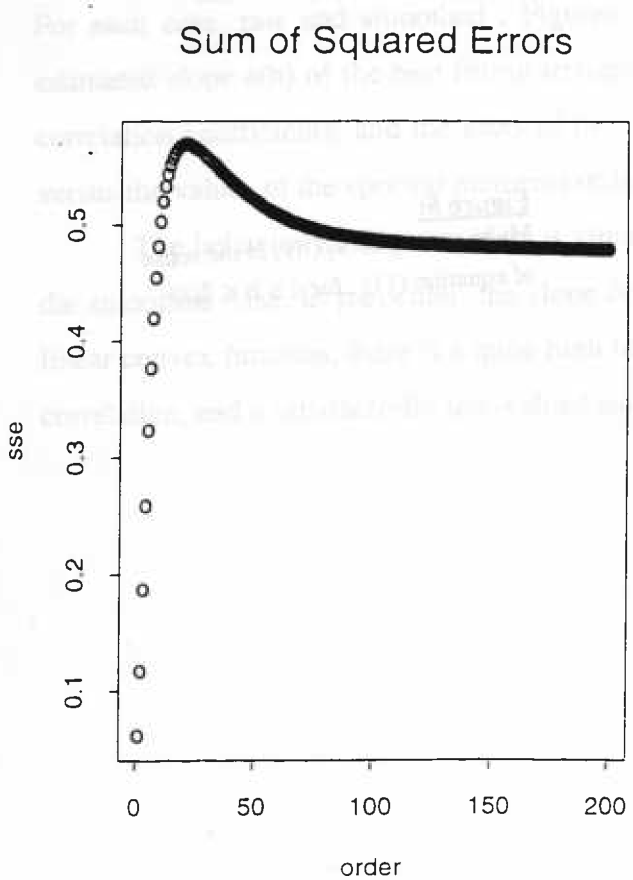

Figure 9:
Multiscaling of $\tilde{S}_\lambda(h)$ in the sense of equation (11), for $1 \leq h \leq 200$.

https://doi.org/10.26219/heal.aueb.5641

Exactly in the same spirit, the multi-scaling behavior of the spectral moments $s_\lambda^*(h)=\int_0^\pi \omega^h \cdot g_\lambda^*(\omega)\,d\omega$, of the normalized spectral distribution, has been investigated. In this task, the normalized density $g_\lambda^*(\omega)$ has been estimated either by the normalized raw periodogram

$$\hat{g}_\lambda^*(\omega_v)=\frac{\hat{g}_\lambda(\omega_v)}{\frac{2\pi}{N}\cdot\sum_{k=1}^{\left[\frac{N}{2}\right]}\hat{g}_\lambda(\omega_k)} \qquad (22)$$

or by the normalized smoothed periodogram

$$\tilde{g}_\lambda^*(\omega_v)=\frac{\tilde{g}_\lambda(\omega_v)}{\frac{2\pi}{N}\cdot\sum_{k=1}^{\left[\frac{N}{2}\right]}\tilde{g}_\lambda(\omega_k)} \qquad (23)$$

Correspondingly, moments of the normalized spectral distribution were estimated by

$$\hat{s}_\lambda^*(h)=\frac{2\pi}{N}\cdot\sum_{v=1}^{\left[\frac{N}{2}\right]}\omega_v^h\cdot\hat{g}_\lambda^*(\omega_v)=\frac{\sum_{v=1}^{\left[\frac{N}{2}\right]}\omega_v^h\cdot\hat{g}_\lambda(\omega_v)}{\sum_{v=1}^{\left[\frac{N}{2}\right]}\hat{g}_\lambda(\omega_v)} \qquad (24)$$

or by

$$\tilde{s}_\lambda^*(h)=\frac{2\pi}{N}\cdot\sum_{v=1}^{\left[\frac{N}{2}\right]}\omega_v^h\cdot\tilde{g}_\lambda^*(\omega_v)=\frac{\sum_{v=1}^{\left[\frac{N}{2}\right]}\omega_v^h\cdot\tilde{g}_\lambda(\omega_v)}{\sum_{v=1}^{\left[\frac{N}{2}\right]}\tilde{g}_\lambda(\omega_v)} \qquad (25)$$

The information of the linear regressions of $\log\left\{\frac{\hat{s}_{\lambda_i}^*(h)}{\hat{s}_{\lambda_0}^*(h)}\right\}$ on $\log\lambda_i$ for $1\le h\le 200$ is depicted in Figure 10, and the information of the linear regressions of $\log\left\{\frac{\tilde{s}_{\lambda_i}^*(h)}{\tilde{s}_{\lambda_0}^*(h)}\right\}$ on

https://doi.org/10.26219/heal.aueb.5641

$\log\lambda_i$ is depicted in Figure 11.

Figures 10 and 11 are strikingly similar to Figures 8 and 9, respectively, and the conclusion to be drawn is that the spectral moments $s^*_\lambda(h)$ of the normalized spectral distribution do comply to the same multi-scaling behavior as the "non-normalized" moments $s_\lambda(h)$, in accord with Definition 4.1 .

https://doi.org/10.26219/heal.aueb.5641

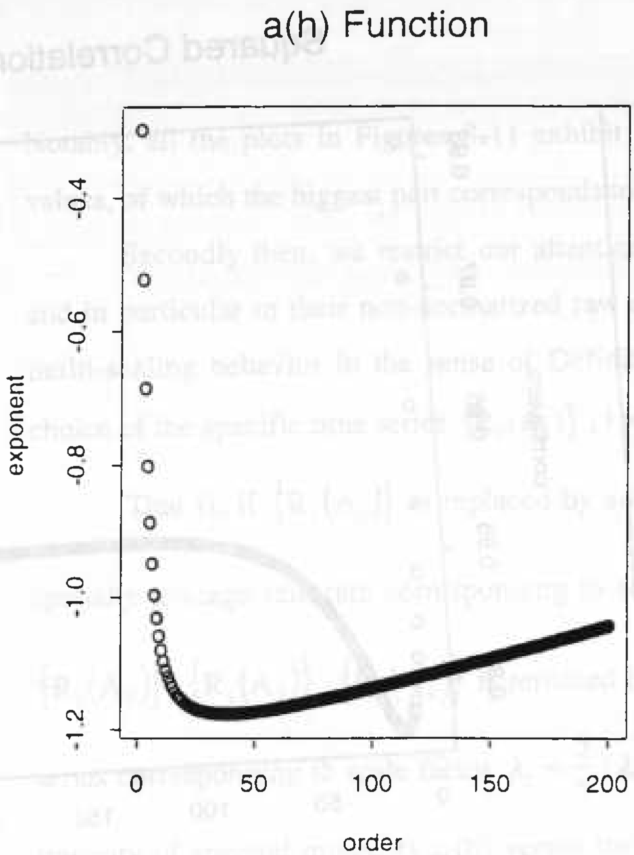

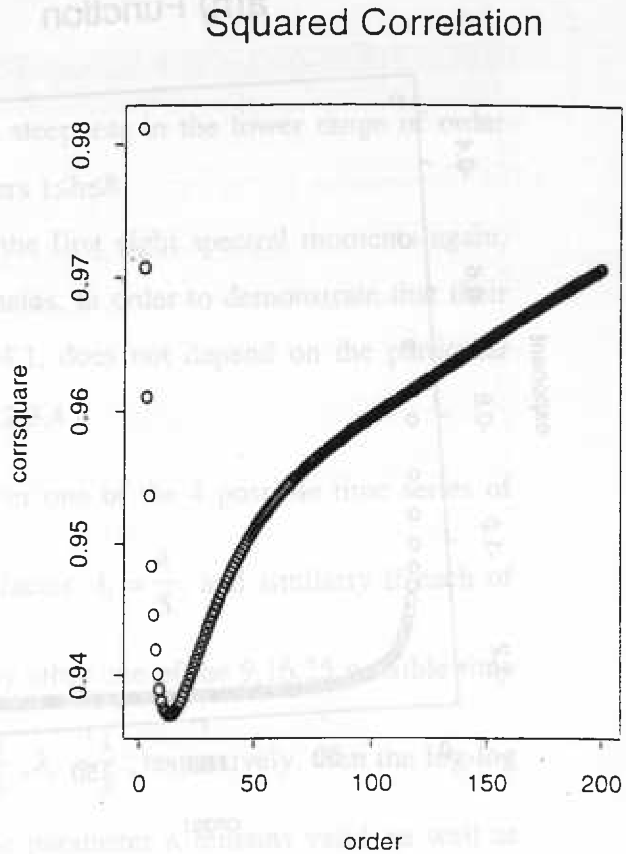

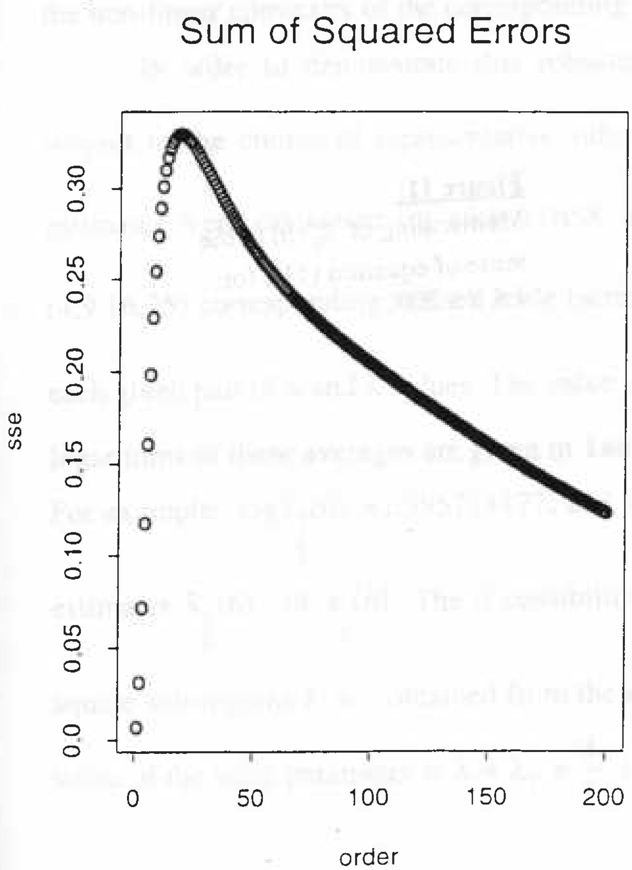

Figure 10:
Multiscaling of $\hat{s}^{*}_{\lambda}(h)$ in the sense of equation (11), for $1 \leq h \leq 200$.

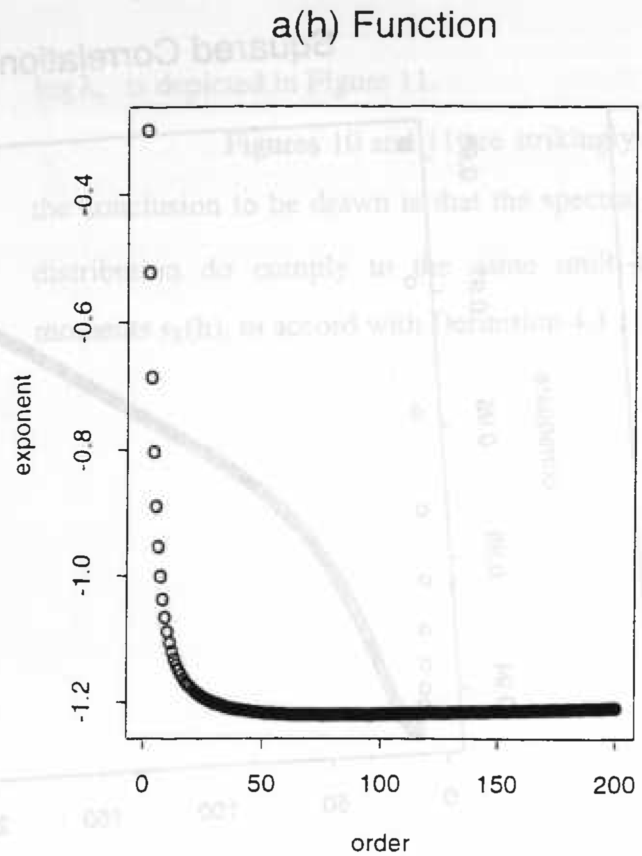

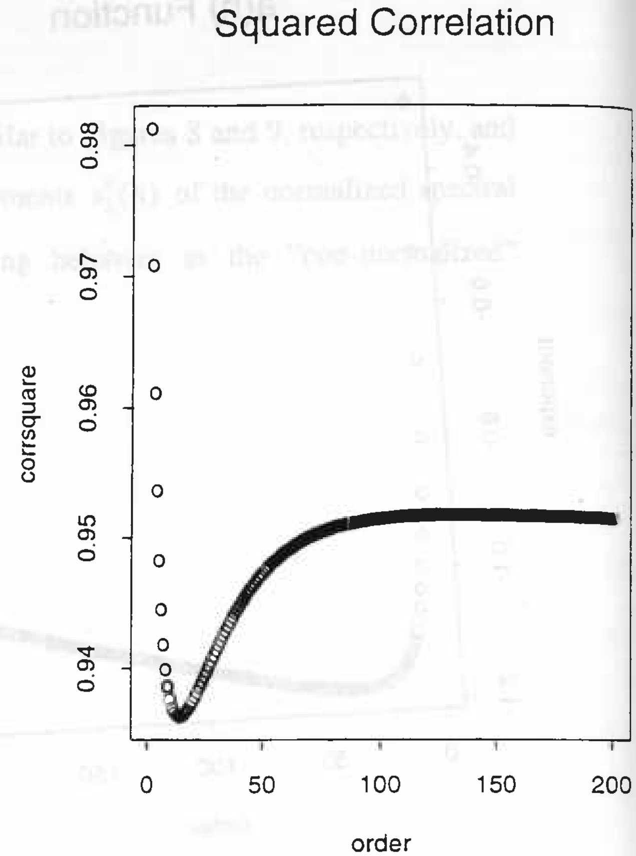

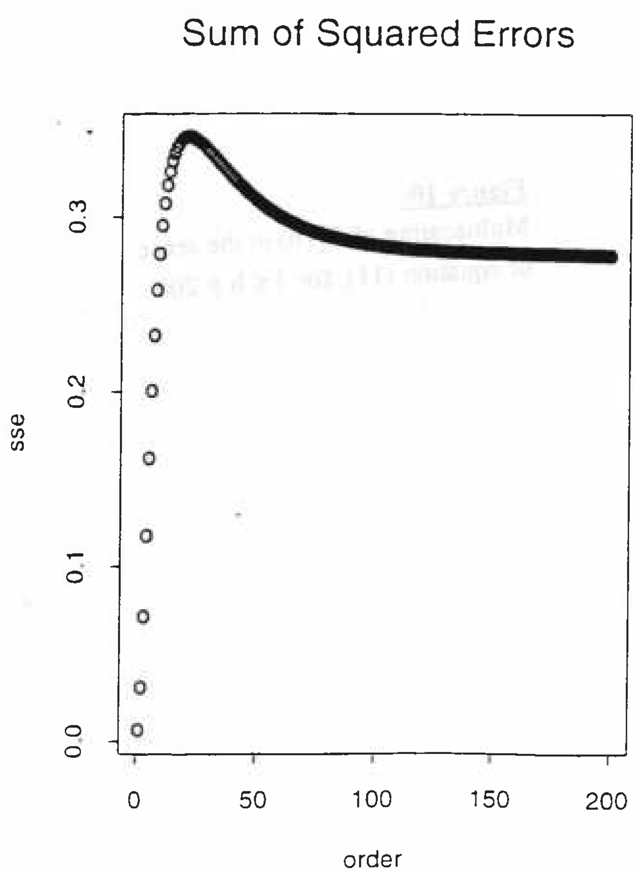

Figure 11:
Multiscaling of $\tilde{s}_{\lambda}^{*}(h)$ in the sense of equation (11), for $1 \leq h \leq 200$.

https://doi.org/10.26219/heal.aueb.5641

Notably, all the plots in Figures 8-11 exhibit high steepness in the lower range of order values, of which the biggest part corresponds to orders $1 \le h \le 8$.

Secondly then, we restrict our attention to the first eight spectral moments again, and in particular to their non-normalized raw estimates, in order to demonstrate that their multi-scaling behavior in the sense of Definition 4.1, does not depend on the particular choice of the specific time series $\{R_t(A_i)\}$, $i = 0,1,2,3,4$.

That is, if $\{R_t(A_1)\}$ is replaced by any other one of the 4 possible time series of spatially average rain-rate corresponding to scale factor $\lambda_1 = \frac{4}{5}$, and similarly if each of $\{R_t(A_2)\}$, $\{R_t(A_3)\}$, $\{R_t(A_4)\}$ is replaced by any other one of the 9,16,25 possible time series corresponding to scale factor $\lambda_2 = \frac{3}{5}, \lambda_3 = \frac{2}{5}, \lambda_4 = \frac{1}{5}$, respectively, then the log-log linearity of spectral moments $s_\lambda(h)$ versus the scale parameter λ remains valid, as well as the non-linear convexity of the corresponding slope function a(h).

In order to demonstrate this robustness of spectral multi-scaling behavior, with respect to the choice of representative sub-region of scale $\lambda = \frac{4}{5}, \frac{3}{5}, \frac{2}{5}, \frac{1}{5}$, the $\hat{s}_\lambda(h)$ estimates were calculated for each $1 \le h \le 8$, and for each one of the possible time series (4,9,16,25) corresponding to each scale factor $\left(\frac{4}{5}, \frac{3}{5}, \frac{2}{5}, \frac{1}{5}\right)$, and then were averaged for each given pair of h and λ values. The value of each such average is denoted by $\bar{s}_\lambda(h)$. The logarithms of these averages are given in Table 4.

For example, $\log \bar{s}_{\frac{3}{5}}(6)$ =1.395714177, and $\bar{s}_{\frac{3}{5}}(6)$ is the arithmetic mean of the 9 possible estimates $\hat{s}_{\frac{3}{5}}(6)$ of $s_{\frac{3}{5}}(6)$. The 9 possibilities correspond one-to-one with the 9 different square sub-regions $\lambda \cdot A_0$, obtained from the scaling of the total square region A_0, when the value of the scale parameter is $\lambda = \lambda_2 = \frac{3}{5}$ (see sub-section 5.1).

https://doi.org/10.26219/heal.aueb.5641

Figure 12 shows the plots of the points with coordinates $(\log\lambda, \log\bar{s}_\lambda(h))$, for each $1 \le h \le 8$, and the best fitting straight line.

The information on the slope, intercept, correlation coefficient, and sum of squared residuals, regarding each one of these linear regressions, is summarized in Table 5.

Figure 13 shows the plot of the slopes a(h) (from Table 5) versus the spectral moments order $1 \le h \le 8$.

Thus, the above analysis shows indeed that in the case of TOGA-COARE like rain rate fields in space and in time, the multi-scaling behavior of the spectral moments in the sense of equation (8), is quite robust with respect to the choice of the time series of spatially averaged rain rate.

https://doi.org/10.26219/heal.aueb.5641

h \ λ	1	4/5	3/5	2/5	1/5
1	-0.4757229	-0.36175634	-0.24889940	-0.14258810	-0.00207401
2	-0.35272564	-0.19997638	-0.05928924	0.096708651	0.244038748
3	-0.10149315	0.080558111	0.240213065	0.391211601	0.578417563
4	0.220015272	0.423667634	0.596357012	0.758518120	0.957016956
5	0.584150154	0.803648838	0.985480174	1.155163440	1.361435506
6	0.976146253	1.207328104	1.395714177	1.570091211	1.782621568
7	1.387408299	1.627290588	1.820474419	1.991085073	2.215538741
8	1.812587470	2.059028963	2.255790588	2.437547920	2.657114974

Table 4 : Values of $\log \bar{s}_\lambda(h)$.

h	slope	intercept	R	S.S.Res
1	-0.656652	-0.432128	0.98154	0.00499
2	-0.831392	-0.289644	0.97377	0.01150
3	-0.933552	-0.026539	0.97489	0.01385
4	-1.008554	0.305559	0.97253	0.01775
5	-1.061069	0.677551	0.97082	0.02093
6	-1.098964	1.075347	0.96962	0.02342
7	-1.123926	1.490138	0.96972	0.02442
8	-1.148275	1.919299	0.96819	0.02684

Table 5 : Slopes , Intercepts , Correlation Coefficients and Sums of Squared Residuals for the regression lines fitted in Figures 12 .

https://doi.org/10.26219/heal.aueb.5641

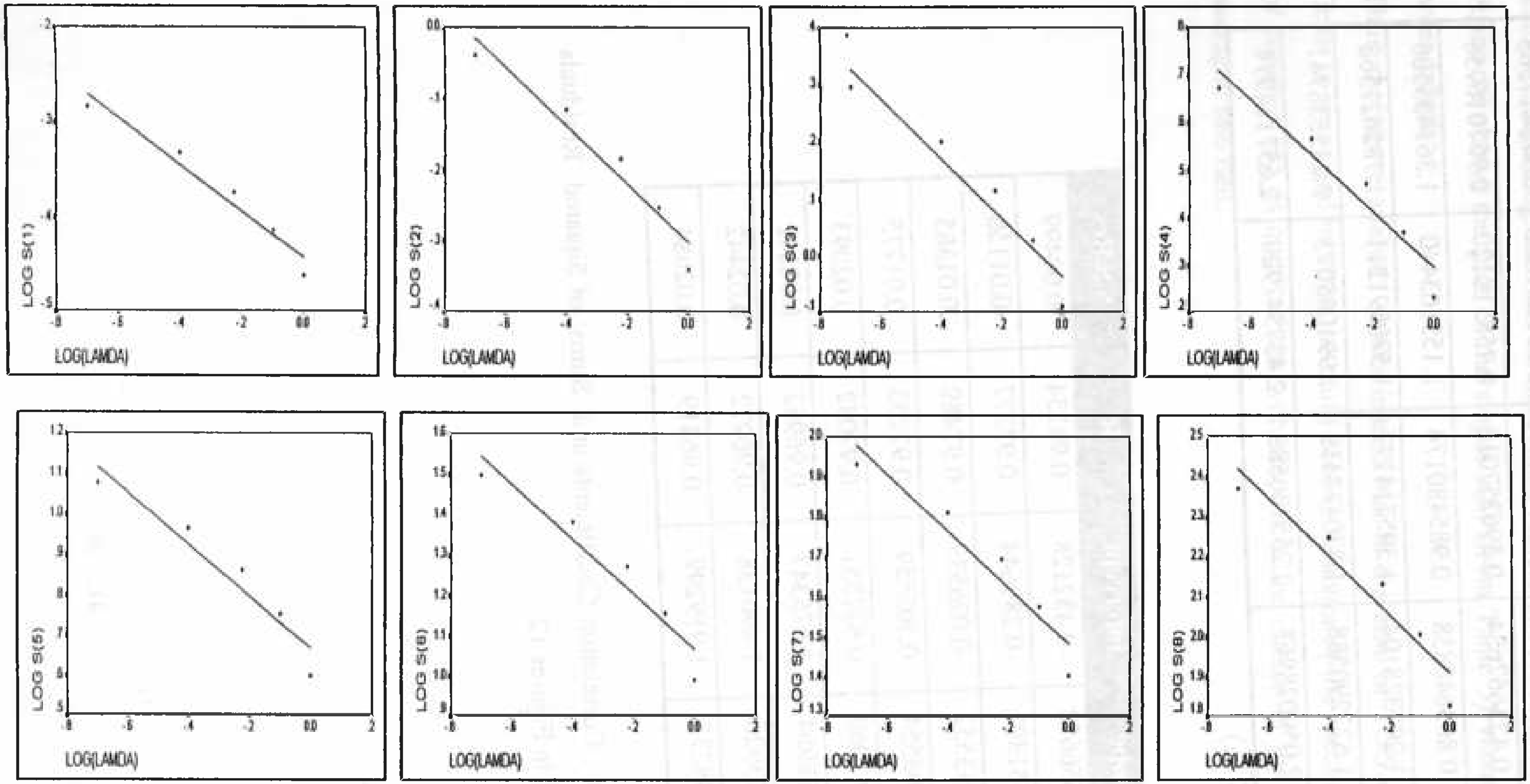

Figure 12:

Plots of $\log \bar{s}_{\lambda}(h)$ versus $\log\lambda$, including best fitting straight lines, for $1 \leq h \leq 8$.

https://doi.org/10.26219/heal.aueb.5641

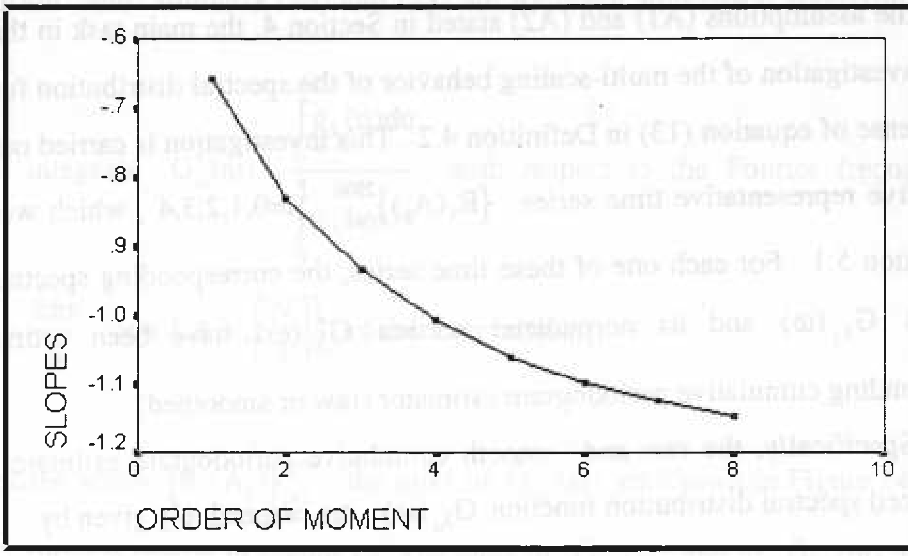

Figure 13 : Plot of the slopes a(h) in Table 5 versus the order h of the spectral moment.

https://doi.org/10.26219/heal.aueb.5641

5.3 Multi-scaling of Spectral Distribution Function

Under the assumptions (A1) and (A2) stated in Section 4, the main task in this sub-section is the investigation of the multi-scaling behavior of the spectral distribution function $G_\lambda(\omega)$, in the sense of equation (13) in Definition 4.2 . This investigation is carried out on the basis of the five representative time series $\{R_t(A_i)\}_{t=1}^{2996}$, i=0,1,2,3,4 , which were defined in sub-section 5.1 . For each one of these time series, the corresponding spectral distribution function $G_{\lambda_i}(\omega)$ and its normalized version $G^*_{\lambda_i}(\omega)$ have been estimated by the corresponding cumulative periodogram estimator (raw or smoothed).

Specifically, the raw and smooth cumulative periodogram estimates of the non-normalized spectral distribution function $G_{\lambda_i}(\omega)$, are respectively given by

$$\hat{G}_{\lambda_i}(\omega_v) = \frac{2\pi}{N}\cdot\sum_{k=1}^{v}\hat{g}_{\lambda_i}(\omega_k) \quad (26),$$

$$\tilde{G}_{\lambda_i}(\omega_v) = \frac{2\pi}{N}\cdot\sum_{k=1}^{v}\tilde{g}_{\lambda_i}(\omega_k) \quad (27).$$

Similarly, the raw and smooth cumulative periodogram estimates of the normalized spectral distribution function $G^*_{\lambda_i}(\omega)$ are respectively given by

$$\hat{G}^*_{\lambda_i}(\omega_v) = \frac{\sum_{k=1}^{v}\hat{g}_{\lambda_i}(\omega_k)}{\sum_{k=1}^{\left[\frac{N}{2}\right]}\hat{g}_{\lambda_i}(\omega_k)} \quad (28),$$

$$\tilde{G}^*_{\lambda_i}(\omega_v) = \frac{\sum_{k=1}^{v}\tilde{g}_{\lambda_i}(\omega_k)}{\sum_{k=1}^{\left[\frac{N}{2}\right]}\tilde{g}_{\lambda_i}(\omega_k)} \quad (29)$$

https://doi.org/10.26219/heal.aueb.5641

Clearly, (26) and (27) are Riemann sum based approximations of the integral $G_{\lambda}(\omega)=\int_{0}^{\omega} g_{\lambda}(u)du$, and similarly (28) and (29) are Riemann sum based approximations of the ratio of integrals $G^{*}_{\lambda}(\omega)=\frac{\int_{0}^{\omega} g_{\lambda}(u)du}{\int_{0}^{\pi} g_{\lambda}(u)du}$, with respect to the Fourier frequencies partition $\left\{\omega_{\nu}=\frac{2\pi\nu}{N},\ \nu=1,2,\ldots,\left[\frac{N}{2}\right]\right\}$ of the interval $(0,\pi]$.

For each of the time series $\{R_{t}(A_{i})\}_{t=1}^{2996}$ the plots of $\hat{G}_{\lambda_i}(\omega)$ are shown in Figure 14 , and the plots of $\hat{G}^{*}_{\lambda_i}(\omega)$ are shown in Figure 15. The plots of $\tilde{G}_{\lambda_i}(\omega)$ and of $\tilde{G}^{*}_{\lambda_i}(\omega)$ are not provided since they are utterly similar to those in Figures 14 and 15 respectively.

https://doi.org/10.26219/heal.aueb.5641

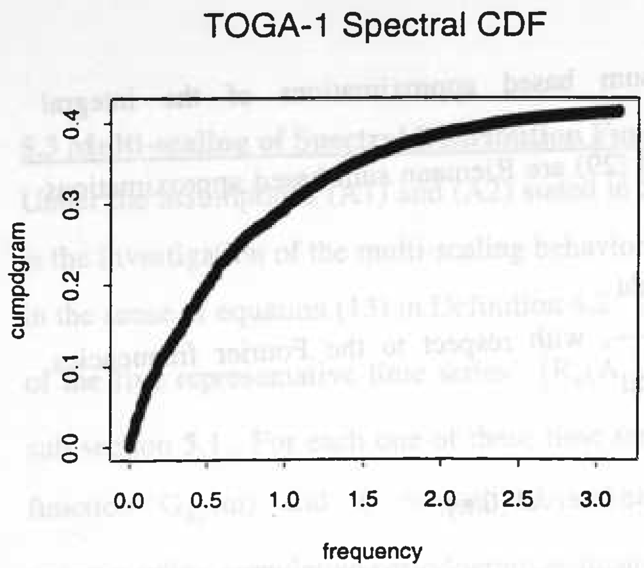

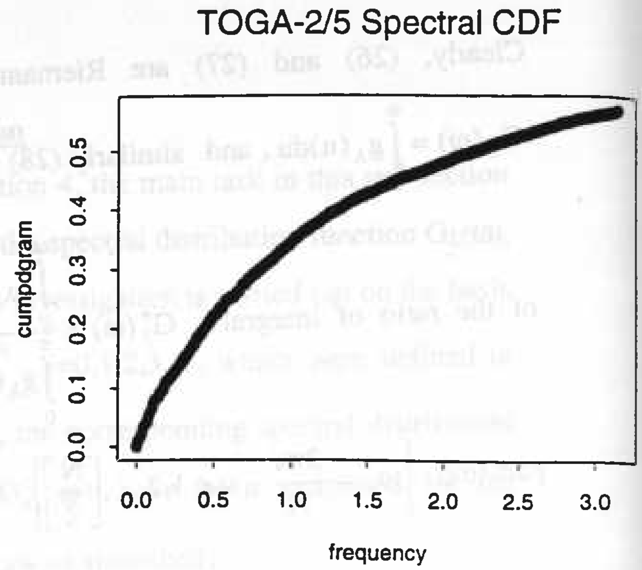

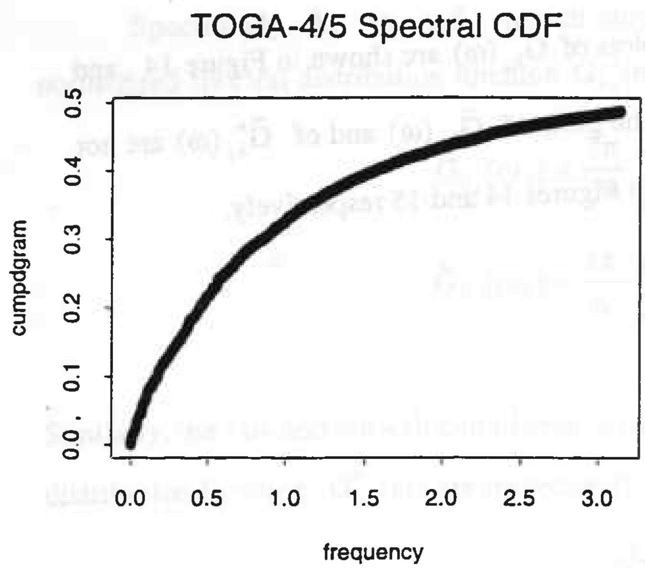

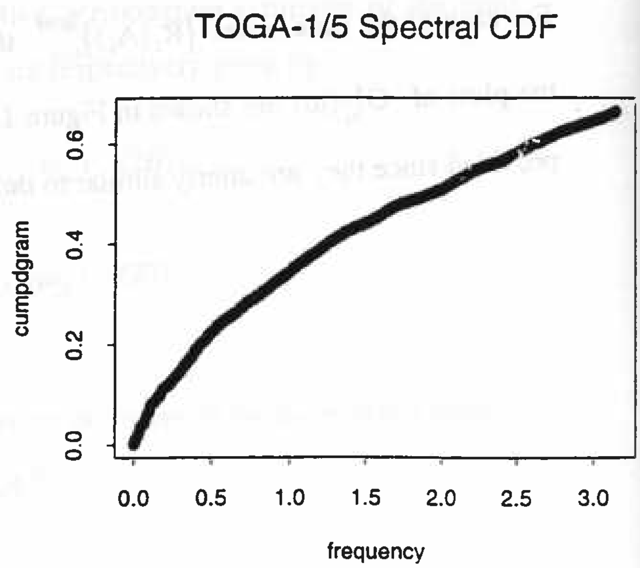

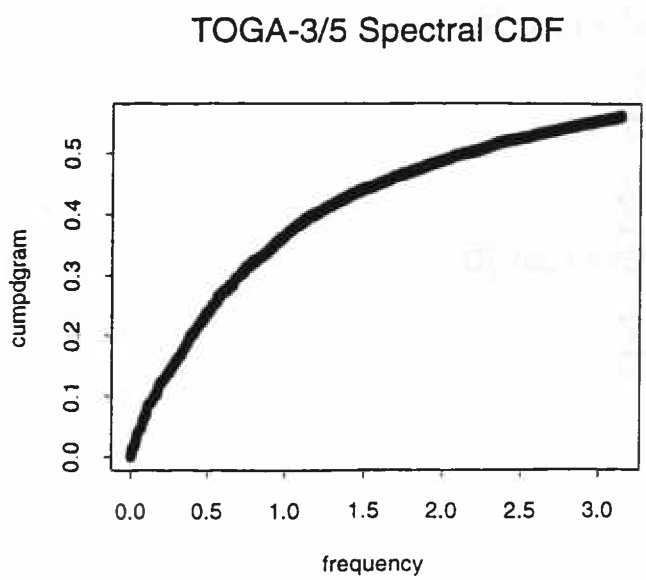

Figure 14:
Plots of $\hat{G}_{\lambda}(\omega)$, for λ=1, 4/5, 3/5, 2/5, 1/5 .

https://doi.org/10.26219/heal.aueb.5641

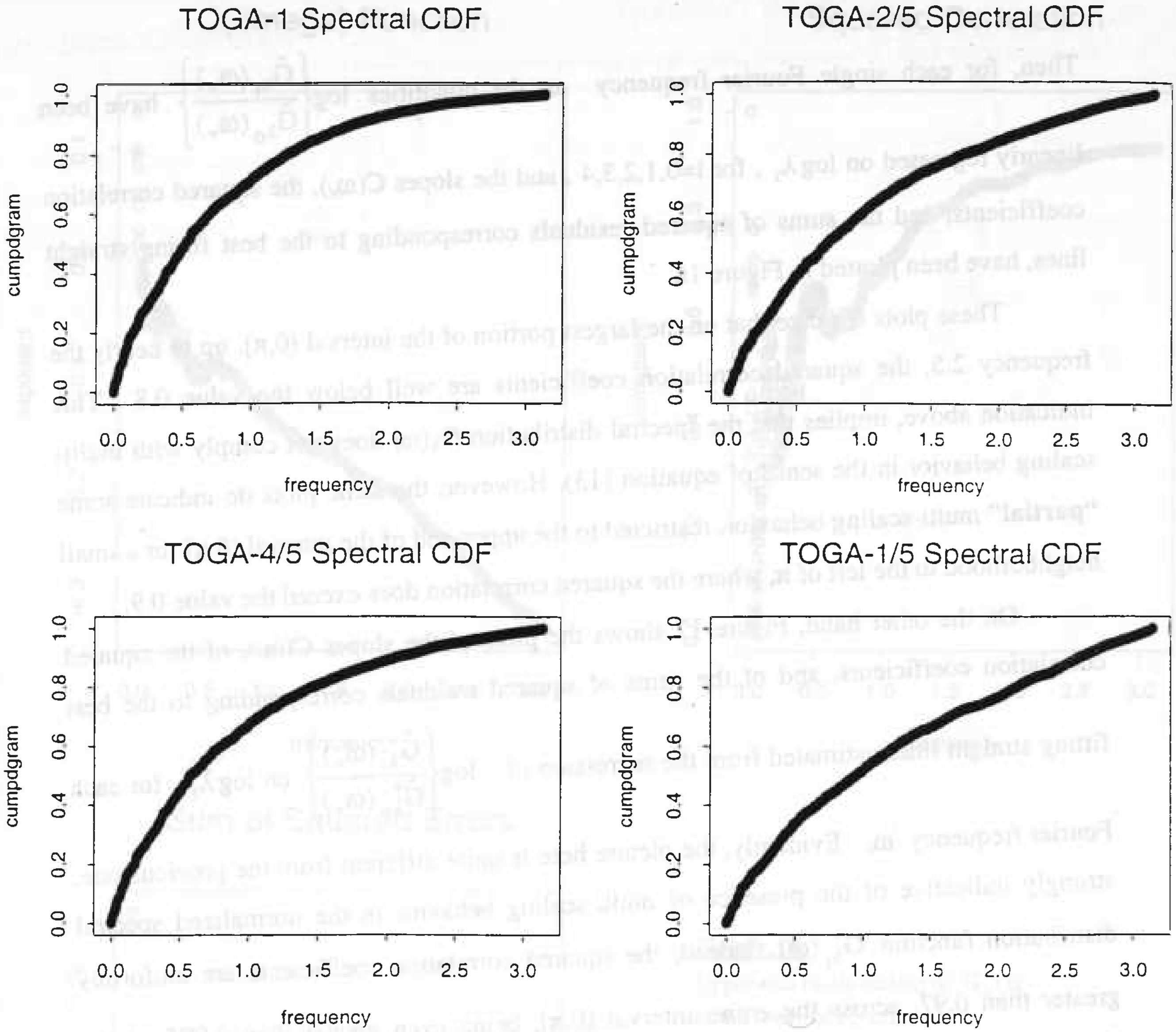

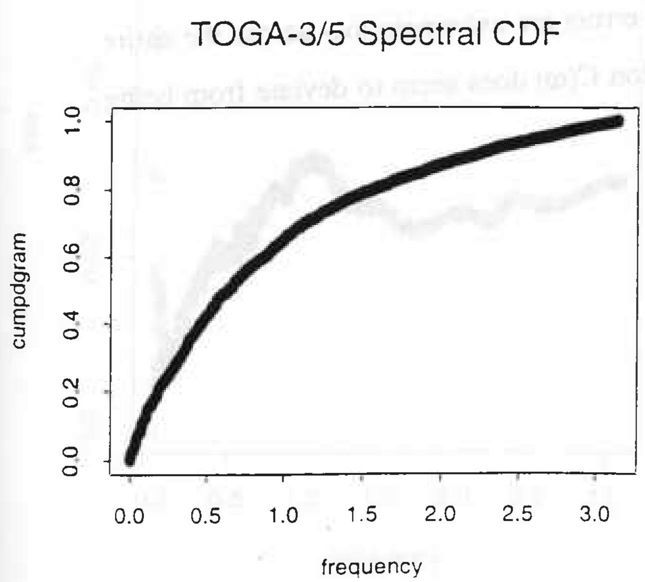

Figure 15:
Plots of $\hat{G}^{*}_{\lambda}(\omega)$, for λ=1, 4/5, 3/5, 2/5, 1/5 .

https://doi.org/10.26219/heal.aueb.5641

Then, for each single Fourier frequency ω_ν the quantities $\log\left\{\frac{\hat{G}_{\lambda_i}(\omega_\nu)}{\hat{G}_{\lambda_0}(\omega_\nu)}\right\}$ have been linearly regressed on $\log\lambda_i$, for i=0,1,2,3,4 , and the slopes $C(\omega_\nu)$, the squared correlation coefficients, and the sums of squared residuals corresponding to the best fitting straight lines, have been plotted in Figure 16.

These plots indicate that on the largest portion of the interval $(0,\pi]$, up to nearly the frequency 2.5, the squared correlation coefficients are well below the value 0.8 . This indication above, implies that the spectral distribution $G_\lambda(\omega)$ does not comply with multi-scaling behavior in the sense of equation (13). However, the same plots do indicate some **"partial"** multi-scaling behavior, restricted to the upper-end of the interval $(0,\pi]$,in a small neighborhood to the left of π, where the squared correlation does exceed the value 0.9.

On the other hand, Figure 17 shows the plots of the slopes $C(\omega_\nu)$, of the squared correlation coefficients, and of the sums of squared residuals corresponding to the best fitting straight lines estimated from the regression of $\log\left\{\frac{\hat{G}^*_{\lambda_i}(\omega_\nu)}{\hat{G}^*_{\lambda_0}(\omega_\nu)}\right\}$ on $\log\lambda_i$, for each Fourier frequency ω_ν . Evidently, the picture here is quite different from the previous one, strongly indicative of the presence of multi-scaling behavior in the normalized spectral distribution function $G^*_{\lambda_i}(\omega)$. Indeed, the squared correlation coefficients are uniformly greater than 0.97, across the entire interval $(0,\pi]$, being even greater than 0.985 on the largest part of it. Moreover, the sums of squared errors are extremely low across the entire interval $(0,\pi]$, and the slope (or exponent) function $C(\omega)$ does seem to deviate from being linear.

https://doi.org/10.26219/heal.aueb.5641

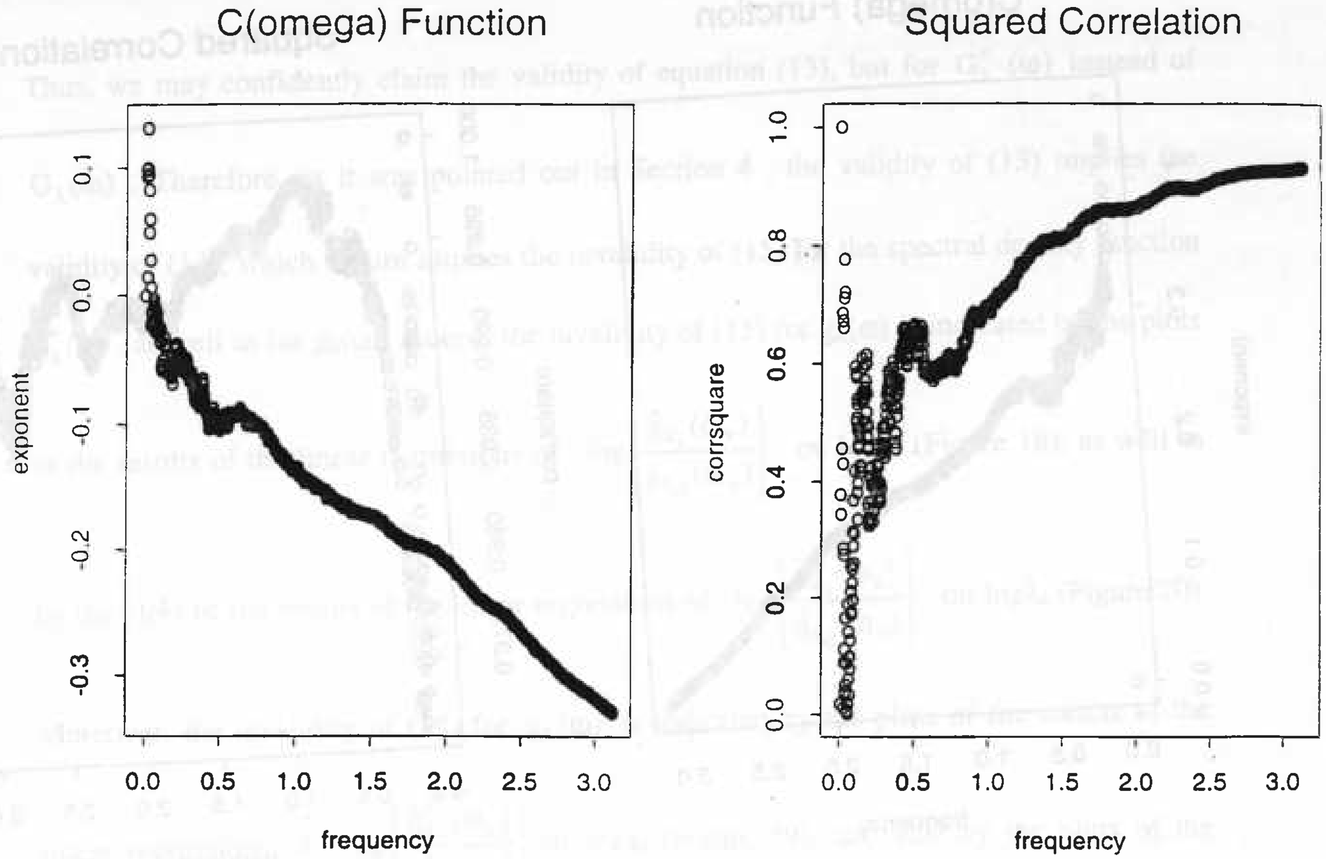

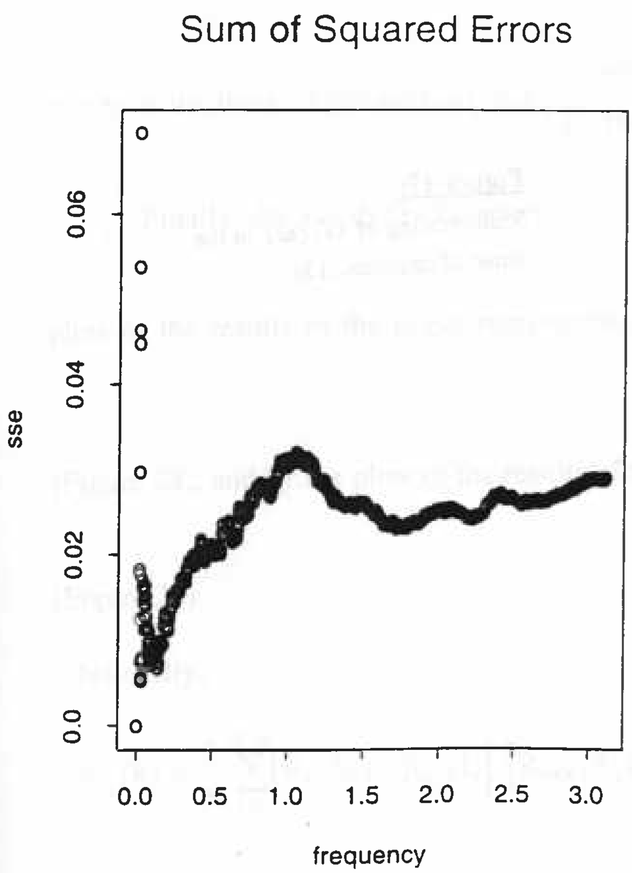

Figure 16:
Upper-end multi-scaling of $\hat{G}_{\lambda}(\omega)$ in the sense of equation (13).

https://doi.org/10.26219/heal.aueb.5641

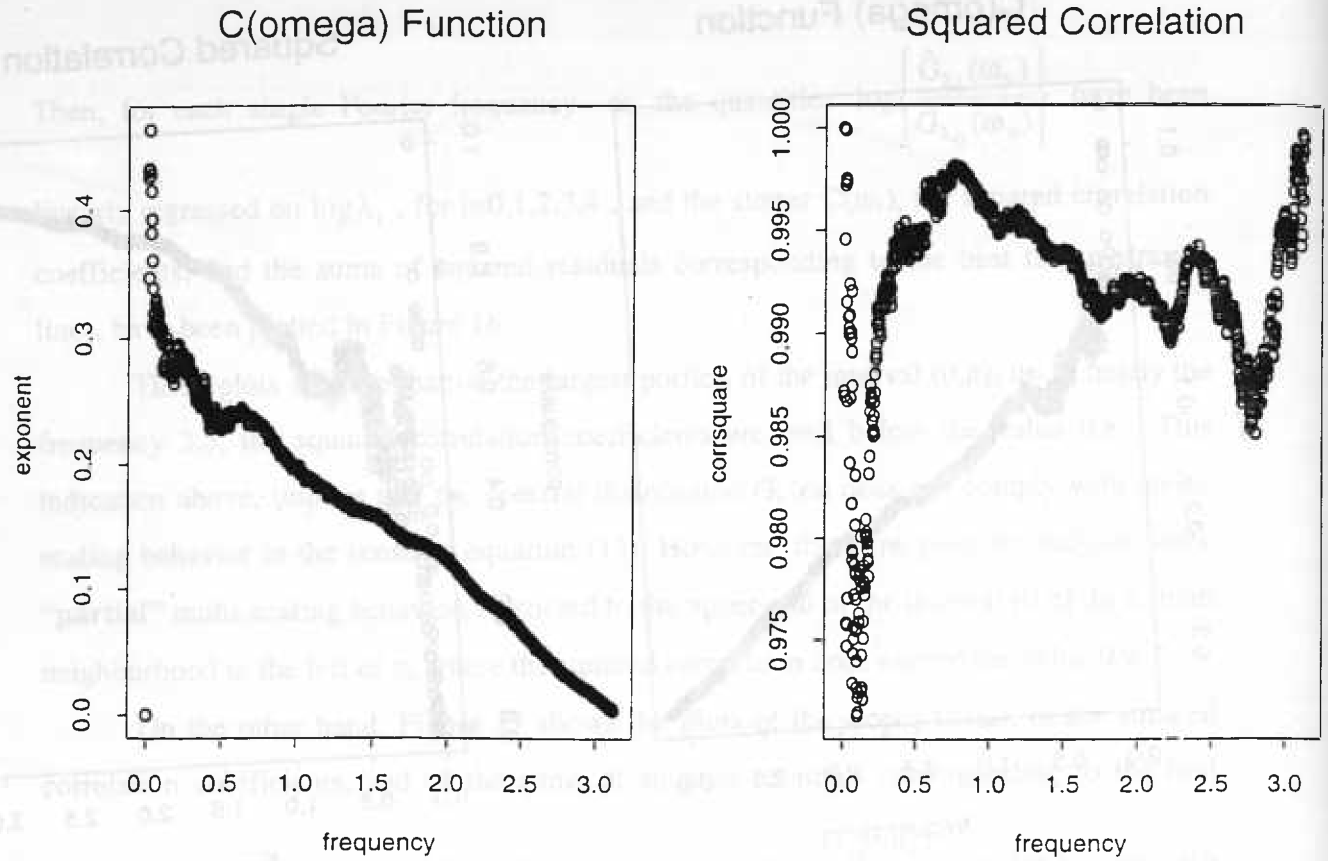

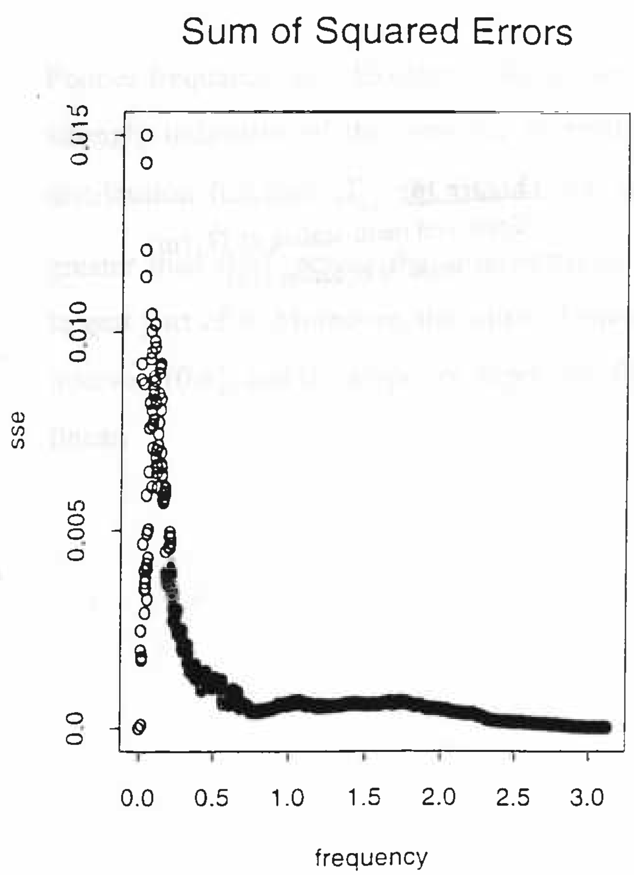

Figure 17:
Multi-scaling of $\hat{G}^{*}_{\lambda}(\omega)$ in the sense of equation (13).

https://doi.org/10.26219/heal.aueb.5641

Thus, we may confidently claim the validity of equation (13), but for $G^*_\lambda(\omega)$ instead of $G_\lambda(\omega)$. Therefore, as it was pointed out in Section 4 , the validity of (13) implies the validity of (14), which in turn implies the invalidity of (15) for the spectral density function $g^*_\lambda(\omega)$, as well as for $g_\lambda(\omega)$. Indeed, the invalidity of (15) for $g_\lambda(\omega)$ is indicated by the plots of the results of the linear regressions of $\log\left\{\frac{\hat{g}_{\lambda_i}(\omega_v)}{\hat{g}_{\lambda_0}(\omega_v)}\right\}$ on $\log\lambda_i$ (Figure 18), as well as by the plots of the results of the linear regressions of $\log\left\{\frac{\tilde{g}_{\lambda_i}(\omega_v)}{\tilde{g}_{\lambda_0}(\omega_v)}\right\}$ on $\log\lambda_i$ (Figure 20). Moreover, the invalidity of (15) for $g^*_\lambda(\omega)$ is indicated by the plots of the results of the linear regressions of $\log\left\{\frac{\hat{g}^*_{\lambda_i}(\omega_v)}{\hat{g}^*_{\lambda_0}(\omega_v)}\right\}$ on $\log\lambda_i$ (Figure 19), and also by the plots of the results of the linear regressions of $\log\left\{\frac{\tilde{g}^*_{\lambda_i}(\omega_v)}{\tilde{g}^*_{\lambda_0}(\omega_v)}\right\}$ on $\log\lambda_i$ (Figure 21).

Finally, the invalidity of equations (16) and (17) is indicated, respectively, by the plots of the results of the linear regressions, for lag $1 \le k \le 2996$, of $\log\left|\frac{\hat{\gamma}_{\lambda_i}(k)}{\hat{\gamma}_{\lambda_0}(k)}\right|$ on $\log\lambda_i$ (Figure 23), and by the plots of the results of the linear regressions of $\log\left|\frac{\hat{\rho}_{\lambda_i}(k)}{\hat{\rho}_{\lambda_0}(k)}\right|$ on $\log\lambda_i$ (Figure 25).

Naturally,

$$\hat{\gamma}_{\lambda_i}(k) = \frac{1}{N}\sum_{t=1}^{N-k}\left[R_t(A_i) - \hat{\mu}_{\lambda_i}(1)\right]\cdot\left[R_{t+k}(A_i) - \hat{\mu}_{\lambda_i}(1)\right]$$

https://doi.org/10.26219/heal.aueb.5641

is the sample auto-covariance at lag k,

$\hat{\rho}_{\lambda_i}(k) = \dfrac{\hat{\gamma}_{\lambda_i}(k)}{\hat{\gamma}_{\lambda_i}(0)}$ is the sample auto-correlation at lag k, and

$\hat{\mu}_{\lambda_i}(1) = \dfrac{1}{N}\sum_{t=1}^{N} R_t(A_i)$ is the sample mean of the time series $\{R_t(A_i)\}_{t=1}^{2996}$,for i = 0,1,2,3,4.

https://doi.org/10.26219/heal.aueb.5641

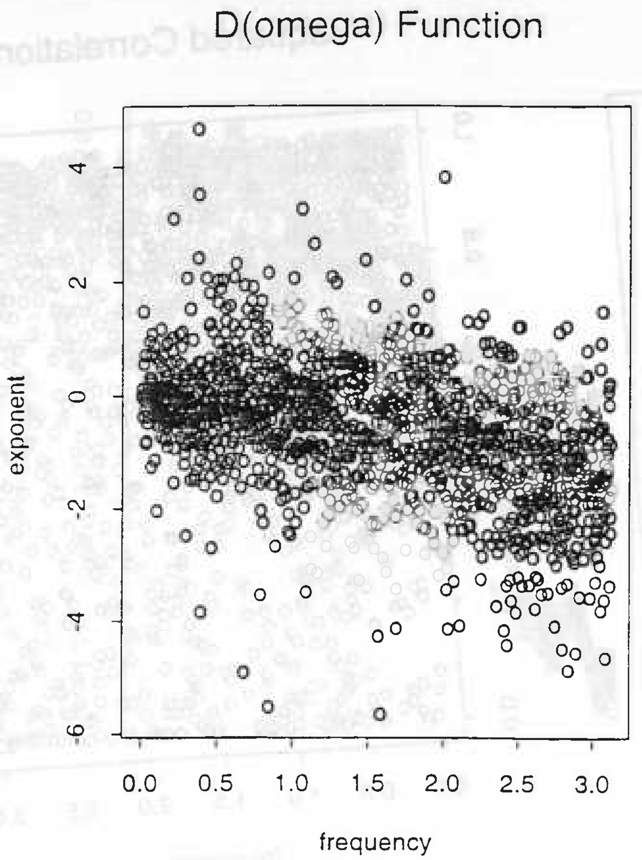

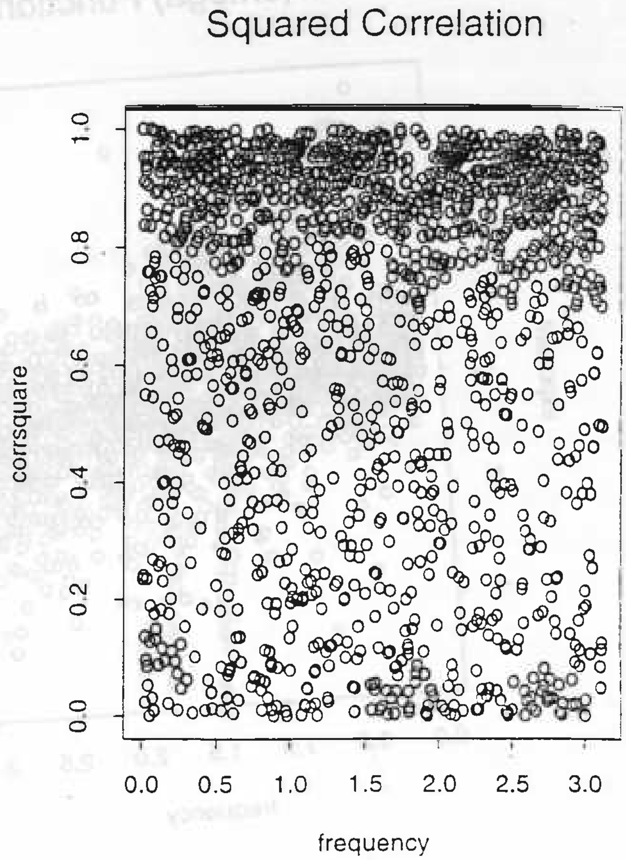

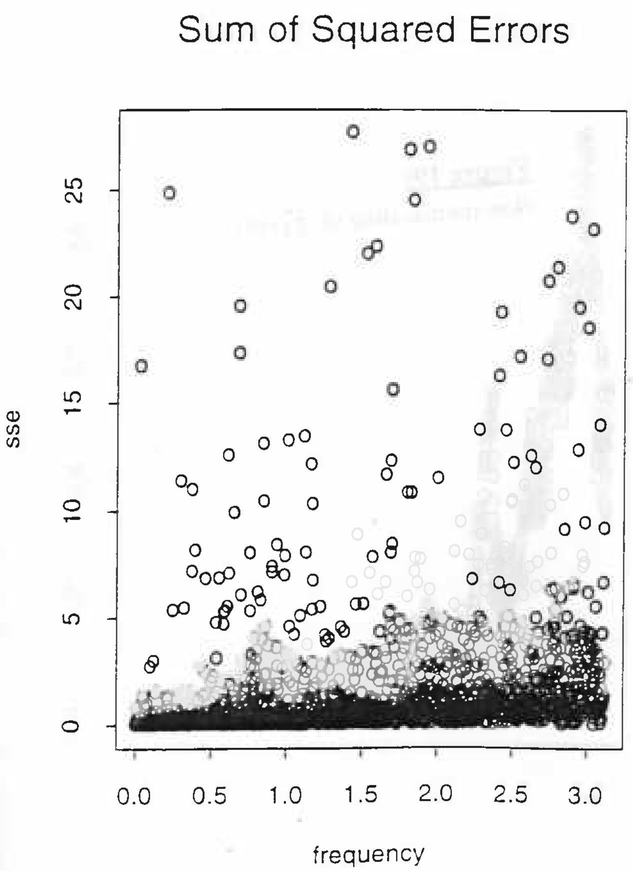

Figure 18:
Non-multiscaling of $\hat{g}_{\lambda}(\omega)$.

https://doi.org/10.26219/heal.aueb.5641

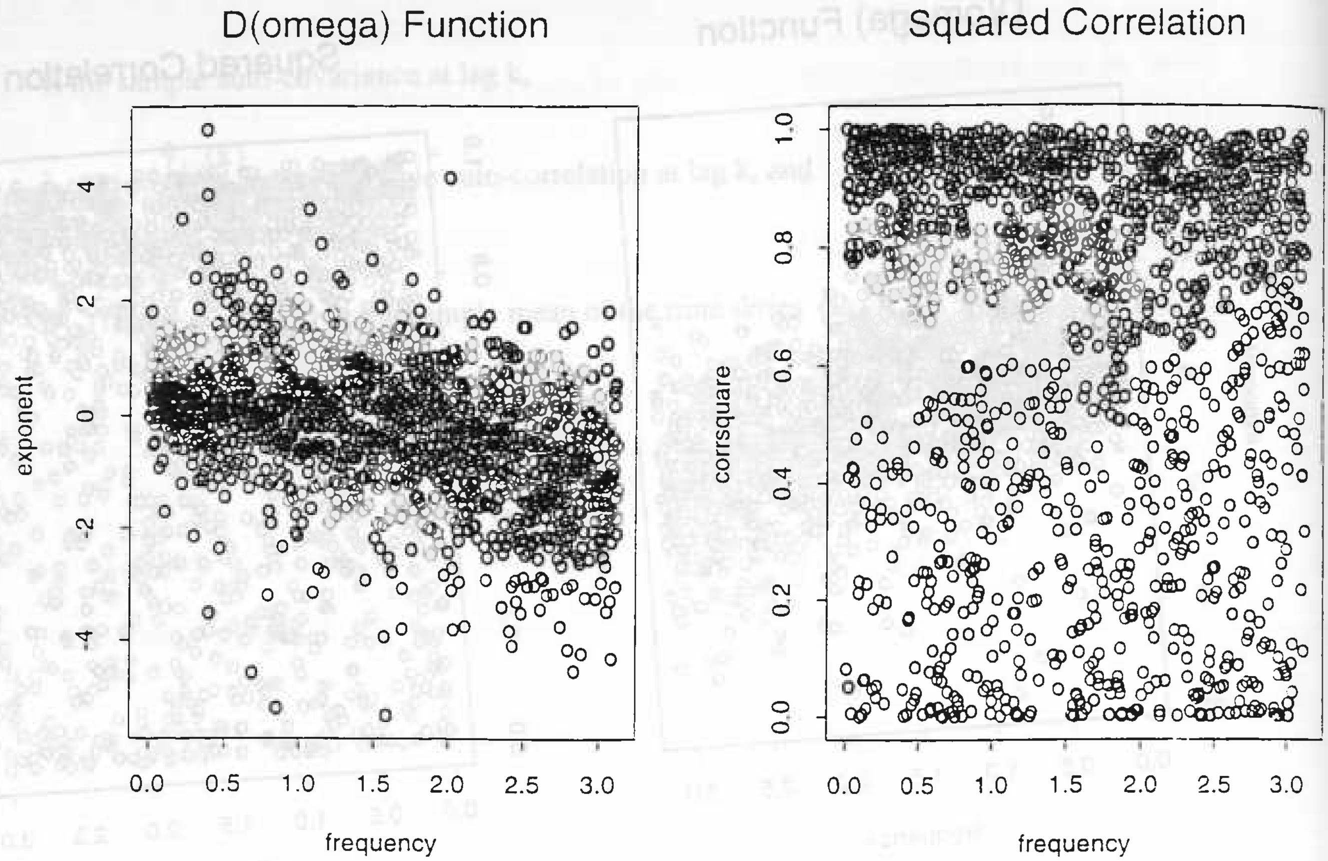

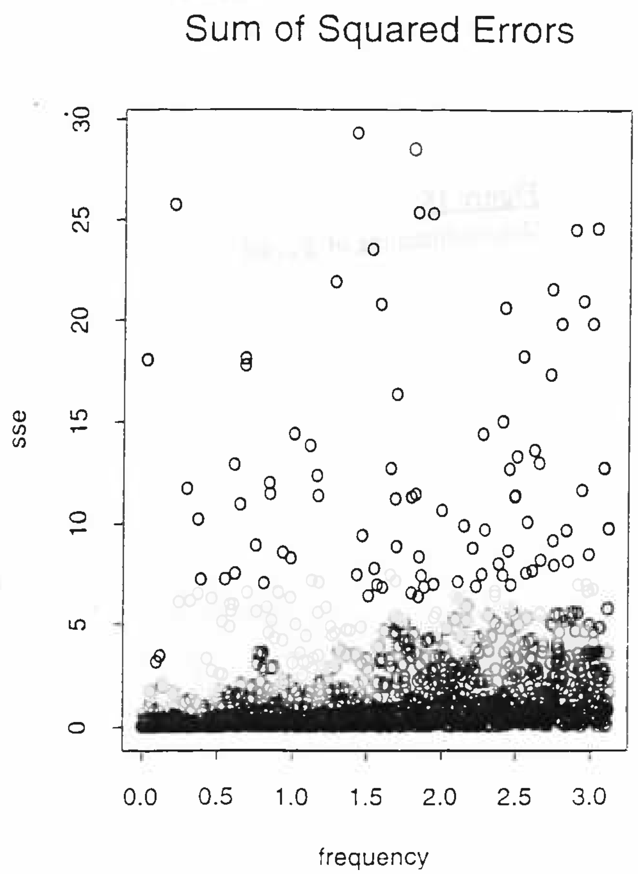

Figure 19:
Non-multiscaling of $\hat{g}^{*}_{\lambda}(\omega)$.

https://doi.org/10.26219/heal.aueb.5641

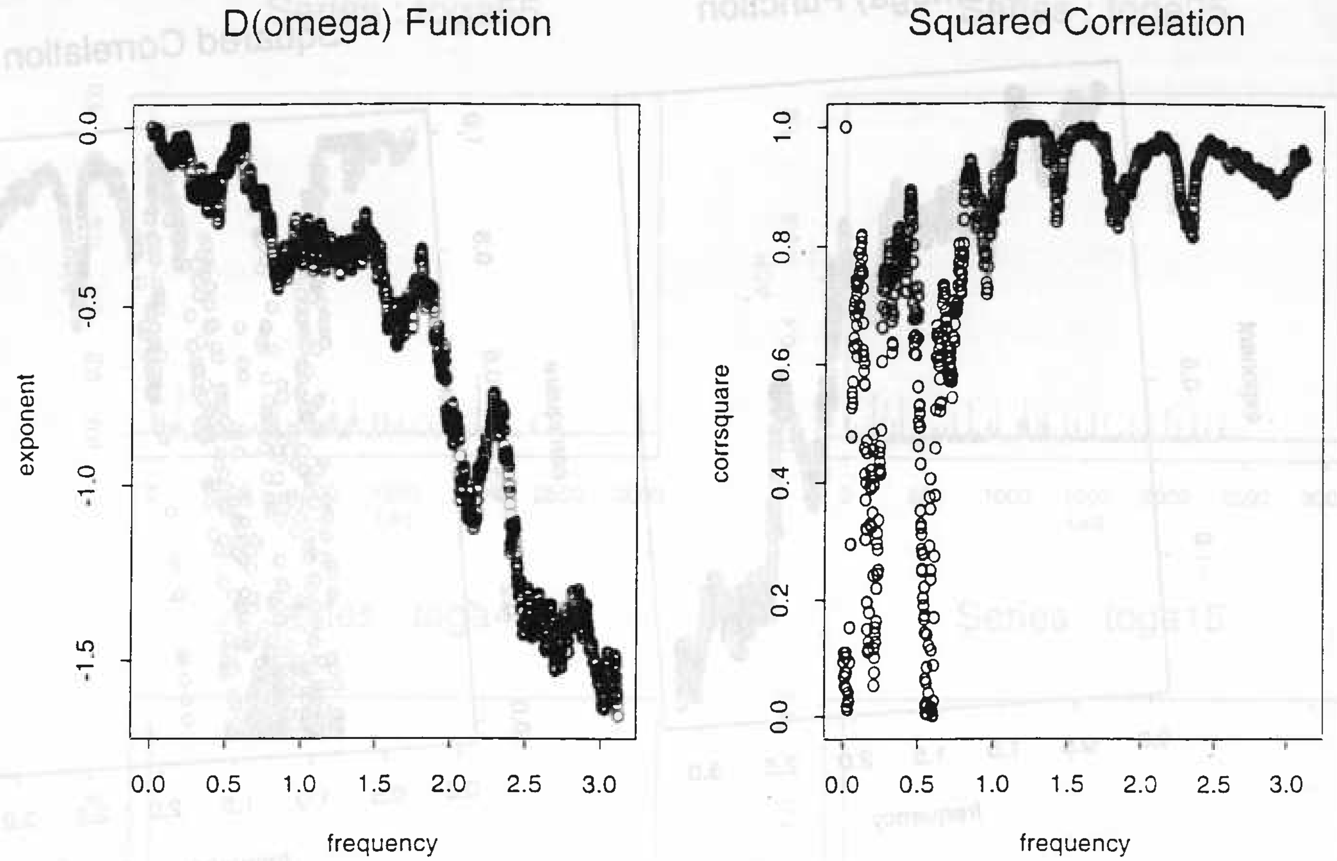

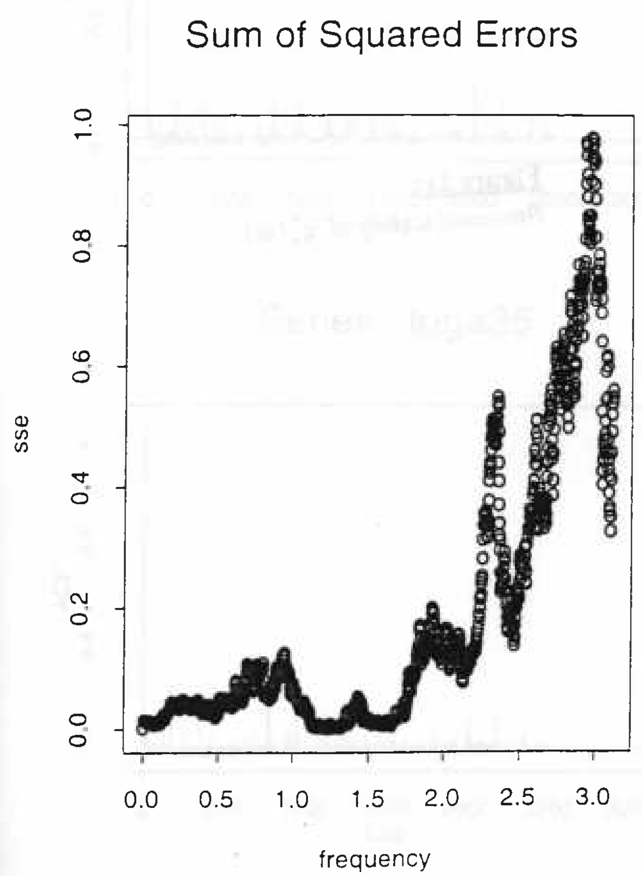

<u>**Figure 20:**</u>

Non-multiscaling of $\tilde{g}_{\lambda}(\omega)$.

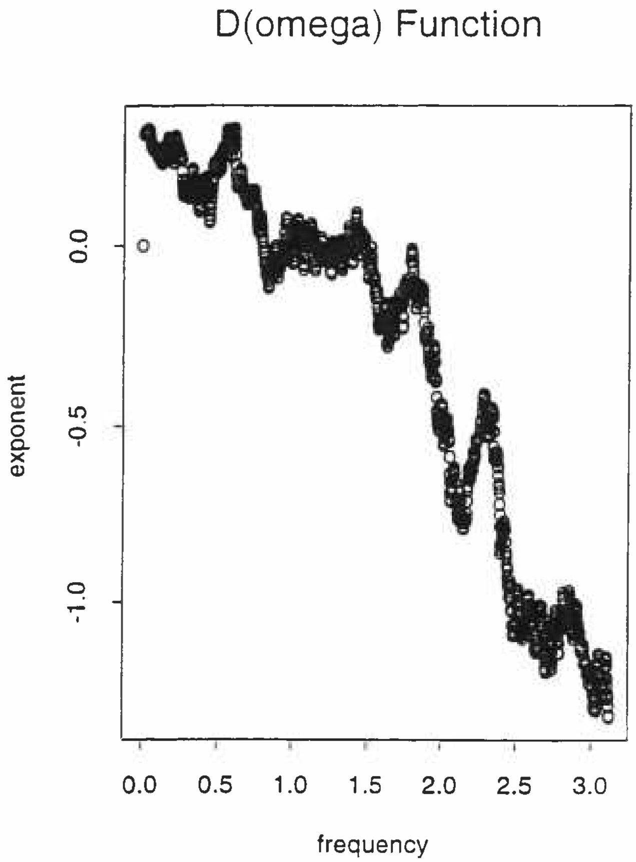

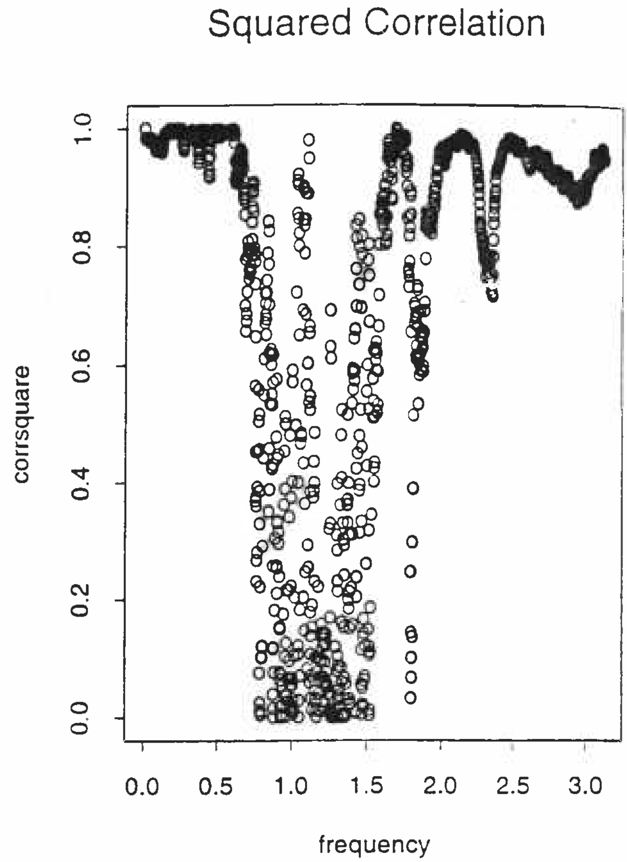

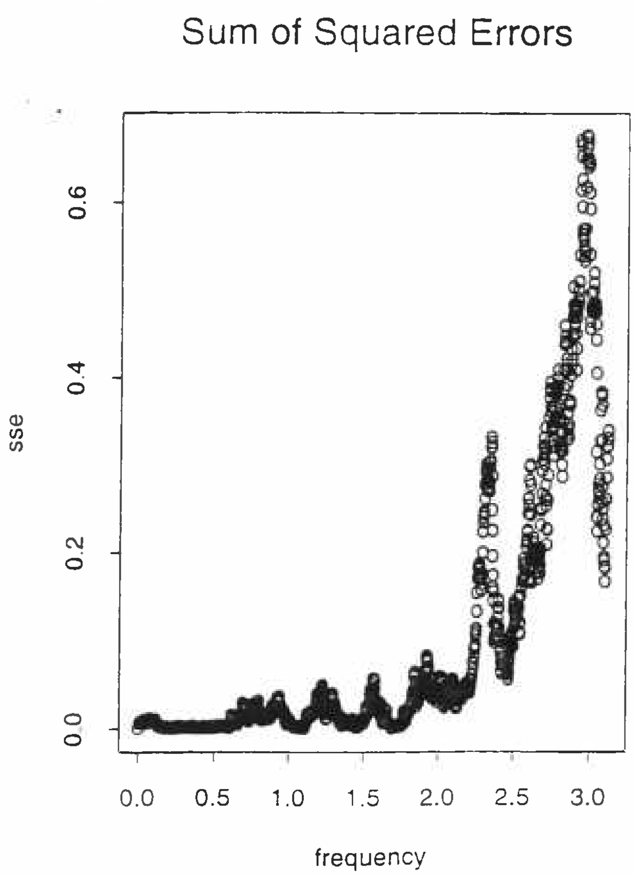

Figure 21:

Non-multiscaling of $\tilde{g}^{*}_{\lambda}(\omega)$

https://doi.org/10.26219/heal.aueb.5641

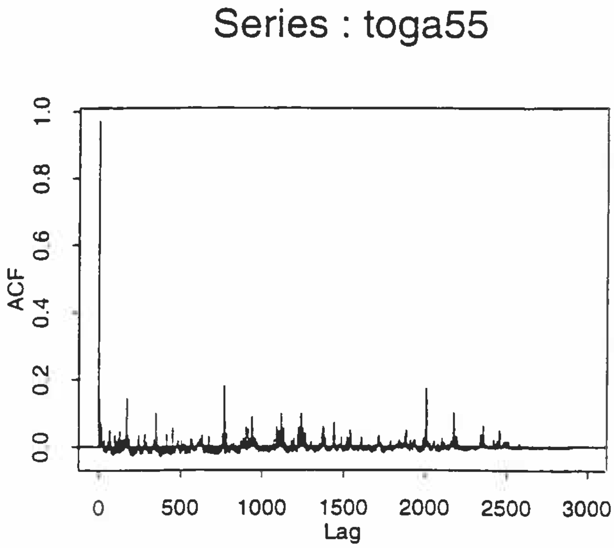

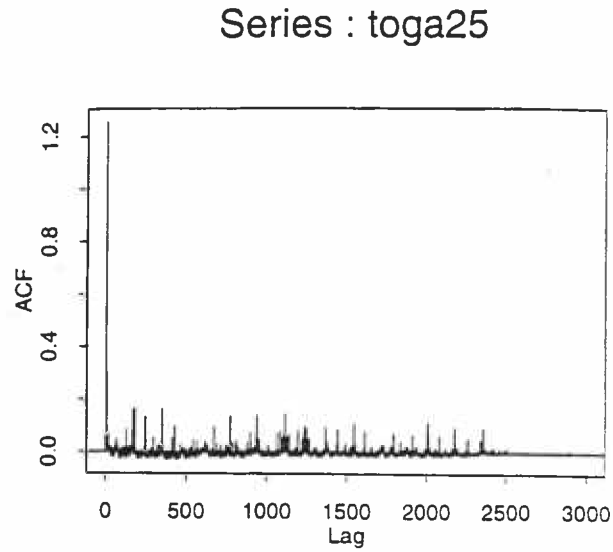

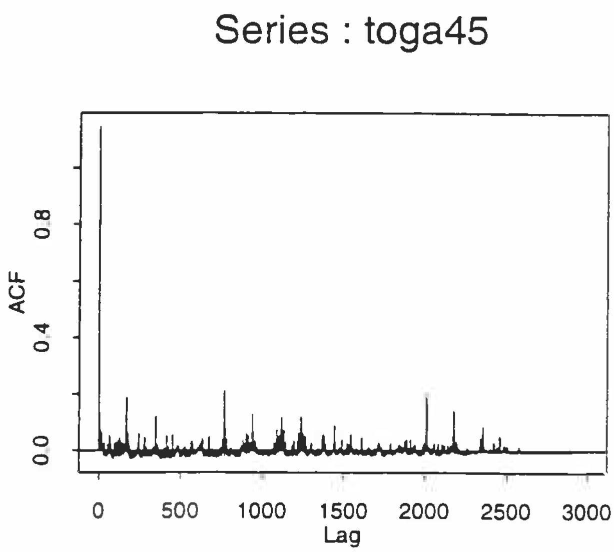

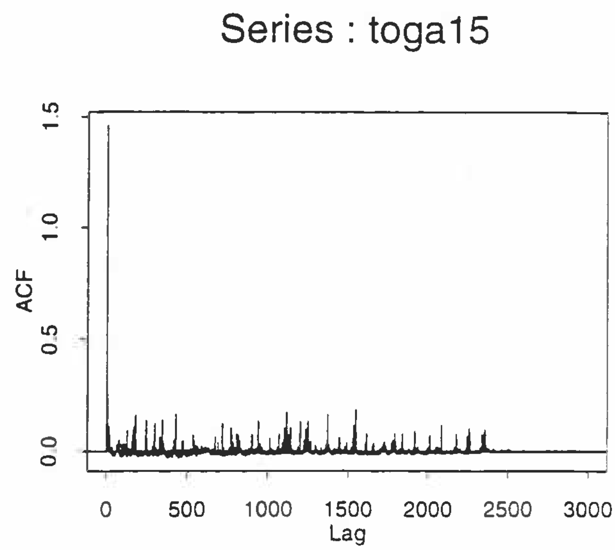

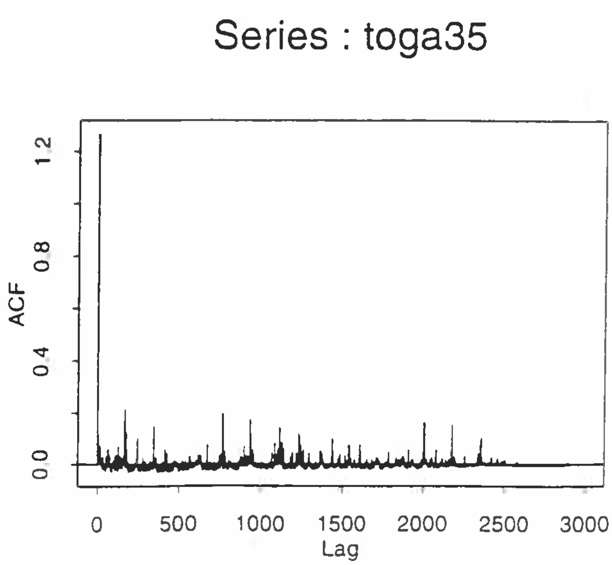

Figure 22:
Plots of auto-covariance for each one of the time series $\{R_i(A_i)\}_{t=1}^{2996}$ i=0,1,2,3,4 .

https://doi.org/10.26219/heal.aueb.5641

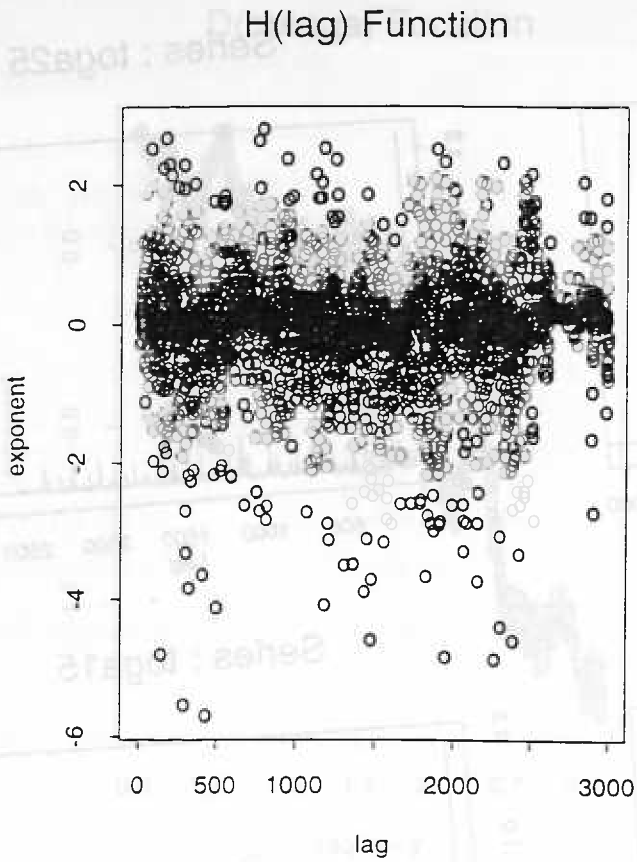

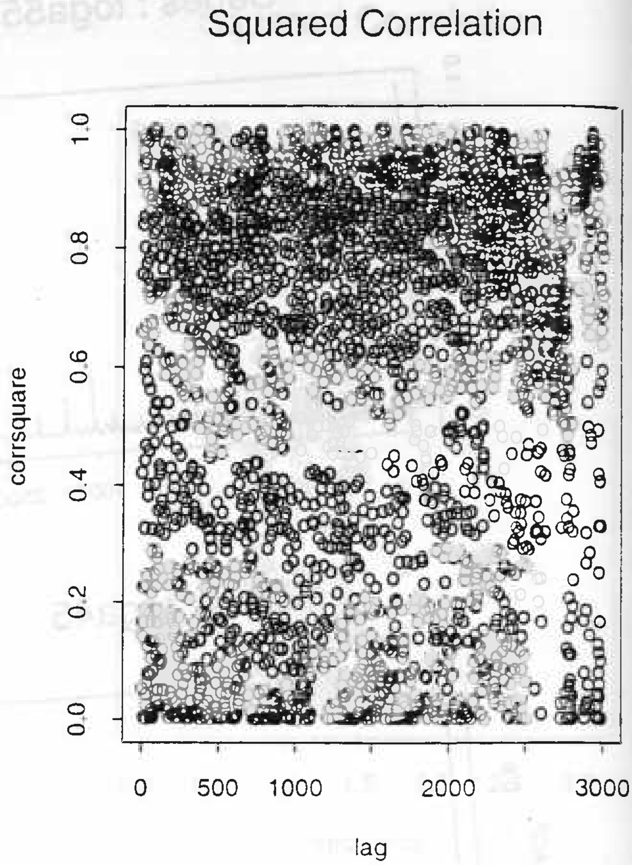

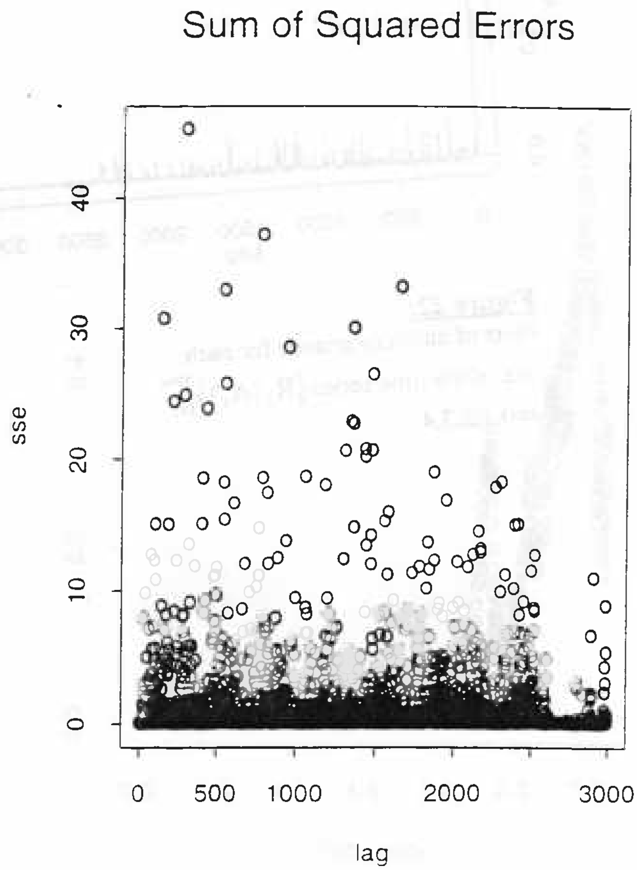

Figure 23:
Non-Multiscaling of $\hat{\gamma}_{\lambda}(k)$, for $1 \leq k \leq 2996$.

https://doi.org/10.26219/heal.aueb.5641

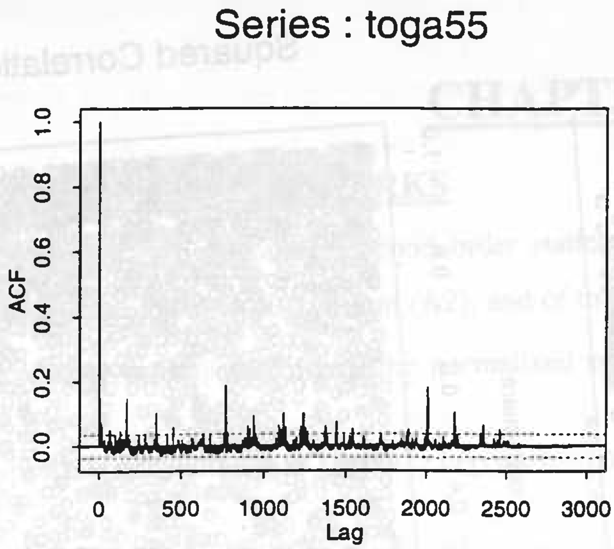

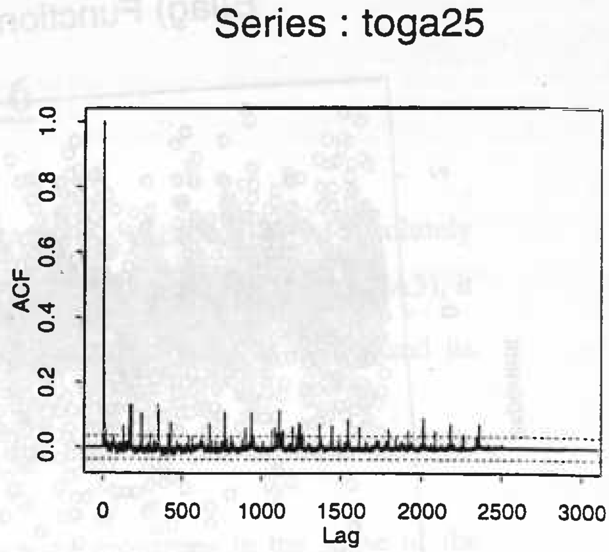

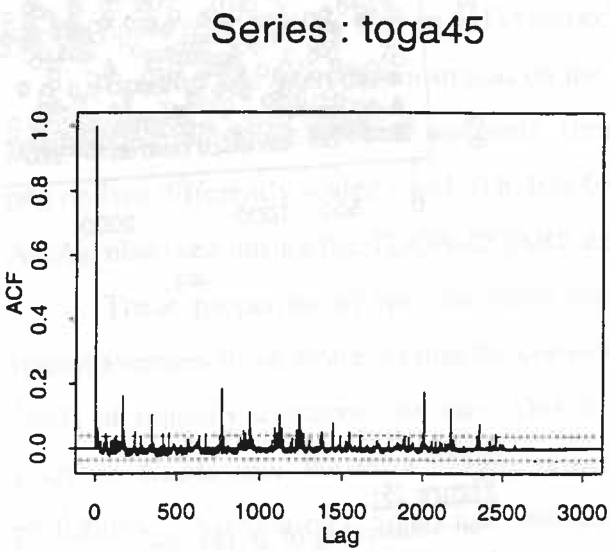

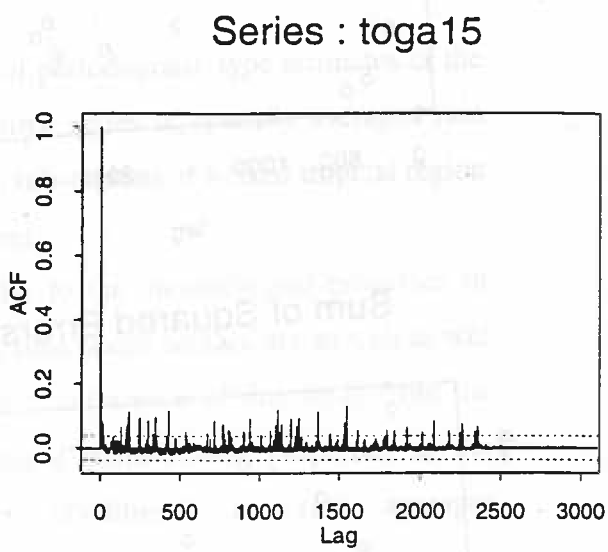

Figure 24:
Plots of auto-correlation for each one of the time series $\{R_t(A_i)\}_{t=1}^{2996}$ i=0,1,2,3,4 .

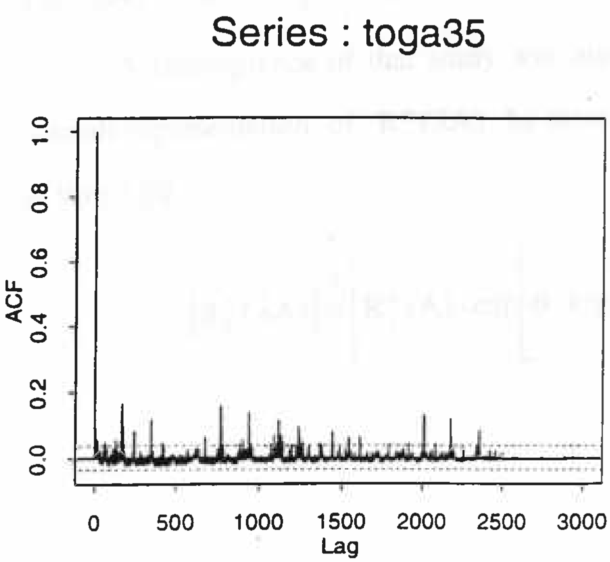

https://doi.org/10.26219/heal.aueb.5641

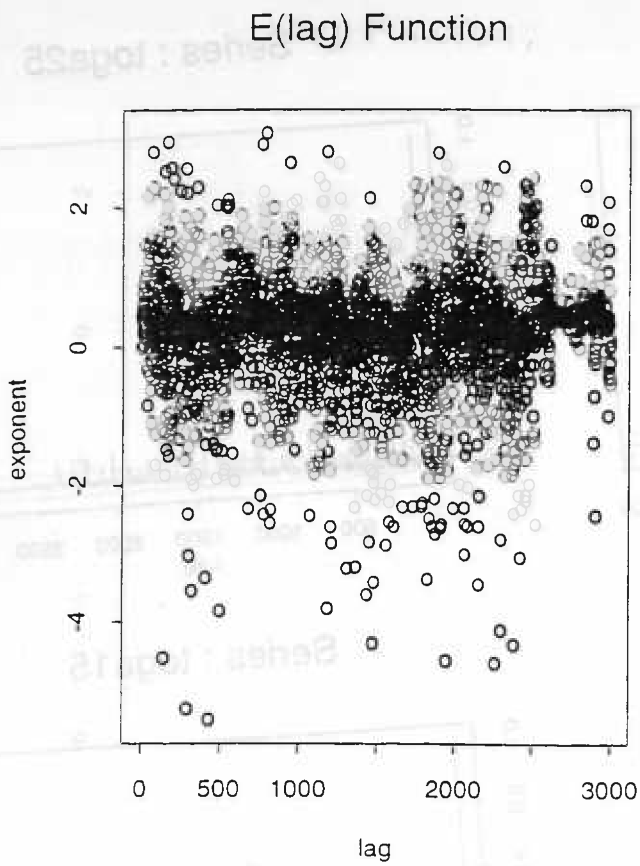

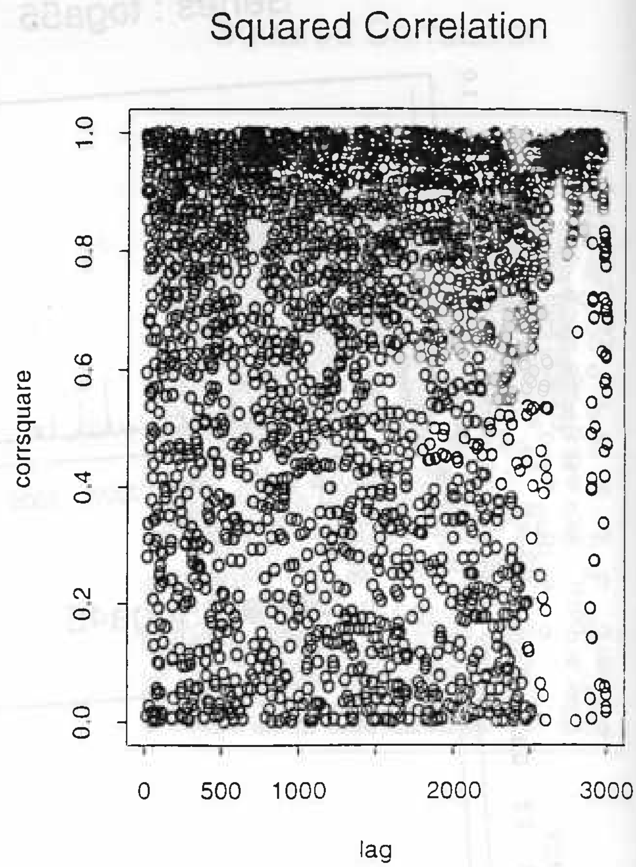

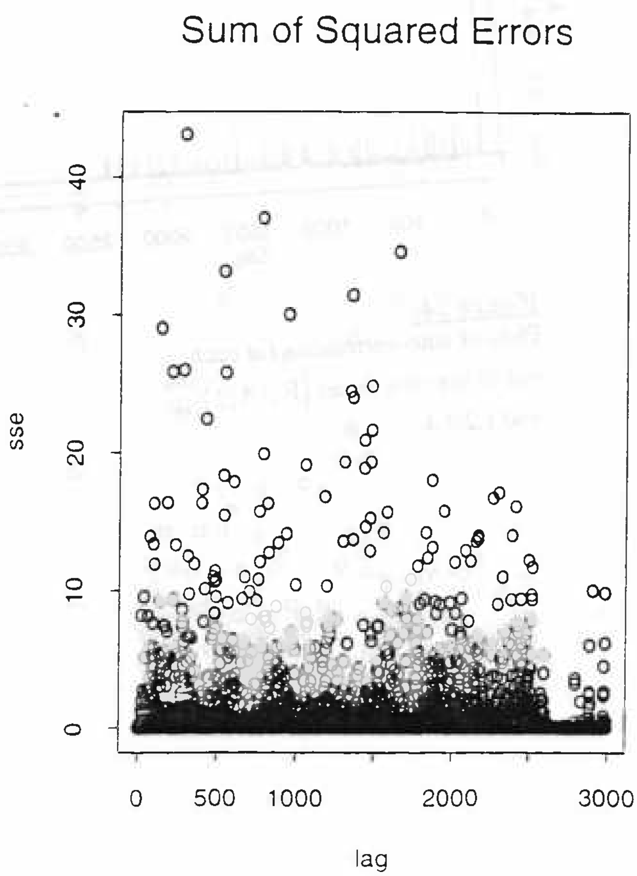

Figure 25:
Non-Multiscaling of $\hat{\rho}_{\lambda}(k)$, for $1 \leq k \leq 2996$.

https://doi.org/10.26219/heal.aueb.5641

CHAPTER 6

CONCLUDING REMARKS

Under the assumptions of second order stationarity (A1), the existence of an absolutely continuous spectral distribution (A2), and of the existence of its spectral moments (A3), it has been demonstrated that, the normalized spectral distribution function $G_\lambda^*(\omega)$ and its spectral moments $s_\lambda^*(h) = \int_0^\pi \omega^h \cdot G_\lambda^*(d\omega) = \int_0^\pi \omega^h \cdot g_\lambda^*(\omega)\, d\omega$, for processes of spatially averaged rain rate $\{R_t(\lambda A)\,;\, t \geq 0\}$, possess multi-scaling properties in the sense of the log-log linear relationships (13) and (11) respectively.

This fact has been demonstrated on the basis of periodogram type estimates of the spectral distribution and of its moments, from real time series of spatially averaged rain rate on five differently scaled (λ=1, 0.8, 0.6, 0.4, 0.2) sub-regions of a fixed tropical region A= A_0 observed during the TOGA-COARE experiment.

These properties of spectral multi-scaling refer to the unconditional processes of spatial averages of rain-rate, so that the corresponding time series contain dry as well as wet spells of spatially averaged rain-rate. This is a point of difference of this study from the study of *Gupta and Waymire (1990)*, which addressed multi-scaling properties of the probability distribution and its moments for conditional on rain averages $\{R_t^+(\lambda A)\,;\, A \in B\,(G)\}$ of a rain-rate field at a fixed time instant t ≥0 .

A consequence of that study was also the postulation of a multiplicative random cascade representation of $R_t^+(\lambda A)$, by means of Lemma 2.2.1, so that at any fixed instant of time t ≥0,

$$\{R_t^+(\lambda A)\} \stackrel{d}{=} \left\{ R_t^+(A) \cdot \exp\left[\theta \cdot \log \lambda + Z_{\log\left(\frac{1}{\lambda}\right)} \right] \right\} \qquad (30)$$

https://doi.org/10.26219/heal.aueb.5641

The random scale process $\left\{ \exp\left[\theta \cdot \log\lambda + Z_{\log\left(\frac{1}{\lambda}\right)} \right] ; 0 < \lambda \leq 1 \right\}$ is parametrized only with respect to the magnifying spatial scale λ, and is apparently the same for every instant of time t.

However, in light of the spectral multi-scaling properties indicated in this dissertation, for unconditional processes of spatially averaged rain-rate, it is conceivable that a similar to (30) representation of the unconditional spatial average may be obtained, with a random scale factor depending on both the spatial scale λ and the time t. This idea is unraveled in the following lines in a rather heuristic manner.

From the spectral theory of weakly stationary processes, and under the assumptions (A1) and (A2), it follows (see *Koopmans (1974), Kedem (1994)*) that, there is a unique complex-valued random measure ξ_λ, defined on the Borel subsets of the interval $(-\pi,\pi]$, and referred to as *random spectral measure*, such that the stationary process $\left\{ R_t(\lambda A) \; ; \; t \geq 0 \right\}$ has the spectral representation

$$R_t(\lambda A) = \mu_\lambda(1) + \int_{-\pi}^{\pi} e^{i\omega t} \xi_\lambda(d\omega) \qquad (31),$$

where $\mu_\lambda(1) = E[R_t(\lambda A)]$ is the stationary mean of the process. Moreover, some operational properties of the random spectral measure are the following:

$$\xi_\lambda(d\omega) = \overline{\xi_\lambda(-d\omega)} \qquad (32),$$

since $R_t(\lambda A)$ is real-valued,

$$E[\xi_\lambda(d\omega)] = 0 \qquad (33),$$

since $\left\{ R_t(\lambda A) - \mu_\lambda(1) \; ; t \geq 0 \right\}$ is a zero-mean process.

Most important is the property of orthogonality, according to which

$$E\left[\xi_\lambda(d\omega) \cdot \overline{\xi_\lambda(d\phi)}\right] = \begin{cases} G_\lambda(d\omega) = g_\lambda(\omega)d\omega \; , & \phi = \omega \\ 0 \; , & \phi \neq \omega \end{cases} \qquad (34),$$

https://doi.org/10.26219/heal.aueb.5641

where $G_\lambda(d\omega)$ is the (un-normalized) spectral distribution (non-random) measure.

Therefore, the corresponding normalized random spectral measure defined by

$$\xi^*_\lambda(d\omega) = \frac{1}{\sigma_\lambda} \cdot \xi_\lambda(d\omega) \quad (35),$$

where σ_λ is the stationary standard deviation of $\{R_t(\lambda A)\,;\, t \geq 0\}$, provides a spectral representation of the standardized stationary process $\{R^*_t(\lambda A)\,;\, t \geq 0\}$.

That is,

$$R^*_t(\lambda A) := \frac{R_t(\lambda A) - \mu_\lambda(1)}{\sigma_\lambda} = \int_{-\pi}^{\pi} e^{i\omega t} \cdot \xi^*_\lambda(d\omega) \quad (36),$$

and ξ^*_λ obviously inherits from ξ_λ the following properties:

$$\xi^*{}_\lambda(d\omega) = \overline{\xi_\lambda{}^*(-d\omega)} \quad (37),$$

$$E\left[\xi^*_\lambda(d\omega)\right] = 0 \quad (38),$$

$$E\left[\xi^*_\lambda(d\omega) \cdot \overline{\xi^*_\lambda(d\phi)}\right] = \begin{cases} \dfrac{G_\lambda(d\omega)}{\sigma^2_\lambda} = \dfrac{g_\lambda(\omega)}{\sigma^2_\lambda} d\omega = g^*_\lambda(\omega) d\omega \ , & \phi = \omega \\ 0 \ , & \phi \neq \omega \end{cases} \quad (39)$$

Now, provided that the normalized spectral distribution function $G^*_\lambda(\omega)$ is scaling in the sense that (see equation (12))

$$G^*_\lambda(\omega) = \lambda^{C(\omega)} \cdot G^*_1(\omega) \quad (40),$$

differentiation with respect to ω yields that (see equation (14))

$$g^*_\lambda(\omega) = \lambda^{C(\omega)} \cdot \left[g^*_1(\omega) + C'(\omega) \cdot G^*_1(\omega) \cdot (\log \lambda)\right] \quad (41).$$

Substituting (41) into (39) one obtains that

$$E\left[\xi^*_\lambda(d\omega) \cdot \overline{\xi^*_\lambda(d\phi)}\right] = \begin{cases} \lambda^{C(\omega)} \cdot \left[g^*_1(\omega) + C'(\omega) \cdot (\log \lambda) \cdot G^*_1(\omega)\right] d\omega \ , & \phi = \omega \\ 0 \ , & \phi \neq \omega \end{cases} \quad (42)$$

The crux of the matter here is that, due to the uniqueness of a random spectral

https://doi.org/10.26219/heal.aueb.5641

measure ξ^*_λ, for each $0<\lambda\leq 1$, it is conceivable that one may obtain a (perhaps complex-valued scalar or even random) function $D_\lambda(\omega)$, which satisfies the "scaling" relation

$$\xi^*_\lambda(d\omega) = D_\lambda(\omega)\cdot \xi^*_1(d\omega) \qquad (43)$$

between the random spectral measures ξ^*_λ and ξ^*_1, and such that it is also consistent with equation (42).

Apparently, a boundary condition which must be met by this function, at $\lambda=1$, is that

$$D_1(\omega)\equiv 1 \; (44).$$

It is also interesting to note that if (43) indeed holds true, subject to the boundary condition (44), then clearly in the case where $D_\lambda(\omega)$ is a non-random scalar function

$$E\left\{\left|\xi^*_\lambda(d\omega)\right|^2\right\} = \left|D_\lambda(\omega)\right|^2 \cdot E\left\{\left|\xi^*_1(d\omega)\right|^2\right\} \quad \text{and equivalently}$$

$$g^*_\lambda(\omega) = \left|D_\lambda(\omega)\right|^2 g^*_1(\omega) \qquad (45).$$

That is, the validity of (43) is equivalent to the validity of (45), a consequence of which is the scaling of the normalized spectral density functions, but in a sense different than that proposed by equation (15).

Thus, if the desired function $D_\lambda(\omega)$ exists, then it follows immediately from equation (36), that

$$R^*_t(\lambda A) = R^*_t(A)\cdot \frac{\int_{-\pi}^{\pi} e^{i\omega t} D_\lambda(\omega)\xi^*_1(d\omega)}{\int_{-\pi}^{\pi} e^{i\omega t}\xi^*_1(d\omega)} \qquad (46)$$

The ratio of integrals on the right side of (46) is a random scale factor involving both the spatial scale λ and the time t, while (46) constitutes a multiplicative random cascade representation of spatially averaged rain-rate processes.

A final remark to be made here, which is apparently consistent with the plots in Figures 3,4,5,14,15 is that the spectrum of a spatially averaged rain-rate process is loosing power as the spatial scale λ is shrinking towards 0 (i.e. $\lambda\rightarrow 0$).

https://doi.org/10.26219/heal.aueb.5641

This observation is consistent with the scaling relation $G^*_\lambda(\omega) = \lambda^{C(\omega)} \cdot G^*_1(\omega)$ indicated by Figure 17. Indeed, since $C(\omega)>0$, for $0<\omega<\pi$, given $0<\lambda_1<\lambda_2\le 1$, one has $0<\lambda_1^{C(\omega)}<\lambda_2^{C(\omega)}\le 1$, whence $0<\lambda_1^{C(\omega)}\cdot G^*_1(\omega)<\lambda_2^{C(\omega)}\cdot G^*_1(\omega)\le G^*_1(\omega)$ or equivalently $0<G^*_{\lambda_1}(\omega)<G^*_{\lambda_2}(\omega)\le G^*_1(\omega)$.

This observation agrees with the intuition that as the spatial scale λ tends towards zero, there is less and less structure or signal to be captured by a process of spatially averaged rain rate, since the very region over which rain rate is averaged, captures less and less of the large scale forcing signal, and eventually degenerates to plain noise.

https://doi.org/10.26219/heal.aueb.5641

REFERENCES

Anselmet, F. , Cagne, Y. , Hopfinger, E. J. , and Antonia, R. A. (1984). High-order velocity structure functions in turbulent shear flows, ***J. Fluid Mech.*** , 140 , 63-89.

Billingsley , P. (1979). ***Probability Measure*** , Wiley, New York.

Chandrasekhar, S . (1943). Stochastic problems in physics and astronomy , ***Rev. Mod. Phys*** , 15 ,1-89 .

Cox, D. R. , and V. Isham (1988). A simple spatial-temporal model of rainfall, ***Proc. Roy. Soc. Lond. Ser. A.*** , 415 , 317-328.

Chatfield, C. (1989). ***The Analysis of Time Series , Fourth Edition***, Chapman & Hall.

Feller, W. (1971). ***An Introduction to Probability Theory and its Applications,***2, Wiley, New York.

Frisch, U. , and Parisi, G. (1985). On the singularity structure of fully developed turbulence, edited by M.Ghil, R.Benzi, and G.Parisi, 84-88, Elsevier North Holland New York.

Gnedenko, B. V.,and Kolmogorov, A.N. (1954). ***Limit Distributions for Sums of Independent Random Variables*** , Addison Wesley, Cambridge, Massachusetts.

Gupta, V. K., and Waymire, E. C. (1979). A stochastic kinematic study of subsynoptic space-time rainfall ,***Water Resources Research*** , 15(3) : 637-644.

Gupta, V. K., and Waymire, E. C. (1989). Statistical self-similarity in river networks parametrized by elevation , ***Water Resources Research*** , 25(3) : 463-476.

Gupta, V. K., and Waymire, E. C. (1990). Multiscaling Properties of Spatial Rainfall and River flow Distributions, ***Journal of Geophysical Research*** , 95 , 1999-2009 .

Gupta, V. K., and Waymire, E. C. (1993). A statistical analysis of mesoscale rainfall as a random cascade , ***Journal of Applied Meteorology***, 32 , 251-267 .

Holley , R. and Waymire, E. C. (1992). Multifractal dimensions and scaling exponents or strongly bounded random cascades , ***Annals of Applied Probability***, 2 , 819-845.

Ito, K. (1984). ***Lectures on Stochastic Processes*** , Tata Inst. , distributed by Springer-Verlag, New York.

Kedem, B. (1994). ***Time Series Analysis by Higher Order Crossings***, IEEE Press.

https://doi.org/10.26219/heal.aueb.5641

Kedem, B. , and Chiu, L. S. (1987). Are rain rate processes self similar?, ***Water Resources Research***, 23 (10) , 1816-1818.

Koopmans, L.H. (1974). ***The Spectral Analysis of Time Series*** , Academic Press.

Lamperti, J. (1962). Semi Stable Stochastic Processes , ***Transactions of American Mathematical Society*** ,104, 62-78.

LeCam, L. (1961). A stochastic description of precipitation , 4th Berkeley Symposium on Math. Stat. And Prob. , Vol. 3 , pp. 165-186 , Univ. of California, Berkeley.

Lovejoy, S. , and Manndelbrot, B. B. (1985). Fractal properties of rain and a fractal model , ***Tellus*** , 37A , 209-232.

Over,T. M. and Gupta, V.K. (1994). Statistical analysis of mesoscale rainfall: Dependence of a random cascade generator on large-scale forcing , ***Journal of Applied Meteorology***, 33, 1526-1542.

Port, S. , C. (1994). Theoretical Probability for Applications , Wiley , New York.

Rodriguez-Iturbe , I., D. R. Cox , and V.Isham , (1987). Some models for rainfall based on stochastic point processes, ***Proc. Roy. Soc. Lond. Ser. A.*** , 410 , 269-288.

Short , D. A. , Kucera , P. A. , Ferrier , B. S. , and Thiele , O.W. (1995). COARE IOP Rainfall from Shipborne Radars : 1.Rain Mapping Algorithms, 27-th Conference on Radar Meteorology, Paper 14 A.2, Proceedings of the American Meteorological Society.

Smith , J. A. and A. F. Karr (1985). Parameter estimation for a model of space-time rainfall , ***Water Resources Research*** , 21(8), 1251-1257.

Taqqu, M. , (1986). A bibliographical guide to self-similar processes and long range dependence, Dependence in Probability and Statistics, edited by E. Eberlein and M. Taqqu , pp.137-162, Birkhauser, Boston, Massachusetts.

Waymire, E. C. , and V. K. Gupta , and I. Rodriguez-Iturbe , (1984). A special theory of rainfall intensity at the meso-β scale, ***Water Resources Research*** , 20(10) , 1453-1465.

Waymire, E. C. (1985). Scaling Limits and Self- Similarity in Precipitation fields , ***Water Resources Research*** , 21(8) , 1271-1281.